

x5

Cranfield Institute of Technology
School of Mechanical Engineering

PhD Thesis

1984

C.O.B. CAREY

RESEARCH AND TESTING OF WORKING FLUIDS
SUITABLE FOR AN ABSORPTION HEAT PUMP
TO HEAT BUILDINGS.

Supervisor: Professor I.E. Smith

January 1984

to NIKLAUS WEHREN

Acknowledgements

I would like to thank Ian in particular,
for making this work both fun and relevant.

SUMMARY

Having outlined the requirements of the heat pump, water and sodium hydroxide are selected as a suitable working fluid and absorbent. The advantages and disadvantages of this particular combination are outlined before dealing with the experimental work. The various components in the system are then discussed with particular attention to the absorber. From the results, suitable improvements to the design are suggested before describing possible alternative absorption systems. The technical details are all presented separately from the main text, in the Appendices.

CONTENTS

	Page	
CHAPTER 1	NATURE OF THE ABSORPTION SYSTEM	1
CHAPTER 2	SELECTION OF SUITABLE FLUIDS	3
CHAPTER 3	THE WATER-SODIUM HYDROXIDE SYSTEM	7
CHAPTER 4	EXPERIMENTAL RIG: CONSTRUCTION AND OPERATION	19
	The generator and condenser	23
CHAPTER 5	DESIGN AND PERFORMANCE OF THE ABSORBER	26
CHAPTER 6	OVERALL SYSTEM PERFORMANCE and DISCUSSION	37
CHAPTER 7	ALTERNATIVE ABSORPTION SYSTEMS	42
	REFERENCES	49
Appendix A	Performance of H_2SO_4/H_2O and $NaOH/H_2O$ System	53
Appendix B	Power available from flashing condensate	55
	Loss in performance from heat pump cycling with dilution required	56
Appendix C	Heat exchanger and general component design	57
Appendix D	Vacuum considerations	68
Appendix E	Absorption process with laminar liquid films.	70
Appendix F	Minimum energy change on mixing	72
	FIGURES	73
	PHOTOGRAPHS	90

FIGURES

	<u>Page</u>
Fig.1. p-T-x diagram for absorption cycle	73
2. A schematic diagram of an absorption cycle	73
3. p-T-x diagram for the NaOH/H ₂ O system	74
4. Theoretical performance for the NaOH/H ₂ O system	75
5. Solution heat exchanger capacity vs. absorber temperature range	76
6. Dependence of maximum COP on temperature lift	76
7. Corrosion chart for nickel with NaOH solutions - courtesy ICI Ltd	77
8. Corrosion chart for austenitic stainless steel with NaOH solutions - courtesy ICI Ltd	77
9. Crystallisation temperature - concentration chart for NaOH solutions	78
10. Crystallisation temperature - concentration chart for NaOH/KOH solutions	78
11. Effect of % KOH on crystallisation temperature	79
12. Effect of % KOH on total % salt necessary for a given temperature lift	79
13. p-T-x diagram for the NaOH/KOH/H ₂ O system with equal weight proportions of salt	80
14. Overall heat transfer coefficient for the condenser coil	81
15. Heat loss from generator and condenser	81
16. Generator/condenser heat ratio for different strengths of solution	82
17. Evaluation of concentration driving potential from p-T-x diagram	82
18. Mass transfer coefficient for different flow rates over the packed column	82
19. Power density against solution flow for the isothermal absorber	83

Fig. 20.	Overall heat transfer coefficient for the isothermal absorber	83
21.	Absorber/evaporator heat ratio for different strengths of solution	84
22.	Solution heat exchanger effectiveness	84
Drawing 1	Schematic diagram of experimental rig	85
Fig. 23.	Materials, heat exchanger areas, etc., of experimental rig.	86
A.1	p-T-x diagram for water/sulphuric acid solutions	87
C.1	Densities of NaOH and NaOH/KOH (1:1) solutions - courtesy ICI Ltd	88
C.2	Viscosities of NaOH and NaOH/KOH (1:1) solutions - courtesy ICI Ltd	88
C.3	Specific heats of NaOH solutions - courtesy ICI Ltd	89
C.4	Conductivity of NaOH solutions - courtesy ICI Ltd	89
photo.1	EXPERIMENTAL RIG	90
photo.2	ABSORBER COIL AND SINGLE HEAT EXCHANGER PLATE	91
photo.3	"SHIMMERING" ON ABSORBER COIL	92

NOTATION

A	area (m^2)	α	thermal diffusivity (m^2/s)
a	speed of sound (m/s)	Γ	wetting rate (kg/ms)
b	breadth (m)	δ	film thickness (m)
C	conductance (m^3/s)	Δ	change in quantity
c_p	specific heat (kJ/kgK)	ϵ	effectiveness % or emissivity
c_f	skin friction coefficient	λ	leak rate (mbar l/s)
D	diameter (m) or material diffusivity (m^2/s)	μ	dynamic viscosity (kg/ms) or chemical potential or micron ($10^{-6}m$)
f	circulation ratio	ρ	density (kg/m^3)
g	gravitational acceleration (m/s^2)	σ	evaporation coefficient or pumping factor or Stefan-Boltzmann constant
h	enthalpy or heat transfer coeff (kW/m^2K)	Gr	Grashof no
h_M	mass transfer coefficient	Le	Lewis no
k	thermal conductivity (W/mK)	Nu	Nusselt no
L	characteristic length (m)	Pe	Peclet no
M^1	relative molecular weight (gMol)	Pr	Prandtl no
m	mass flow (kg/s)	Re	Reynolds no
p	pressure (N/m^2)	Sh	Sherwood no
Q	heat input or output (W)		
q	volume flow (m^3/s)		
R	recirculation ratio		
R_o	universal gas constant		
S	pumping speed (m^3/s)		
T	absolute temperature (K) unless otherwise specified		
t	temperature ($^{\circ}C$)		
U	overall heat transfer coeff		
u	velocity (m/s)		
V	volume (m^3)		
v_g	specific volume (m^3/kg)		
W	wetting density (kg/m^2s)		
x	concentration %		

Suffixes

g)	vapour
r)	
f)	liquid
l)	
o	pure water
s	solution
m	mean
Δp_g	pressure drop from skin friction
Δp_d	pressure drop from one dynamic head

CHAPTER 1

NATURE OF THE ABSORPTION SYSTEM

The attraction of the absorption system lies in its ability to evaporate and condense a fluid at two different temperatures but at the same pressure, thus obviating the need for a vapour compressor. This is achieved by condensing the vapour into an 'absorbent' which must have the properties of a lower vapour pressure than the working fluid in addition to a high degree of mutual solubility. The vapour pressure - temperature relationship is shown in Fig.1 for various strengths of absorbent solutions: it may be seen that a stronger absorbent solution increases the temperature at which it exerts the same vapour pressure as the pure fluid.

The working fluid is evaporated at a low temperature accepting heat from an ambient source and it is then condensed into an absorbent solution at a higher useful temperature; as the absorbent solution is diluted the temperature lift is reduced until effective heat pumping no longer occurs. Since there is not an infinite supply of absorbent or working fluid, some means of concentration is necessary so that both fluids may be recycled for the process to continue. Normally concentration has been achieved by distilling the working fluid out of the absorbent solution and the energy required for this is delivered at a sufficiently high temperature so that the resulting condensation occurs at a similarly useful temperature as in the absorber.

The various temperatures for equilibrium conditions in the cycle are shown in Fig.1 and a schematic diagram of the main components of the system in Fig.2. A pump is necessary to deliver the solution to the generator at the pressures determined by the appropriate condensation temperatures; however the power requirements have a negligible effect on the performance of the system on account of the fluid being a liquid and virtually incompressible. A heat exchanger is employed between the strong and weak absorbent solutions flowing to and from the absorber to reduce the heat input to the generator by minimising the direct transport of heat. Although this component does not exchange heat with any source outside the system, its performance is one of the most influential factors in determining the overall performance of the system as will be discussed in more detail in Chapter 3. Reducing the capacity of this heat exchanger is attractive not only on account of its size and cost but also to lessen the overall performance's sensitivity to

ineffective heat exchange in this component. Consequently low solution flow rates between absorber and generator are particularly desirable and this is the main reason for selecting absorbents and working fluids which have a strong chemical affinity for one another.

For the absorption heat pumping process to work the mixing of absorbent and working fluid need only be a physical process involving an increase of entropy without any chemical affinity between the two fluids. The presence of the latter is reflected in a heat of solution on mixing, and the effect of this 'chemical bonding' between fluid molecules is to reduce the amount of absorbent necessary to produce a given temperature lift between absorber and evaporator: this results in lower solution flow rates between generator and absorber thereby reducing the capacity of the solution heat exchanger.

However, working fluid/absorbent combinations that exhibit this behaviour also have a disadvantage which offsets the benefits mentioned to a certain degree. This is illustrated by defining the coefficient of performance (COP) as the ratio of the heat delivered in the absorber and condenser to the heat input to the generator, (Fig.2). The quantities of heat exchanged in each component is largely the latent heat of vaporisation of the working fluid; the existence of a heat of solution between absorbent and working fluid increases the heat of vaporisation in the absorber and generator but not the condenser. Consequently the heat of solution put into the generator appears directly at the absorber and represents another direct transport of heat between these components.

Further details of the cycle will be discussed at a later stage with specific reference to the fluids used in this work; however, (Ref.1-5) give a more generalised treatment of the absorption system. In particular a report by Haseler (Ref.1) is recommended giving both an excellent theoretical explanation of the cycle, and also a thorough description of desirable properties for working fluids and absorbents. In addition the data provided on suitable working fluids is comprehensive and, surprisingly, few additions can be made five years on from its writing.

CHAPTER 2

SELECTION OF SUITABLE FLUIDS

The correct selection of a working fluid and absorbent is crucial to the success of an absorption heat pump for any given application. There is a considerable amount of literature on the subject which has mostly generated from the requirements of the refrigeration industry, (Ref.3-5); however, these cannot necessarily be applied to a heat pump system since there are certain operational aspects which make this a very different machine. The most important differences are that heat pumps, both for industrial and domestic applications, operate at different temperatures from refrigeration machines, in addition the temperature lifts between those components rejecting heat and those accepting heat are considerably higher. In the selection of a suitable working fluid and absorbent it is this temperature lift that is the first criterion to be satisfied. Consequently the relevant temperatures of operation will be discussed in some detail.

This work has been orientated to the heating requirements of domestic buildings in Great Britain, and in particular those buildings with existing gas fired systems for central heating and domestic hot water. There is an annual replacement of over 200,000 gas boilers in Britain (Ref.6) and if these could be substituted with gas fired heat pumps having a COP of about 1.5 there would be fuel savings of the order of one third.

Over two thirds of the domestic heating requirements are for central heating, Leach (Ref.7), with the majority of these systems employing hydronic distribution via radiators. Although the mean radiator temperature necessary for satisfactory heating is a subject of much debate, it is generally agreed that return water temperatures of 55 - 60°C are the minimum allowable during winter periods for existing systems (Ref.8). However, Wood (Ref.9), also identifies a sizeable market for new gas central heating systems in both existing and new homes. In both cases lower water temperatures may be acceptable either by employing larger heating surfaces, or, in the latter case, on account of higher insulation standards. However, domestic hot water requirements presently account for almost a third of the total, this fraction increasing in the better insulated houses. If existing capacities of storage tanks continue, then this water must be heated to temperatures of at least 55 - 60°C Leach (Ref.7).

Thus it is reasonable to specify that such a heat pump must be capable of delivering heat at a temperature of 60°C at least.

To establish the temperature lift required the source of low temperature must now be considered. Air is the most likely ambient heat source for the heat pump. There are problems such as noise from the fan and inherently poor heat transfer possibly aggravated by frost, but these problems are common in the development of vapour compression heat pumps.

Considerable work has been carried out studying ground source evaporators but their installation and cost combined with operational problems such as freezing of the ground, may make them less attractive, in spite of a higher and more uniform temperature of the ground than the air. Heating systems are normally designed for a "design day" of -1°C ambient air temperature and data show that temperatures below this occur for less than three percent of the heating season (October-May) (Ref.10). If the heat pump was unable to operate below this temperature some sort of direct heating would be necessary and this is very easily achieved within the system of an absorption heat pump and will be explained in a later chapter.

From the previous considerations it has been established that the heat pump must be capable of accepting heat at temperatures down to -1°C ambient air temperature and delivering heat at a minimum temperature of 60°C . If one takes an arbitrary temperature difference of 5°C across heat exchangers it is apparent that temperature lifts of greater than 70°C are required within the heat pump, and it is this criterion which must be met through the selection of working fluids.

One notable combination is the ammonia/water system which is indeed capable of providing these temperature lifts. However, because the absorbent, water, is to some extent volatile, it is not possible to evaporate pure ammonia vapour from the generator and 'rectification' of the vapour mixture is necessary resulting in a lower COP. Alefield (Ref.11), has suggested the addition of a salt such as lithium bromide, which reduces the rectification requirement considerably and this seems a course well worth pursuing despite reports of the solution being highly corrosive (Ref.12). Another problem of the ammonia/water system is the necessity for a high pressure solution pump which would have to work across pressures of 35 bar. Work in this area has been carried out by Fitt (Ref.13), which also includes novel designs for reducing the power requirement.

Much time has been spent trying to find suitable organic fluids, and several successful absorption refrigeration units were built in the 1930's (Ref.3). However, for heat pumping applications the higher generator temperatures encountered ($>150^{\circ}\text{C}$) can result in uncertainties regarding the stability of the absorbent and working fluid. In addition the use of working fluids with latent heats of vaporisation an order of magnitude less than inorganic fluids, can result in a low COP. This is on account of the high mass flow rates required both in the working fluid and the absorber requiring a very large solution heat exchanger: this problem may be avoided if solutions of sufficiently low heat capacity can be employed. Steimle (Ref.14), has identified several potential organic fluid combinations but there is as yet insufficient data on their high temperature stability.

A potentially promising combination was methanol with a mixture of lithium and zinc bromides as the absorbent, which was demonstrated of pumping from -10°C to 74°C , Shamarka (Ref.15). But the instability of this mixture at typical generator temperatures was revealed by Koebel (Ref.16), and confirmed in these laboratories (Ref.17).

Water remains as an attractive working fluid being completely innocuous, stable, cheap, and having the highest latent heat of vaporisation of any pure liquid. Despite there being two potentially good absorbents, viz. sulphuric acid and sodium hydroxide, both of which are capable of providing very high temperature lifts, there remains the problem of water freezing in the evaporator at temperatures below 0°C .

Although evaporation of water vapour from ice was considered, it appears inconceivable how ice may be formed internally while maintaining an acceptable rate of heat transfer. An alternative is to employ an antifreeze additive to the water: initial tests demonstrated that water could be successfully evaporated at temperatures down to -5°C , and as a result the automatic exclusion of water is unjustified.

The two absorbents for water already mentioned, sulphuric acid and sodium hydroxide, are both capable of providing a high temperature lift with a theoretically good performance, and App.A shows vapour pressure data of each absorbent with first order calculations of COP. The slightly higher performance (ca. 5%) of sulphuric acid over sodium hydroxide makes it the more attractive absorbent, coupled with the fact that the components are totally miscible over all the temperatures likely to be encountered. However, there is one important drawback common to both these absorbents, and that is their highly corrosive nature in aqueous solutions. Although there is considerable information on compatible materials in the

literature, it was not clear as to which of the absorbents was more favourable from a corrosion point of view.

There are very few materials which will resist corrosion by sulphuric acid over the full temperature and concentration range that would be encountered in an absorption heat pump. Discussions with ICI (Ref.18) indicated that fused silica enamel coating or tantalum plating are the most likely candidates: the latter is prohibitively expensive and enamel coatings are unattractive both from heat transfer considerations and the thermal shock which would be unavoidable in a gas fired generator. Sodium hydroxide solutions are considerably less aggressive and suitable materials for components are detailed in the following chapter.

Despite the previous work that has been undertaken on various chemical storage and heat pumping projects employing sulphuric acid and water (Ref.19 - 21), it is the problem of corrosion that precludes the use of this pair. Hence sodium hydroxide and water was selected as a potential working combination, which justified further investigation.

CHAPTER 3THE WATER-SODIUM HYDROXIDE SYSTEM

The major attributes of using sodium hydroxide/water for an absorption heat pump will be discussed first including predicted performance, before mentioning the problems associated with its use and explaining the methods of overcoming them.

The advantages of using water are obvious and have been stated in the previous chapter; however, further explanation is necessary to illustrate the benefits attributed to its high latent heat of vaporisation as compared with any other working fluid. The mass flow rates of working fluid and absorbent are both directly related to the latent heat of vaporisation since a condensation process in both the condenser and absorber is the method by which heat is delivered. Employing water as a working fluid reduces these flow rates considerably; for a 10 KW heat output, a water flow rate of around 0.1 l/min may be compared with about 2 l/min for a typical fluorocarbon working fluid. The major benefits are from a lower absorbent flow rate for this reduces the size of the solution heat exchanger. Other factors such as concentration change, specific heat of absorbent solution, fraction of absorbent in solution, etc., also determine the solution heat exchanger size but it will be seen that the latent heat has a major influence.

A comparison will be made with two other absorption systems which are also capable of providing the temperature lifts specified in the previous chapter. These are the ammonia/water system and the trifluoroethanol/n-methylpyrrolidine (TFE/NMP) system, the latter combination being one of the most promising candidates to emerge from an extensive search for suitable organic compounds by Steimle et al (Ref.14).

The relative mass flow rate between weak absorbent solution and working fluid is given by

$$f = \frac{x_s}{\Delta x}$$

from which the following factor may be defined

$$n_1 = \frac{(f-1)C_p \Delta T}{\Delta h_o}$$

This is a ratio of heat to be exchanged between weak and strong solution for a given heat input to the evaporator. Comparing systems for heat pumping applications one should strictly define ratios involving heat outputs from absorber and condenser but this becomes a lengthy calculation and is not possible for systems without extensive data.

In addition a comparison may be made between the minimum pumping energies needed for each system by defining the factor

$$n_p = \frac{f\Delta p}{\rho\Delta h_o}$$

The above factors are calculated for an evaporation temperature of 0 °C, a condenser and minimum absorber temperature of 50 °C and a generator temperature of 150 °C.

for NH₃- H₂O : f = 4.28 ; n₁ = 1.15 ; n_p = 6.56 x 10⁻³

for TFE-NMP : f = 3.04 ; n₁ = 0.86 ; n_p = 0.205x10⁻³ (Ref 22)

for H₂O-NaOH : f = 4.03 ; n₁ = 0.33 ; n_p = 0.019 x 10⁻³

Despite the higher heat capacity of the sodium hydroxide solutions as compared with the organic pair, the high latent heat of vaporisation of water results in by far the lowest requirement in terms of solution heat exchanger capacity. The pumping energies are also shown to be truly minimal on account of the system operating at a low pressure.

The use of a salt, sodium hydroxide, as an absorbent has the immediate advantage of eliminating the need for rectification in the generator thereby avoiding a potential source of loss in performance. Although not necessary for all liquid absorbents, the two other systems mentioned above require rectification as a result of a relatively high absorbent vapour pressure in the generator. Despite the potentially excellent performance of the NaOH/H₂O system as shown by the theoretical curves in Fig.4, strong absorbent salt solutions may have high viscosities (up to 0.02 kg/ms) which can hinder performance of components such as absorber and solution heat exchanger; this is to some extent counteracted by the high thermal conductivities of sodium hydroxide solutions (at least 10% greater than pure water).

The theoretical performance curves in Fig.4 have been evaluated from the NaOH/H₂O p-T-x chart in Fig.3, by the same method outlined in App.A. The results do not take into account temperature differences across heat exchangers, and equilibrium conditions are assumed in the

absorber and generator. However, the curves do serve the purpose of emphasising the importance of an effective solution heat exchanger. An ineffective heat exchanger is particularly detrimental to performance at low absorber temperature ranges where small concentration changes (<3%) result in high solution flow rates ($f > 20$).

The loss in performance for high absorber temperature ranges is due to the increasing heat of solution for the stronger solutions reflected by the steepening of the concentration lines on the p-T-x chart. Although these conditions allow a smaller solution heat exchanger to be employed, as shown in Fig.5, the need to achieve concentration changes >9% requires an exceptionally large absorber. In addition Fig.5 shows that the temperature lift between evaporator and absorber does not greatly affect the heat exchanger size and that for best performance, 80%-90% effective heat exchangers should be sized for a capacity between a half and a third of the total heat output of the system. However it may not be possible to attain the necessary concentration changes in the absorber for these conditions and this would result in larger flow rates with a greater demand for an effective heat exchanger.

One final point which may be derived from theoretical considerations is the relatively low degree of sensitivity of the systems performance to temperature lift as compared with a vapour compression heat pump; the variation of COP with temperature is shown in Fig.6.

As with all absorbent combinations the NaOH/H₂O system is not without problems, the important ones being;

1. The freezing of water in the evaporator at temperatures below 0°C.
2. Unfavourable heat transfer rates for the evaporation of water at low pressures.
3. Long term protection of components from the highly corrosive solutions.
4. Crystallisation problems of caustic solutions at low temperatures.

1.

As mentioned in the previous chapter, water vapour had been successfully evaporated from antifreeze solutions at temperatures of -5°C. Typical antifreeze components might

be calcium chloride or ethylene glycol, the former depressing the freezing point by 15°C for 18% weight content in the solution. A convenient choice would be to use sodium hydroxide itself since this would keep the number of substances in the system to a minimum and would not necessitate the fluid in the evaporator to be completely isolated; an 18% solution depresses the freezing point of water by as much as 27°C . A possible disadvantage of using the absorbent as an antifreeze additive is that it will lower the vapour pressure of the water thereby reducing the temperature lift available between absorber and evaporator. Inspection of the p-T-x chart in Fig.3 shows that a 12% solution, with a freezing point of -15°C , will reduce this temperature lift by less than 3°C .

Whatever antifreeze is used, two precautions must be taken; firstly the pure water vapour must not come into contact with any colder surface which is below 0°C thereby condensing as ice, and secondly provision must be made for introducing the water to the antifreeze without any freezing occurring. As will be explained in the next section, the evaporator design will very likely employ a falling film of water and antifreeze (ca 1mm thick), evaporating from surfaces which are either heated by a liquid or are in direct contact with air. Consequently all heating surfaces below 0°C will be covered by antifreeze solution ensuring no vapour contact. Although the vapour is likely to be colder than any heating surface and so without a temperature gradient to encourage condensation, it would be unwise to allow a situation commonly found in vapour compression units where a two phase flow of working fluid passes through tubes where both vapour and liquid are in contact with the heating surfaces.

If ice was to form inside the evaporator it is unlikely that it would be as serious as the normal external frosting problem that occurs at higher air temperatures. Since an air source heat pump would require provision for external defrosting, this could also serve for internal defrosting.

Such an evaporator could not be envisaged as a once through device, for there would be a need to re-circulate the antifreeze and mix it with the incoming condensate. Rather than employ a pump for this process, the energy from the flash evaporation of the hot condensate could be utilised to drive a simple vapour lift pump. App.B shows calculations evaluating the maximum available energy from the flashing of condensate, which should be more than adequate for the purpose.

It might be argued that the fresh water should be mixed with the antifreeze in the condenser thereby avoiding pure

condensate flashing to evaporator pressures and temperatures with the possibility of ice forming. However the mechanism of flashing is a sufficiently inefficient process in reducing the temperature of the liquid condensate (and this has been verified from experiments) that the condensate enters the evaporator in a superheated state above 0°C. The water might then be mixed with the antifreeze without the latter having to be pumped up to condenser pressure. If a vapour lift pump was employed such mixing would occur within the pump.

2.

The development of a low temperature evaporator using water as a working fluid poses a second important problem, a low rate of heat transfer through the liquid to its surface and an unknown liquid-vapour interfacial temperature drop.

The vapour-liquid interface to wall temperature difference has been investigated by Raben et al. (Ref.23) in their experimental study of nucleate pool boiling, at various pressures in the range of 13 - 1000 mbar. The results show temperature gradients which are almost an order of magnitude larger at a pressure of 13 mbar as compared with atmospheric. The heat transfer coefficients at this low pressure, for non-nucleate boiling are approximately 200W/m²K for a wall superheat of 3 to 10°C.

This low rate of heat transfer at low pressures may be attributed to the diminishing contribution of convective heat transport and the disappearance of nucleate boiling in liquid pools. As a result absorption chillers normally employ spray or falling film evaporators. In the latter case the heat is transferred by conduction through a thin water film and the heat transfer can accurately be predicted by using the Nusselt equation, (Ref.24). However, the temperature drop owing to interfacial resistance still cannot be predicted with certainty. The magnitude of this temperature drop may be estimated from Kinetic theory by the equation;

$$\frac{\dot{m}}{A} = \left(\frac{M}{2\pi R} \right)^{\frac{1}{2}} \sigma \left(\Gamma \frac{P_v}{T_v}^{\frac{1}{2}} - \frac{P_f}{T_f}^{\frac{1}{2}} \right)$$

This shows that for a given fluid and evaporating mass flux \dot{m}/A the interfacial temperature drop, $T_v - T_f$ increases with decreasing values of system pressure, P_v and evaporation coefficient σ . For a mass flux of 0.01 kg/m²s (25 kW/m²) Sukhatme et al. (Ref.25), used this formula to calculate the interfacial temperature drop for water at decreasing pressures. For an evaporation coefficient of 1.0, values of 0.0015 °C at 1000 mbar, and 0.06°C at 13 mbar were calculated.

However, the correct value of σ to employ is a matter of debate, and is the largest source of uncertainty in the estimation of the interfacial temperature drop. For the generally accepted value of $\sigma = 0.04$ for water, (Ref.26), the above calculated temperature drops would be 0.063°C and 3°C respectively for a heat flux of 25 kW/m^2 . Although Gallagher-Daggitt et al. (Ref.19), reported a value of σ as low as 0.005 at 13mbar and applied it with apparent success to their falling film evaporator, this should not be regarded as being conclusive.

An estimate of interfacial temperature drop on one commercial absorption chiller which employs water in a falling film evaporator, suggests that the value of σ lies between 0.014 to 0.03 depending on the assumed value of saturation vapour pressure inside the evaporator. Even at the lower value of 0.014 the overall heat transfer coefficient of the evaporator would be the order of $1.3 \text{ kW/m}^2 \text{ K}$. However, the value of σ at lower pressures corresponding to the evaporation of water at sub-zero temperatures requires confirmation for this type of evaporator.

3.

The corrosive nature of aqueous sodium hydroxide solutions is a particular problem that arises in the development of an absorption heat pump employing such solutions. Although there is a considerable choice of materials available for use in an experimental apparatus for short term exposure only, this is not the case when designing commercial units for a typical life of ten years continuous use.

Apart from silver and gold, both too expensive, the most resistant material to hot caustic solutions is nickel. Fig.7 shows corrosion rates for various strengths and temperatures of solutions and it can be seen that only above 120°C for 75% solutions, does the corrosion rate exceed 0.025 mm per year. However rather than use sheet nickel or nickel clad steel in the construction of components such as the generator and solution heat exchanger, a very much more attractive method is to employ "electroless" nickel plated components. This is a chemically deposited nickel alloy (92% Nickel 8% Phosphorus) which has extraordinarily low corrosion rates,

viz. 73% NaOH at 132°C $0.025 \mu/\text{year}$ deaerated
 $2.3 \mu/\text{year}$ aerated (Ref.27)

This is not only more economically attractive than sheet

nickel (see Table 1), but also has considerable appeal from a manufacturing point of view. A component such as a solution heat exchanger may be constructed from a material of favourable thermal conductivity i.e. copper, and then totally immersed in the nickel solution. Unlike electrolytic methods of plating there are no problems with 'throwing' the electrolyte over convulated components, since the nickel is deposited out of solution uniformly over the whole surface. An additional advantage of electroless nickel plating is that it produces a very hard coating (>500 VPN), so thin coatings would not be susceptible to damage.

Detailed information on such plating techniques is given in Gawrilov (Ref.28), describing the various solutions employed, methods of plating, and specifying important design criteria. One particular property which can limit the thickness of coating in a component is the ratio of surface area to be plated, to volume of solution retained and in a solution 'plate' heat exchanger this may be as high as $1 \text{ m}^2 / \text{l}$, However, discussions with Poeton Ltd. (Ref.29), indicate that this may be avoided if the plating solution is circulated through the component.

A possible alternative to nickel is to employ 'Ni-resist' cast irons (B.S.3468:1974) containing 20-30% Ni. These have excellent corrosion resistance to strong hot sodium hydroxide solutions and in particular the NiCr 30.3 grade would have maximum resistance to attack with corrosion rates of the order of 0.05 - 0.125 mm/year for 80% solutions at 180°C (Ref.30). Table 1 shows that this material is attractive from an economical point of view and its use would be particularly applicable to the generator where the cast iron also has excellent resistance to hot gas side corrosion, as this material is conventionally employed in domestic gas fired boilers.

There are two factors which can prevent the use of cast irons and these should be mentioned although they are unlikely to be of importance in this instance. Firstly iron can pass into solution and reduce the purity to an unacceptable level; secondly stress corrosion cracking can be a source of failure in components which are highly stressed.

Mild steels and ferritic stainless steels would not be suitable in any of the absorber, solution heat exchanger or generator components, having inadequate corrosion resistance. Austenitic stainless steels might be marginally acceptable in the absorber from inspection of the corrosion rates shown in Fig.8.

Copper and copper alloys have surprisingly good resistance to dilute sodium hydroxide solutions, particularly if oxygen is absent. Although not suitable for any of the

	price	rate μ /year	required thickness for 10 year life	$\text{£}/\text{m}^2$
<u>Ni 200</u>	£8/kg [Jan 84]	125-25	1.5 mm sheet	136
<u>electroless Ni</u>	5p/thou/in ² [Jan 84] (0.051 p/ μ /cm ²)	2.3-0.25	23 μ (< 1 thou)	117-11
<u>Ni resist iron</u>	30% Ni £1.39/kg [Jun 83]	125-50	1.25-0.5 mm	12.6-5.0 * 30
	20% Ni £1.06/kg [Jun 83]	250-200	2.5-2.0 mm	19.2-15.4 * 23

* for a minimum casting thickness of 3 mm.

Table 1: Costs of suitable materials

	t_s	<u>NaOH</u> kg H ₂ O/kg strng. soln.	<u>NaOH/KOH 1:1</u> kg H ₂ O/kg strng. Soln.
$T_4=70^\circ\text{C}$	0°C	1	0.16
	20°C	0.15	no dilution
$T_4=100^\circ\text{C}$	0°C	1.23	0.44
	20°C	0.29	0.17

Table 2: Dilution requirements

strong solution components, it would be particularly applicable to the evaporator where dilute sodium hydroxide solutions might be employed as an antifreeze. The addition of nickel as an alloying agent will further improve resistance.

What has not been mentioned is the nature of the corrosion and its products. Unfortunately there is little information on this aspect of the subject and its relevance warrants further research. Firstly the corrosion rates given have been largely for aerated solutions and the effect of air on this might or might not be detrimental. For instance the presence of oxygen might enhance the formation of a protective oxide, or it might be the cause of a corrosive chemical reaction. Secondly the nature of the corrosion might be in the form of pitting and if the corrosion rates have been evaluated by a weight loss method then this underestimates the actual thickness required. Finally, and possibly the most important factor, is whether any gaseous products result from the corrosion reaction. Any non-condensable gas in an absorption heat pump would considerably reduce its performance and possibly lead to an inoperative machine, particularly if the heat pump is operating at subatmospheric pressures; in such a case the partial pressure of the non condensable gas may be of a similar order of magnitude to the vapour pressures of the liquids. An exception to this is when hydrogen is a corrosion product; by employing a heated palladium cell in the machine, hydrogen is allowed to diffuse out of the system although preventing any ingress of atmospheric gases such as N_2 , O_2 . Such cells are commonly employed in $H_2O/LiBr$ chillers where hydrogen is a product from the corrosive aqueous lithium bromide solutions.

Despite these unknown factors an approximate cost comparison can be made between some of the aforementioned materials and this is shown in Table 1. The prices are of course dependant on quantity of product and in particular this has been most difficult to determine for the cost of electroless nickel plating where manufacturers are unaccustomed to large quantities of a single product (>100,000per year).

4.

Another major problem with the use of sodium hydroxide solutions as an absorbent is that they have an inconveniently high crystallisation temperature. Inspection of the p-T-x chart in Fig.3 shows that for the necessary absorber temperatures, solutions of 60-65% must be used and while remaining liquid during the running of the heat pump, on cooling, these solutions crystallise at

temperatures between 60°C and 50°C. This is shown on the p-T-x diagram by the crystallisation boundary, below which salt hydrates are formed. A clearer indication of the proximity of crystallisation temperature to operating temperature is shown in the 'equilibrium' phase diagram for sodium hydroxide/ water in Fig.9.

For the solution concerned the monohydrate is formed on cooling, containing 69% NaOH. The quantity of hydrate formed in solution will depend on the initial concentration and temperature, but even the more dilute absorbent solutions of 60% will contain about 50% monohydrate at 10°C and this would certainly be unacceptable in the heat pump where partial, if not complete, blockage of equipment would be encountered.

The obvious method to avoid this, on complete shutdown of the apparatus, is to dilute the solutions with sufficient water till the crystallisation temperature has been lowered to an acceptable level. Water might be bypassed from the evaporator or condenser to the absorber where the diluted solution might then be pumped to the generator to mix with the remaining strong solution. Alternatively all the strong solution may first be transferred from the generator to the absorber before mixing. It would seem preferable to use water from the condenser for dilution as this would make use of the available pressure difference for pumping. However, the use of cold evaporator water should not be ruled out on account of it encouraging freezing of the strong solution, for the 'heat of solution' evolved on mixing would counteract this. On start up the dilute solution would be strengthened by boiling off the water in the generator during which period the absorber would not be delivering heat although the condenser would.

Great difficulty was encountered in the experimental work when running the experimental rig with temperature lifts between evaporator and absorber of over 50°C. This was due to the fact that solution concentration gradients were necessary in the absorber for mass transfer and therefore stronger solutions than those predicted by the p-T-x chart had to be employed. The net effect was to bring the crystallisation temperature of the absorbent solutions unacceptably close to the absorber operating temperatures. Although the concentration gradients could have been reduced with further experiments to optimize the absorber design, it was considered that investigations should be undertaken to find an additive to the sodium hydroxide to reduce the crystallisation temperatures.

Various substances were investigated (Ref.31), but the only significant improvement was achieved by the addition of potassium hydroxide. Potassium hydroxide alone is no better than lithium bromide as a suitable absorbent for

water suffering from too high a crystallisation temperature preventing adequate temperature lifts. However, the salt combination of NaOH and KOH results in a remarkable improvement of crystallisation temperatures whilst still providing solutions capable of high temperature lifts between evaporator and absorber. The reduction in crystallisation temperature depends on the amount of KOH added and the results of three salt mixtures are given in Fig.10 and Fig.11. Comparison is also made between solutions having equilibrium temperature differences of 100°C since such solutions may have to be employed while producing lower lifts of 70°C , on account of concentration gradients in the absorber. A disadvantage of using such salt mixtures is that a larger percentage of salt by weight is needed to produce a given temperature lift as shown in Fig.12, and hence a larger solution heat exchanger is likely. The problems encountered with crystallisation were sufficiently great to warrant the use of such a salt mixture and a NaOH:KOH weight ratio of 1:1 was selected as the most promising. The results of the vapour pressure measurement tests were used to plot a p-T-x chart shown in Fig.13.

Despite the significant improvement of the salt mixture as compared with pure NaOH, dilution of absorbent solutions is still necessary on shutdown of the apparatus. The amount of water that must be added to prevent crystallisation depends on the temperature to which the system will fall. Table 2 gives some typical requirements and shows the marked reduction by the addition of KOH.

Unfortunately any dilution necessary will result in a lower performance of the heat pump because when the solution is being reconcentrated only the condenser is delivering heat. The deterioration in performance is largely dependant on the frequency to which the heat pump cycles; if the system is shut down for periods longer than a day then the performance loss will be small, but if the heat pump is cycling, say every half hour, this could be more serious.

Appendix B gives an estimation of the reduction of performance for a generalised case, comparing a system with no dilution and a system with dilution. For a heat pump cycling more frequently than every hour it is unlikely that the system temperature will drop below 20°C , though of course this depends on the time constant of the machine determined by the thermal capacity, insulation etc,. If we take solutions with equilibrium temperature lifts of $0-100^{\circ}\text{C}$, then a dilution requirement of 0.17 kg water/kg strong solution is necessary; one result gives a reduction in heat output of about 5%.

Despite this loss in performance, it is not necessary that the system delivers a reduced amount of heat during the

reconcentrating period. Both the generator and condenser could be increased in size such that the condenser delivers the full heat output albeit at a reduced efficiency. As the generator may well already be sized for a larger output, to give direct heating on exceptionally cold days by transferring heat directly from generator to absorber where it may be delivered to the cooling water, all that would be required is to increase the capacity of the condenser; this would necessitate a larger area by at least doubling the capacity of the condenser.

The previous sections have highlighted the important problems concerned with operating a heat pump employing water and caustic salts as the working substances, and in addition methods of overcoming these problems in a commercial system have been outlined. What first had to be practically demonstrated however is that such solutions were indeed capable of sufficiently high temperature lifts in a heat pump and that such a system could work with an adequate degree of performance.

CHAPTER 4

EXPERIMENTAL RIG : CONSTRUCTION AND OPERATION

An experimental heat pump rig was designed and constructed for the purposes of testing a variety of working fluids and absorbents that might have been chosen. Although initially sized for use with methanol and LiBr/ZnBr_2 , it was very easily modified for the $\text{NaOH/H}_2\text{O}$ system. The system was designed to deliver a heat output of around 3kW, as this seemed a suitable value from which a larger unit might be developed; avoiding the significant stray losses of a smaller system and yet not too ambitious an undertaking for a development sized unit.

Drawing 1 and Fig.23 show the detailed layout of the rig showing materials used, surface areas of heat exchangers and instrumentation. The detailed design of heat exchangers, pipe diameters, etc., is shown in App.C, and also the relevant properties of sodium hydroxide solutions are given. The later use of NaOH/KOH salt mixtures as an absorbent did not affect the solution properties sufficiently to warrant redesigning components; viscosities and densities were evaluated for these solutions and are also shown in the appendix.

Employing glass vessels for the major components was a great benefit in that one was able to see the behaviour of fluids in the system, such as wetting of absorber surfaces, nature of boiling in generator and evaporator, etc,. Even when the rig was fully insulated provision was made for 'windows' so that observations could be made.

Another feature of the rig was that it could easily be dismantled for alterations. This was useful for cleaning the system before adding fresh inventories and in particular for changes to the absorber design. However, the presence of many removable joints and gaskets meant that it was extremely difficult to provide a vacuum tight system for effective operation. As already mentioned the presence of any non condensible gas in an absorption heat pump operating at subatmospheric pressures will degrade the performance considerably as the vapour has an additional resistance at the condenser and absorber surfaces through which it has to diffuse.

Continuous evacuation was necessary although leaks were reduced to a value below 10^3 mbarl/s. This was achieved by 'balancing' the leak rate with an equivalent evacuation rate by means of a needle valve in series with a vacuum pump. The system was initially evacuated to the vapour

pressure of the working fluid through a diaphragm valve which was subsequently closed (see Drawing 1). The needle valve was then adjusted until there was no further pressure rise in the vessel.

On account of the rig having to operate at two different pressures, a balancing valve was necessary for both absorber/evaporator and generator/condenser, each being connected in parallel to one vacuum pump. These valves were placed at the top of the absorber and condenser since both components are at a lower pressure than evaporator and generator respectively. Any non condensible would accumulate on the surfaces of these components since their direction of flow would be the same as that of the water vapour.

By using this technique the quantity of vapour passing out of the system was reduced to a minimum; however, some loss was inevitable and this was measured by means of a liquid nitrogen trap placed upstream of the vacuum pump. Experimental tests showed that less than 1% of the vapour being generated at maximum power output was transferred out of the system. App.D gives details of the pump down times, acceptable leak rates, and other vacuum related problems associated with the rig.

Operation

To operate the rig the following procedure was adopted:

The system was evacuated to < 0.1 mbar having assured a maximum permissible leak rate of 10^{-3} mbarl/s. The evaporator was charged with 2-3l. of distilled, deaerated water sufficient to immerse the electric heating element. An inventory of 3-4 litres of absorbent solution was charged to the generator, at a strength that avoided crystallisation at room temperature. The pressures in the absorber/evaporator and generator/condenser were the vapour pressures of the two liquids at room temperature, typically 14 mbar and 0.5 mbar respectively.

The generator heater was then switched on, controlling the power by the variac. This was kept below 400W initially to avoid excessive thermal gradients in the solution arising from the high heat fluxes (40 kW/m^2). Otherwise violent kettling noises were produced from the cavitation of vapour bubbles leading to possible damage of the immersion heater.

After 10-20 min the solution attained a sufficiently high vapour pressure to generate water condensate in the adjacent condenser vessel. With no cooling water flowing through the condenser coil, the pressure and temperature in the generator and condenser continued to rise. At the

lower pressures the vapour bubbles in the generator were of the order of several centimetres in diameter and the nucleate boiling was quite violent, however, at condenser temperatures above 30°C (42 mbar) the bubbles were less than 1cm dia. and the liquid surface in the generator was considerably less disturbed, The power to the heater could now be increased up to values of 1.5 kW without excessive cavitation or bubbling.

When a suitable pressure and temperature was attained in the condenser, the water was turned on to a flowrate such that a steady pressure was maintained. Condensate was fed to a separate receiver to avoid collecting in the condenser vessel next to the generator, otherwise there would be an unnecessary reflux of condensate from the generator separating plate resulting in direct heat transfer from heater to cooling coil. App.C shows that any radiant or convective losses between generator and condenser are minimal and are a source of negligible direct heat transfer.

To prevent any solution being carried over with the vapour from generator to condenser, a metal cap was placed over the connecting orifice to offer a more tortuous path for the vapour. This proved to be adequate with the condensate having a pH value of 7-8; if however, the cooling flow rate was increased suddenly at low pressures it was possible for the solution to surge violently and pass through to the condenser.

The pressure drop between the generator and condenser was measured by means of a water manometer connected to the two vessels with small bore capillary tubes. Even at high generator powers (1.5 kW +) the pressure drop was less than 1.5 mbar, which is less than 1% of the total pressure. Since the generator solution was well mixed from the nucleate pool boiling, there were no large temperature gradients in the liquid and its temperature was the same as the vapour temperature to within 1-2 °C. Consequently the strength of the solution could be deduced from the p-T-x chart knowing the generator and condenser temperature. Tests on samples taken from the generator confirmed these concentrations to within 1% by weight, which was sufficiently accurate for the absorber analysis to be carried out.

Having obtained a suitable strength of solution in the generator, valve 22 in Drawing 1 was opened to allow solution to be fed to the absorber. With the packed column absorber, sufficient solution was collected at the bottom of the column before turning on the solution pump and circulating liquid through the absorber heat exchanger. The 3-way valve was adjusted to keep the liquid level in the absorber constant for a given absorber recirculating flow, thus ensuring that the return flow of

absorbent to the generator was balanced with the generator-absorber flow.

When the solution in the absorber was at a sufficiently low temperature below its equilibrium temperature at the corresponding pressure, water commenced to evaporate in the evaporator, cooling this vessel at a rate determined by the conditions in the absorber. When an appropriate temperature in the evaporator was attained the power to the immersion heater was turned on and controlled by the variac to maintain an approximately constant temperature. Despite the violent 'explosions' of water generated from the high heat fluxes and large specific volumes of water vapour, there was no danger of damage to heater or vessel on account of the low energy and dynamic head in the vapour. This is also the reason why no water was carried through the pipe to the absorber.

Having established the operation of the system, control had to be implemented to maintain a reasonable degree of steady state performance. This was achieved by manual operation of the flow rate valves and variacs. The low thermal capacity of the condenser compared to the generator (see figure 23) meant that the pressure in these components was more quickly controlled by the condenser cooling water flow than the electrical heater power. In the absorber however, the thermal response of the system was more complicated and is discussed later.

If it was necessary to change the concentration^{of} solution in the generator without altering the pressure there, then the generator power and condenser cooling water flow had to be changed simultaneously. Typically an increase of 5% by weight in the concentration of the solution would take 15 minutes for a generator power of 1kW, neglecting heat losses from the generator and condenser.

Initial running of the rig showed that the generator and condenser worked extremely well; the absorber was identified as the component needing further development and requiring investigation on the heat and mass transfer characteristics. Since much of the work was centred on this component it will be discussed separately in the following chapter.

The performance of the heat pump could not be calculated with sufficient accuracy from a total heat balance, on account of the large inventory of solution in the generator. For instance, if equilibrium conditions gave heat outputs from absorber and condenser of 600W. and 400W. respectively with a generator input of 700W, then a COP of 1.43 would be realised. If the condenser was delivering 500W., giving a 10% error in COP, this would be an excessive flow of water of 0.04g/s.; evidence of this would only be apparent from a rise in generator

temperature of as little as 1°C every ten minutes. Although the heat pump could be operated continuously for several hours control could not be maintained within such limits.

To evaluate the performance it was necessary to study the behaviour of the generator and condenser separately from the absorber and evaporator. When running the latter components the whole unit would be operating with sufficiently constant conditions to give results on the performance of the solution heat exchanger.

The Generator and Condenser

As there was negligible pressure drop between these components enabling the vapour temperatures to be used as an adequate method of determining the concentration, it remained to evaluate the heat transfer coefficient in the condenser and verify the heat of vaporisation of solutions by comparison with the p-T-x chart. The performance of the generator was not being studied on account of the unrealistic design compared to that of a gas fired unit. Although heat and mass transfer coefficients were not evaluated, a maximum heat flux of 200 kW/m^2 was possible in the generator above pressures of 50 mbar without the onset of 'burnout'; the critical heat flux was not evaluated.

A range of heat transfer coefficients evaluated from the log mean temperature difference of cooling water and vapour temperature in the condenser, are shown in Fig.14. At all values of condenser heat outputs, the approach temperature difference between the vapour and cooling water outlet was less than 1°C , on account of the very low cooling water flowrates. In a development unit the flow rates would be considerably higher with lower temperature differences across the heat exchanger.

Since the approach temperatures were so small (often reading zero since the thermocouples were only accurate to within 0.5°C), two approach temperatures were used in the calculation giving an optimistic and pessimistic value. Also two areas of condenser surface were taken as the condenser coil was closely wound making some of the external tube surface possibly redundant.

The results show a steady increase in heat transfer coefficient with condenser heat output as compared to a virtually constant theoretical value. As expected App.C shows the major resistance to heat transfer to be on the internal cooling water side and this is even greater when

laminar flow exists, as was the case for all experiments undertaken. The discrepancy of the results in Fig.14 may be due to the inability to predict accurately this internal coefficient, being a function of position in the coil (see App.C). A small contribution to the higher heat transfer at higher flow rates is the longer length of tube over which the flow has not yet become fully developed. There may also be an underwetting of the coil externally, at low powers where there is a considerable variation in temperature over the condenser surface. Higher water flow rates reduce the temperature change in the cooling water resulting in more uniform condensation.

It was next necessary to evaluate the heat of vaporisation of the generator solution since the magnitude of these values greatly affect the performance of the heat pump as explained in the introduction. The generator and condenser heat loss to ambient at typical operating conditions first had to be found. Although the vessels were covered with 40-80mm of glass fibre insulation, further insulation could have been provided to the generator. However the heat loss could easily be measured by finding the power necessary to keep the condenser and generator at specific temperatures: by measuring the condensate collected over a certain period of time, the generator and condenser losses could be separated. All experiments were undertaken with an initial inventory of solution in the generator which was subsequently concentrated as water was distilled to the condenser: there was no flow of solution through the solution heat exchanger. Admittedly the concentration of solution in the generator would change over this period increasing the temperature and so making the heat loss vary with time, but the quantities of water generated to supply the condenser heat loss are negligible.

The results for the heat loss from the generator and condenser are given in in Fig.15. For condenser temperatures between 50°C and 90°C the heat loss from this component is less than 20% of the total heat loss for generator temperatures greater than 130°C. This total heat loss could sometimes amount to as much as 50% of the total heat input to the generator which emphasises the importance of its evaluation. Experiments were performed over a range of water flow rates to evaluate the generator heat input to condenser output ratios, Q_g/Q_c . Evidence of minimal direct heat transfer between generator and condenser was given by comparing the condensate, collected over a period of time, with the heat output from the condenser coil. By including the sensible heat in cooling the vapour from generator to condenser temperature (about 10% of the total heat output) the former quantity was always within 5% of the coil output to the cooling water.

The ratio Q_g/Q_c may be used as an indication of the latent

heat of vaporisation of the solution having allowed for the heat loss Q_1 (found from Fig.15), and for the sensible heat in the vapour contributing to Q_c . During experiments steady state conditions were maintained for at least 20-30 min. before taking results; since the generator temperature would increase over this time the experimental results in Fig.16 are shown with horizontal bars. In addition vertical bars are shown for the heat loss Q_1 being $\pm 50W$ from the value deduced from the curve in Fig.15. This allows for an error of at least 15% in estimating the latter which can be seen to have a significant effect on the ratio Q_g/Q_c at low generator powers.

For comparison, the heat ratio Q_g/Q_c has been calculated from the p-T-x diagram in Fig.13, using the Clausius-Clapeyron equation as outlined in App.A. It is particularly interesting to note that the experimental results give heat ratios well below those evaluated from the p-T-x chart, even allowing for errors in the heat loss from generator and condenser. A possible explanation is that the p-T-x diagram is in error. However this would have required an error of at least 100% in the pressure readings (at pressures <20 mbar) which is unlikely. There are no other reasons that can be put forward for this behaviour. Despite this discrepancy though, the effect of the heat ratio Q_g/Q_c and the corresponding heat of vaporisation of solutions is not as significant as other factors in the evaluation of the COP. This is shown later in Table 3 on page 38 where two extreme experimental values of Q_g/Q_c are taken.

CHAPTER 5DESIGN AND PERFORMANCE OF THE ABSORBER

A major part of the experimental work was undertaken to investigate various absorber designs with a view to maximising the heat and mass transfer coefficients. This is important since it is undesirable to have large driving potentials across the absorber surfaces; for the heat transfer coefficient this is realised by large temperature differences between cooling water and absorbent solution thereby reducing the effective temperature lift over which heat is being pumped. A large driving potential for mass transfer is brought about by having solutions of a bulk concentration considerably stronger than those given by the equilibrium temperature and pressure in the absorber, the use of such overstrong solutions decreases the performance of the heat pump and increases the problems associated with crystallisation.

In a low pressure absorption system that uses water as a working fluid, it is imperative that the pressure drop between evaporator and absorber is kept to a minimum since at evaporation temperatures of -10°C the pressure in the evaporator is only 2.5 mbar. This precludes the use of bubble absorbers where vapour is bubbled through the absorbent solution until fully absorbed; 2.5 mbar corresponds to a head of solution less than 2cm in depth and the high specific volume of the vapour would require enormous bubbles.

The absorber has to take the form of a liquid in vapour system with the vapour occupying the larger volume. This typically requires the absorbent to be dispersed as a film over a solid surface with vapour coming into contact at the free surface of the liquid. The film might be simultaneously cooled as vapour condenses into the absorbent solution as is the case with vertical wetted wall absorbers, or it may be circulated through a separate heat exchanger as in the case of a packed column absorber. Both arrangements allow for recirculation of solution at a rate different to that of the absorber/generator flow.

The heat and mass transfer coefficients are fundamentally controlled by the hydrodynamic conditions existing in the absorber: the respective dimensionless groups, the Nusselt number and Sherwood number, may be related to the film Reynolds number by an assortment of theoretically and empirically derived relationships. The most significant factor affecting the nature of the film flow is whether it is in a laminar or turbulent condition. This is

determined from the value of the film Reynolds number defined as,

$$Re = \frac{4\Gamma}{\mu}$$

Γ is the mass flow rate of solution per unit breadth of film expressed in kg/sm, and it is an important parameter in the design of an absorber. For turbulence to occur $Re > 1600$, with a solution having a viscosity of 0.02 kg/ms a wetting rate of 8 kg/sm is required: the solution pump has a maximum delivery of about 30 g/s, which would require a film breadth of 2.5mm if turbulence was to be achieved. A reduced viscosity would not have alleviated the situation and it was apparent that all forms of absorbers studied would be operating in the laminar regime. Indeed the benefits to be accrued from a turbulent film flow remain uncertain and they would have to improve the heat and/or mass transfer coefficients considerably to warrant the very high pumping rates required.

Having established the nature of the flow the characteristics of the absorption process may be qualitatively analysed with the help of theoretical and experimental data. Many studies of absorption problems have considered the heat and mass transfer separately neglecting the coupling between these processes. This is acceptable where the heat released on absorption is small; however in absorption heat pumps the mass transfer in the absorber is initiated specifically to produce a temperature change. One of the more recent and very relevant studies specifically orientated to this problem is a report by Grossman (Ref.32), where the simultaneous heat and mass transfer is analysed for the absorption of vapour into a laminar liquid film.

The most significant result is the tendency for Nu and Sh to fall to a constant value when the respective thermal and concentration boundary layers have become fully developed. The distance to achieve this fully developed condition depends in particular on the wetting rate Γ and App.E evaluates a variety of conditions. Having attained a developed boundary layer, the constancy of Nu and Sh indicates that lower wetting rates are desirable since the heat and mass transfer coefficients are inversely proportional to film thickness, this being a function of wetting rate ($\delta \propto \Gamma^{0.33}$). However, the results of App.E show that even for extremely low wetting rates (1 g/sm) the concentration boundary layer has not yet become fully developed after at least 0.5m. It is evident that the condition of the film in a packed column or falling^{film} absorber is going to be a transient one with a rapidly changing thermal and concentration profile across the thickness of the film.

The theoretical results of Grossman indicate that in this transient region the heat and mass transfer coefficients depend in the following way, for both an adiabatic and isothermal absorption process;

$$h \propto \Gamma^{0.02}$$

$$h_M \propto \Gamma^{0.27}$$

From these relations, it appears favourable to increase the wetting rate although its effect is a weak one, particularly for the heat transfer coefficient.

Quantitative analysis is not possible for two reasons: firstly to evaluate the mass transfer coefficient it is necessary to have a reasonably accurate value of the diffusivity of the solutions employed, which could only be obtained from additional experimental work. Secondly, and more importantly, the use of this and other data on the properties of the absorbent solutions is of limited value since the majority of absorber designs will consist of a number of solid elements over which the film will fall (e.g. a piece of packing or a tube). Between each element there will be a degree of bulk mixing of the fluid which improves absorption considerably: however, the lack of data on this 'mixing' makes the mass transfer coefficient almost impossible to predict.

With the previous points in mind, several types of absorber were constructed and studied. Initially a packed column absorber was employed using the solution pump also to circulate solution through a separate absorber heat exchanger. The potential advantages in such an absorber were in the ability of the column to provide a very high surface area per volume for solution to pass over, giving maximum opportunity for a large liquid/vapour interface. The less stringent requirements on the heat transfer (see App.E) were catered for with a compact plate heat exchanger, similar to that used for the solution heat exchanger.

The packed column was designed for an acceptably low pressure drop (<0.2 mbar) and the details are outlined in App.C. With a maximum dry surface area of 2.5m², good liquid distribution is imperative in order to wet as much of the packing as is possible. A rose was used to give a liquid spray providing one liquid stream for every 10cm²- 20cm², two to three times the recommended distribution (App.C).

The purpose of the experiments was to evaluate the mass transfer coefficient, h_M , in the packed column since it was this that limited the power output of the absorber and not the absorber heat exchanger. Although normally expressed in units of m/s, it is thought that the units of kW/m² solution defined in Fig.18 on page 82 are more

convenient for design purposes. The evaluation of this coefficient involves a number of estimations each of which can be a possible source of error.

The power output of the absorber is evaluated from the heat delivered to the absorber heat exchanger water, since the specific heat and flow rate are more accurately known than that of the absorbent solution. This does assume, however, that the total heat of the circulating solution is transferred to the cooling water, without any being lost through the pipes, flow meter and heat exchanger. Despite these components being well insulated, it is necessary to bear in mind that the absorber power output is a slight underestimation.

The second quantity to evaluate in the determination of the mass transfer coefficient is the surface area over which absorption is taking place. This is particularly difficult in the case of a packed column since the distribution of the liquid over the packing is not exactly known. Two distinctions may be made between the active surface and wetted surface; the former is that surface covered by a flowing film of solution including the augmentation by ripples on the vapour/liquid interface. The wetted surface, on the other hand, includes surfaces covered by stationary layers of solution which contribute little to absorption; such stagnant zones are typically formed at points of contact between packing. Ramm, (Ref.33), summarises the results of various authors who have estimated these areas as a function of wetting density, W , (solution flow rate per unit cross sectional area of packed column): for the highest values of wetting density employed in experiments, $13 \text{ kg/m}^2 \text{ hr}$, the minimum estimated active wetted area is as little as 8% of the total dry surface of packing.

The liquid rate may be alternatively expressed as the flow rate per unit periphery of packing ; this is related to wetting density, by the expression

$$\Gamma = \frac{W}{S}$$

where S is the surface area/unit volume of packing. For a given solution and method of distribution there exists a minimum wetting rate Γ_{min} on account of surface tension effects. When operating at this minimum wetting rate any increase in liquid flow increases the periphery and hence area over which the film is flowing. Having attained the maximum periphery over which the film can be distributed, further increase in liquid flow rate increases Γ but adds little to the active area.

For design purposes, however, the mass transfer coefficient is best evaluated on the total dry surface

area of packing since having established the maximum flow rate at which the wetting rate is still a minimum, then this is the best one can obtain, any further increase in flow rate resulting in a thicker film without more packing becoming wetted.

Finally the concentration driving potential across the film must be evaluated from the temperatures and sample analyses taken on the inlet and outlet solutions in the packed column. The temperatures give the effective solution strengths with reference to the p-T-x chart and knowing the evaporator temperature. Since the calculated pressure drop between the absorber and evaporator is very small <0.2 mbar this does not contribute to increasing the driving potential significantly, (see Fig.17). The equilibrium concentration is found from vapour pressure tests on samples from the absorber. Results gave typical driving potentials of 4-12% depending on absorber conditions.

The results of tests are shown in Fig.18 for a variety of absorber circulation rates and heights of packing. The first conclusion that may be drawn from the results is the distinct increase of the mass transfer coefficient at a circulation rate of about 20cc/s. This was due to the sudden improvement in distribution from the rose above this flow rate, from one stream of solution to 10-20 streams. At this flow rate of 20cc/s the wetting rate is calculated to be 4×10^{-3} kg/sm: further increase in flow rate only shows a slight improvement in mass transfer coefficient as expected.

The second point is the initial increase of the mass transfer coefficient with the reduction in height of packing. This shows that with adiabatic absorption, the highest absorption rates occur over the first few cm. of packing before the heat released into the film prevents further effective absorption. Since the rose was maintained at a fixed position in the column a greater active wetted area was provided by the liquid streams where lower packing heights were employed. Although this area was only equivalent to 4% of the area of 'dry' packing for a height of 3cm., this might have been a significantly greater proportion of the 'active wetted' surface, providing a considerable contribution to absorption.

Despite the small improvement of the mass transfer coefficient with increasing flow rates above 20cc/s, a greater advantage to be gained is the lower temperature difference between inlet and outlet solutions (typically 3°C for 40cc/s as compared with 6°C for 20cc/s). This allows higher cooling water temperatures to be employed in the absorber heat exchanger.

Experiments were also undertaken to study the effect of using a spray absorber. A Lavan type BT/6 nozzle was used to provide a solid cone spray of solution in the 150mm diameter column. However the experimental circuit did not allow flow rates greater than 20cc/s on account of the pressure drop developed across the nozzle (>2bar). Since the spray pattern was not fully developed at these flows and no significant improvement in absorption rate was observed, the investigation was abandoned. The high pressure drop across the nozzle, especially for viscous solutions, illustrates the inherent inefficiency of such a method in producing a large droplet surface area by hydrodynamic shear forces.

Having studied a variety of adiabatic absorbers, attention was turned to the isothermal absorber where the film of solution is simultaneously cooled. The advantages to be gained by using this method are;

i)

A circulating pump is not necessary if a sufficient absorber surface can be wetted with the generator absorber flow rate. This also encourages the elimination of all pumps with the replacement of the solution pump by a vapour lift pump.

ii)

The hold up of solution in the absorber is kept to a minimum. For similar power outputs the isothermal absorber employed had a hold up of less than 100cc as compared to the packed column absorber which held up to 200cc/l of packing in addition to 140cc in the absorber heat exchanger.

iii)

Employing solutions which had crystallisation temperatures close to absorber operating temperatures, allowed considerably more flexibility in the variation of absorber cooling water flow. If crystals were observed, the water flow rate was reduced and the crystals melted as absorption continued. If such a situation was to arise with an adiabatic absorber, the outlet to the absorber heat exchanger would immediately become blocked.

A study was made on the possible use of a wetted wall falling film isothermal absorber with particular reference to work by Salazar (Ref.34). By introducing the solution tangentially to the internal wall of a vertical tube the liquid/vapour interface was increased due to complex wave formation, and the film thickness reduced; this improved the absorption process as compared to a vertical falling film. However, the calculated pressure drops (>2.5 bar) through the tangential entry holes seemed unacceptably high to achieve the necessary flow behaviour.

It appeared far more beneficial to improve absorption by bulk mixing of the film rather than increasing the wetting rate and film Reynolds number. This is most simply achieved by distributing the solution over a series of horizontal tubes; as the film passes over each tube mixing occurs before it is re-established on the tube below. The degree of mixing is likely to depend on the separation distance between tubes; if the tubes are touching, the film will not separate from each tube and it is likely that a stagnant portion will form at the contact points. If, however, the tubes are sufficiently far apart for the film to separate into droplets then the energy imparted to the solution from gravity will be used to mix the solution as it splashes onto the next tube. Too large a separation might result in the solution splashing off the tube completely without the film becoming re-established.

A spiral tube was constructed being considerably easier to manufacture than a bundle of horizontal tubes with vertical manifolds. The tube was made of 6mm diameter stainless pipe, sufficiently flexible to be formed into a 135mm diameter spiral for the existing absorber vessel. A spacing of 6mm was considered necessary for the film to separate from each tube and this was shown to be satisfactory: the resulting pitch angle of the coil was less than 1.3° .

Particular effort was made to encourage good wetting at low flow rates. Reports of treating the surface of the metal by scouring or roughening apparently improved the wetting (Ref.36); it was considered that a deeper deformation of the surface than that produced from emery paper would be beneficial. Attempts to knurl the pipe proved unsuccessful but a series of vertical grooves approximately 0.1mm deep were cut with a die. The two uppermost turns of the coil were left untreated for comparison.

A truncated cone (see photo. 2) was used to distribute the film to the top of the coil, for two reasons. By forming the film on a small perimeter and then increasing it, the wetting rate is reduced with distance until it reaches the edge of the cone. This method was considered to be less sensitive to levelling than a horizontal V-trough placed directly over the coil. In addition it was thought that the hysteresis effect may be reduced; this is displayed by the differences in minimum wetting rate on increasing and decreasing the flow rate. Ramm (Ref.33) lists results where Γ_{\min} varied by as much as a factor of five depending on whether the flow was increased or decreased; the method of distribution had an important effect however, on these results and a similar conical distributor had provided the lowest wetting rates as compared to other methods.

Although it was not necessary to use the previous absorber heat exchanger, provision was made for recirculating solution over the coil. However, the majority of the experiments were performed without recirculation for the reasons mentioned earlier.

Since there was the possibility of crystallisation which occurred on regions of the coil cooled by the inlet water, a parallel flow arrangement was adopted between solution and cooling water. This avoided crystals forming at the bottom of the coil preventing solution flowing to the pump inlet.

The power outputs and concentration driving potentials for the mass transfer coefficients were evaluated by the same method as the packed column absorber. However, the active wetted area of the coil was estimated on inspection of the flow behaviour, rather than use the total dry coil area. The reason for this was that the distribution and coil design had not been optimised, for an isothermal absorber should ensure 100% wetting of the absorber surfaces. In the case of a packed column a situation would exist where the best distribution had been achieved and yet there would still exist a percentage of dry or stagnant surface, thus the mass transfer coefficient has to be evaluated on total surface area.

Several effects were noticed when running the rig with the coil absorber. Firstly the coil was at best 30% wetted unless recirculation was employed. Although the first five to ten coils would be well wetted the angle of the coil allowed solution to flow laterally along the tube to the support struts; the solution then flowed down these struts thereby leaving the surface unwetted further along the tube. This behaviour was more noticeable at lower flow rates (<5cc/s), when the lower half of the coil was almost redundant in providing any absorption. Despite this, the mass transfer coefficient appeared independent of flow rate, an increase in the latter only providing an increase in wetted area.

A particularly interesting phenomenon was observed when large temperature differences existed across the thickness of the film. Normally the behaviour of the solution was to dribble from tube to tube, spreading along the tube in both directions and then retracting to form a drop. If the tube was fully wetted this behaviour was realised by a transient change in thickness of the film. However, when the film temperature difference was sufficiently large, a violent shimmering took place across the film. Any incipient drop would be drawn upwards into the film, and spread along the length of the tube with rapid changes in film thickness. This behaviour would either be intermittent or under certain conditions it would exist continuously and on several coils (see photo 3).

A thermocouple was inserted in the uppermost coil and it was found that 'shimmering' only commenced for temperature differences between the liquid film and metal surface of over 30 °C. The cause of such behaviour is thought to be in the sudden inversion of the film leading to rapid absorption; the heat released from the condensing vapour produces sudden changes in surface tension with a resultant climbing film. The cause of this inversion would be due to some local exposure of solution that had been cooled well below its equilibrium temperature; the rapid absorption at this point would disturb more stable film around it, and hence the effect would continue. Unfortunately this phenomenon could not be produced over a sufficiently large area to establish whether or not high absorption rates were present. Indeed if this was the case it would be hard to reap the benefits for a domestic heat pump application. Since the return central heating water temperature is likely to be within 10°C of the absorber operating temperature, then overstrong solutions must be used to provide equilibrium temperature differences of over 30 °C. This would lower the performance of the heat pump, although possibly allowing very small absorbers to be built.

Experiments were performed with generator/absorber flow rates of 2-9 cc/s and circulating factors, f , of 20-60. On account of the cooling water being at very low flow rates, 2-5 cc/s, the exit temperature was always less than 3°C below the absorber temperature. The solution inlet temperature to the absorber was generally superheated by 7-20°C but this did not prevent absorption taking place on even the uppermost coil. Fig.19 gives the power densities in kW/m², for a variety of solution flow rates over the absorber coil; the vertical bars show the effect of an error in the estimated wetted area by 5% of the total coil area. It is interesting to note the lower power densities that are obtained with recirculation of solution over the coil, despite a larger wetted area of 30-40% total area as compared with 20-25% for a single pass arrangement. On account of the maldistribution that occurred as the solution passed down the coil, a minimum wetting rate may only be specified for the top coil. This was found to be about $12-15 \times 10^{-3}$ kg/sm.

Heat and mass transfer coefficients were calculated by the same methods as outlined previously. Both properties were evaluated at a variety of absorber power outputs from 0.3 to 1.2 kW, and with a range of flow rates. The mass transfer coefficient remained remarkably constant within values of 1.1-1.4 kW/m², and as a consequence results have not been shown. The experimental heat transfer coefficient is shown in Fig.20, with the theoretical internal heat transfer coefficient also given; it is likely that this will be the limiting factor since the

external absorption process will result in coefficients an order of magnitude higher, being essentially a condensation process (App.E). The higher experimental values, nearly a factor of three in some cases, cannot be satisfactorily explained; the error in estimating the wetted area has already been accounted for (vertical bars), and the calculation of the logarithmic mean temperature difference will not increase this significantly. The theoretical coefficient was found using the same method as for the condenser (see App.C) and it may be possible that the length/diameter ratio of the pipe was too large, since the major part of the absorption took place on the first few coils. However, taking this into account would only result in an increase of heat transfer coefficient to $0.75 \text{ kW/m}^2\text{K}$.

The high concentration difference across the thickness of the solution film (5 to 15%), necessary for effective absorption, meant that the full temperature lift between absorber and evaporator could never be realised. This was particularly serious on account of it being the most crucial factor of the whole experimental work. The majority of tests were undertaken at evaporator temperatures of between -3°C and 3°C yet the highest absorber temperatures achieved for these conditions were only 65°C to 68°C . An encouraging point was that the absorber heat output was in no way affected by the degree of temperature lift obtained, the highest outputs occurring for lifts of over 65°C . There was a slight tendency for the temperature lift to fall at lower pressures; a reduction of about 3°C in lift was observed for a fall in evaporator temperature from 10°C to 0°C . Although experiments were performed with pure water, instances occurred when a small overspill of solution into the evaporator allowed temperatures of -5°C to be reached while still maintaining evaporator inputs of 500W. At these higher heat inputs, the water temperature was remarkably uniform throughout its depth being within 1°C ; this was because the violent nature of the boiling kept the inventory well stirred. However at lower heat inputs (<250W.) the vapour bubbles would be more intermittent (one every 3-5s.) and the water near the immersion heater might be more than 4°C higher than the vapour temperature.

For comparing absorber heat output to evaporator input ratios to deduce the heat of vaporisation of the solutions, it was necessary to evaluate the external heat gain to the evaporator for operating temperatures below that of the room. This was done by circulating a known volume of solution around the absorber coil while keeping the evaporator at a constant temperature, without any power input from the heater. After a certain time the increase in volume of solution could be found to calculate the amount of water evaporated, knowing the density and

strength of the solution. For an evaporator temperature of 0°C and room temperature of 15°C the steady state heat input was found to be between 40W and 60W.

The heat output in the absorber was found from the heat delivered to the cooling water; an additional amount of heat from the absorber is used to heat the water vapour from evaporator to absorber temperatures, but this is less than 3% of the total. The results are shown in Fig.21 with vertical bars for an error in the evaporator heat input of $\pm 20\text{W}$. The equilibrium temperature lift is used as opposed to the achieved temperature lift, since the former is a direct indication of the strength of solution used. Heat ratios evaluated from the p-T-x diagram are also shown for comparison. Although the results are somewhat scattered they generally show a lower heat of vaporisation than that predicted from the p-T-x diagram, in accord with the results from the generator/condenser tests. If this is correct then it would be beneficial to the performance of the heat pump as explained in the first chapter.

Neither the packed column or coil absorber showed any significant advantage over each other with regards to the concentration driving potential and hence available temperature lift. The packed column was slightly better, with a lower approach concentration Δx_{app} of one or two percent; however the solution inlet temperature really defines the maximum cooling water temperature allowable, and in this respect the adiabatic absorber was no better.

Considering the operation of either absorber, the falling coil was by far the easier to control. This was in part due to the bad design of the experimental rig, using one pump both to recirculate solution and return a portion back to the generator. The 3-way valve could sometimes prove difficult to balance and it would have been expedient to employ two separate pumps. This would not be attractive in a final design, and with the added complication of potentially hazardous crystallisation in the absorber heat exchanger, the isothermal absorber is considered the better arrangement.

Improvements for better absorption are discussed in the next chapter, having shown its particular relevance to the overall performance of this heat pump system. This can only be done when the solution heat exchangers role has been evaluated, for these two components are completely interdependant.

CHAPTER 6OVERALL SYSTEM PERFORMANCE and DISCUSSION

During all the experiments on the absorber, the performance of the solution heat exchanger was monitored from the inlet and outlet temperatures of the weak and strong solution flows. Experiments were performed with solution strengths of 65-80% and concentration changes of 1.5-3%; this is because high circulation factors, f , of 20-60 were necessary to obtain sufficiently large heat outputs from the absorber (>400W).

The results are shown in Fig.22 against the solution heat exchanger power, $Q_{s.h.x.}$; this has been calculated using a specific heat of 3kJ/kgK , a possible overestimate if the values of pure sodium hydroxide solutions are inspected in App.C. The performance of the heat exchanger is relatively insensitive to its capacity, over the specified flow rates and temperature differences; however, the penalty to the overall performance of the heat pump is increased at the higher capacities.

This is surprising since for the range of flow rates that were employed, the Reynolds number did not affect the Nusselt number (see App.C) and hence a decrease in performance would have been expected at the higher solution heat exchanger capacities. A likely explanation is that better distribution across the surface of the plates occurred at higher flow rates, thus increasing the effective area over which heat was being exchanged.

Sufficient information is now available to make some tentative predictions on the overall performance of the heat pump. The method outlined in App.A is used to calculate the COP, with a variety of data taken from the experimental work and the results are presented in Table 3. Figs.16 and 21 have been used to evaluate the heats of vaporisation of the solutions, and the solution heat exchanger effectiveness is taken as 70% and 80%. A concentration driving potential of 15% is assumed to be necessary for an absorber/evaporator temperature lift of 65°C . A mean specific heat of 3kJ/kgK is taken for the solutions and as already mentioned, this is probably an overestimate; a value of 2.7kJ/kgK would increase the COP by about another percent.

with reference to Appendix A:

$$T_e = 0^\circ\text{C} \quad T_c = 70^\circ\text{C} \quad T_A = 65^\circ\text{C}$$

$$T_2 = 170^\circ\text{C} \quad (77\% \text{ solution})$$

$$\alpha + \beta \approx f C_p \Delta T_{12} \quad \text{for } f > 15$$

$$\text{at } 70^\circ\text{C}; \Delta h_o = 2.33 \text{ MJ/kg}, (1-x)\Delta h_o = 2.24 \text{ MJ/kg}$$

Δh_g MJ/kg	f	ϵ	$(\alpha+\beta)$ MJ/kg*	COP
1.3 x 2.33 = 3.0	20	80	1.3	1.53
	20	70	1.8	1.47
	40	80	2.4	1.41
1.6 x 2.33 = 3.7	20	80	1.2	1.46
	20	70	1.8	1.41
	40	80	2.4	1.37

$$* C_p = 3 \text{ kJ/kgK}$$

Table 3: Evaluation of COP

The predicted performance is remarkably good for these high values of circulation flow f , but considerable improvements could be made by reducing these with a better absorber and this can be done in two ways. Firstly the high concentration driving potentials may be reduced with better mixing of the solution since the improvement in absorption that was predicted with higher wetting rates Γ , has not been realised experimentally. It is uncertain whether a larger spacing between horizontal tubes, in an isothermal absorber, would improve mixing to any great extent but there are no obvious alternatives other than a mechanically stirred absorber.

The second, and far more encouraging method of improving absorber performance is to increase the wetted area of the absorber. The coil absorber used in experiments provided a particularly bad distribution of solution, principally on account of the pitch angle being too steep. A higher flow rate did improve wetting but this could only be achieved by recirculation, if the flow through the solution heat exchanger is limited to maintain a low circulation ratio. It is felt that an improved absorber design could achieve larger wetted areas before recourse is made to employ recirculation, with the added complication of a pump.

The obvious improvement would be to reduce the pitch angle of the coil by employing a larger diameter, however, it would be necessary to also increase the diameter of pipe, otherwise the cooling water pressure drop would become unacceptably high for a central heating circulating pump; consequently the pitch and pitch angle is also increased and this would tend to nullify the effect of an increased coil diameter. An alternative design could employ horizontal tubes with vertical manifolds; the reduced pressure drop would allow smaller pipes and a greater number for a given height, thus increasing the stirring effect. These modifications will require the heat pump to be accurately levelled to within 1° which, although not uncommon with some existing commercial chillers, is an inconvenience with regards to installation.

The surface tension is a particularly important factor on the wettability of a surface and plays an important role in the hydrodynamic conditions existing in an absorber. Indeed it is changes in this property which provides the forces necessary for the 'shimmering' behaviour discussed earlier. There is some contradiction in the literature as to whether a high or low surface tension is beneficial to the wetted area, (Ref.33,37,38), but two distinctions must be made between film breakdown during absorption and the establishment of a film at a minimum flow rate Γ min.. The former occurs when there are large changes in surface tension due to the heat released on absorption. The value of Γ min. however, depends not only on the surface tension and method of distribution, but also on whether the surface is convex or concave. This point is made by Haselden (Ref.36),

"

Surface tension causes a smooth film on the inside of a vertical tube to be in a state of stable equilibrium, whereas the equilibrium of a uniform film on the outside of a tube is unstable. A thin-walled cylinder exposed to internal and external pressure is analogous. A state of dynamic equilibrium can however exist in a convex liquid film under the influence of rippling, though the film thickness will be required to be greater than for a stable non-rippling concave film. Thus the existence of factors leading to high surface tension and uniform film thickness will be favourable to the achievement of a thin concave film whilst conditions of low surface tension combined with rippling will be favourable for the convex film. "

For a coil absorber a low surface tension becomes desirable and since tests on a torsion balance gave values of 0.10-0.12 N/m for solutions of 50% + strength, this indicated the possible use of 'surfactants' as suitable additives to lower the surface tension. Although these

experiments did not reproduce the true conditions present in an absorber, there was no noticeable change in surface tension with temperatures between 20 and 50°C although the higher temperature was that of the bulk test sample, not the true surface temperature. The error is unlikely to be more than 20% which is sufficiently accurate to see if a surfactant has a noticeable effect on surface tension.

One of the problems of using surfactants is their stability at high temperatures in particularly aggressive media such as sodium hydroxide solutions. A promising group of compounds however, is a perfluorinated variety of surfactant with the highly stable carbon-fluorine bond present in the molecule and if these prove unstable it is unlikely that there will exist any other suitable compound.

If one is restricted to the high values of surface tension for such strong salt solutions it may prove beneficial to employ an absorber with concave surfaces; this could be achieved with a falling film on the internal wall of a vertical pipe. However it is likely that the degree of curvature would also play an important part in the stability of the film, and pipes of a small diameter may be necessary. Although a wetted wall absorber has the advantages of simplicity and the requirement to establish a film only once, at the top, it is unlikely that these factors will outweigh the advantages of mixing that are present in a coil absorber.

CONCLUSIONS

The work on the experimental rig demonstrated that it is possible to operate a low pressure absorption heat pump with temperature lifts between absorber and evaporator of about 65°C and yet still maintain a remarkably good degree of performance. Although the COP was derived by assimilating the performance of various components independantly, the majority of values over a range of conditions, were more than 1.4 and some were above 1.5 which is particularly encouraging. Significant improvements would be realised by redesigning the absorber with improved wetting and it is considered that this is possible without a recirculation pump. The experimental work has also shown that water may be used successfully to pump heat from temperature below 0 °C; this is particularly significant considering the dearth of suitable working fluids. Although the temperature lifts initially specified between absorber and evaporator, were never fully realised the results have shown that winter operation is possible with careful evaporator and absorber design. The crystallisation problem has been alleviated considerably with the addition of potassium hydroxide, and the detriment to performance has also been shown to be minimal. However, the successful automatic dilution of strong solutions, when the system shuts down for long periods of time, has yet to be realised and this should be a primary requirement for a development unit. The feasibility of using water and caustic salts in an absorption heat pump has been proven and areas for further development work have been highlighted. The final chapter outlines some different heat pump cycles although still embodying the basic absorption principle.

CHAPTER 7ALTERNATIVE ABSORPTION SYSTEMS

Absorption systems to date have achieved the concentration of absorbent solution by the distillation of the working fluid, this process being easy to achieve even with absorbents of high volatility such as in the ammonia/water system. By carrying out this process at a suitable pressure the energy may be partially recovered at a useful temperature in the condenser since the latent heat of vaporisation of the working fluid is a significant proportion of the energy input to the generator. However a considerable increase in performance is potentially possible if the absorbent and working fluid could be separated without the need for vaporisation. For example if we take the first set of conditions used to evaluate the COP in Table 3;

$$\begin{aligned} \Delta h_s &= 1.3 \times 2.33 = 3.0 \text{ MJ/kg} \\ (\alpha + \beta) &= 1.2 \text{ MJ/kg} \quad (\text{see App.A for defn. of } \alpha \text{ and } \beta) \\ \text{COP} &= 1.53 \end{aligned}$$

without evaporating the water in the generator;

$$\begin{aligned} \Delta h_s &= 0.3 \times 2.33 = 0.7 \text{ MJ/kg} \\ \text{COP} &= 2.18 \end{aligned}$$

As already mentioned in the introduction the absorption process relies on the lowering of vapour pressure of a working fluid by the addition of either a liquid or solid solute. This is fundamentally a 'colligative' property depending on the number rather than the nature of the solute molecules; the latter behaviour gives a modification to the intermolecular forces and results in an additional 'enthalpy' of mixing with corresponding heats of solution. If though we first consider an ideal solution where there is no enthalpy change on mixing, the thermodynamics may be more simply analysed to illustrate the essential energy changes, although a more extensive treatment maybe found in any standard physical chemistry text, (Ref.39,40).

The chemical potential μ , defined as the molar Gibbs function, allows the free energy of a system ($G=H-TS$) to be extended to a situation with more than one component and so may be used to indicate the direction for spontaneous energy change in systems containing several substances. For equilibrium to exist in a system either between phases of one component or components of one phase, etc., the principle of uniform chemical potential applies.

For a single component, by definition

$$\mu = \frac{\partial G}{\partial n} \quad p, T \quad n = \text{no. of moles present}$$

At constant pressure the chemical potential may be shown to vary with temperature according to

$$\left(\frac{\partial \mu}{\partial T} \right)_p = -S$$

The stability of a phase of a single component system at a particular temperature may be easily deduced from this expression, and is shown below in Fig.a

Since the entropy in most systems is positive we have a negative gradient, becoming steeper for each phase with a higher entropy, $S_{\text{gas}} > S_{\text{liq}} > S_{\text{sol}}$: at the boiling point and freezing point the equilibrium between phases is validated by the equality of chemical potential.

The chemical potential of a component, in an ideal solution, may be expressed as:

$$\mu(\text{soln}) = \mu(1) + RT \ln x \quad x = \text{mole fraction of component}$$

and is indeed one definition of an ideal mixture.* $\mu(1)$ is the chemical potential of the pure component at the same temperature and pressure as the solution. What the above equation shows is that the chemical potential of a component is reduced by an amount $RT \ln x$ (since $x < 1$), when in a multicomponent system. In a two component system, if the solute B is taken to be involatile and insoluble in the solid solvent A, the chemical potential of the liquid is only altered and the reduction results in both an increase in boiling point and decrease in freezing point as shown in Fig.b.

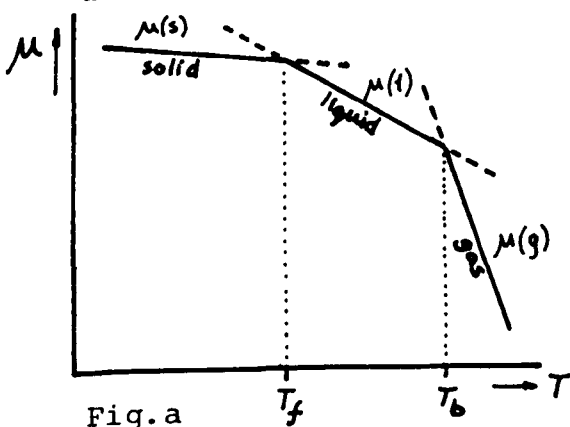


Fig.a

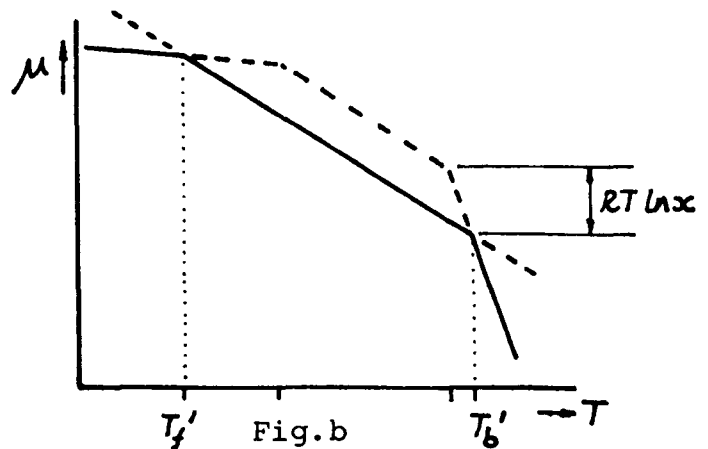


Fig.b

* Several assumptions are made in stating ideality, the most important ones being that the pressures are not excessive ($> 3 \text{ bar}$), the vapour behaves as an ideal gas, and there is no change in volume on mixing.

Specifying a particular working fluid and temperature lift between evaporator and absorber, it is then possible to evaluate the absolute minimum energy required for separation of absorbent and working fluid. This is outlined in App.F for water, with a temperature lift of 70°C a minimum work input to the system of 630 kJ/kg is required to separate the water from the absorbent. This gives a value for COP of;

$$\text{COP} = \frac{(\Delta h_0)_{\text{abs}}}{\Delta h_{\text{sep}}} = \frac{2500}{630} = 4.0$$

For comparison, the Carnot performance may be given, for the same temperature lift from 0°C to 70°C ;

$$\text{COP} = \frac{T_h}{T_h - T_l} = \frac{343}{70} = 4.9$$

Since a method of separation involving work rather than heat has been postulated, the former result is considerably closer to the Carnot COP than a conventional absorption system.

Liquid mixtures exhibiting partial immiscibility is one potential method of separation, relying in particular on the non-ideal behaviour of the solute/solvent mixture where the disturbance of intermolecular forces plays an essential part. These mixtures exist in a homogeneous single phase over a temperature range up to a 'consolute' temperature above or below which the mixture separates into two phases. The composition of each phase depends on the mixture and temperature but it is unlikely that either phase will consist of a pure component: as a consequence the working fluid will consist of a mixture evaporating over a temperature range.

Fig.c is a phase diagram of a two component mixture having an 'upper consolute' temperature below which a two phase mixture exists. The bubble and dew point curves have also been included, to illustrate the processes that would be undergone in such an absorption system: The physical representation of such a process is shown in Fig.d.

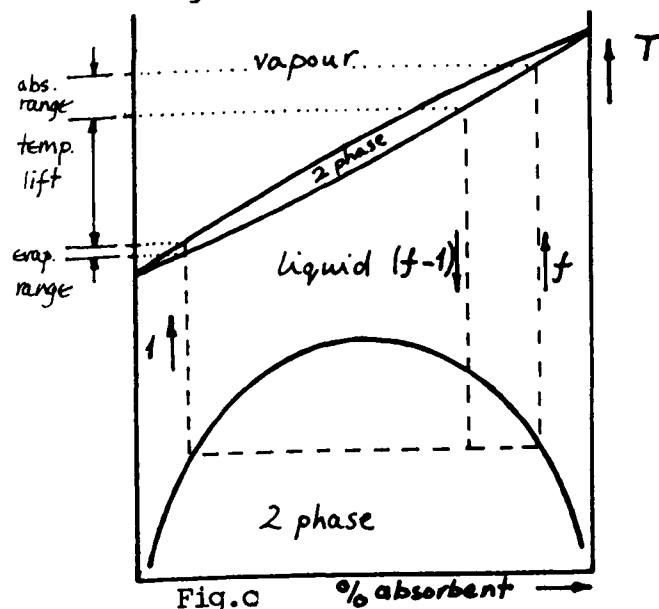


Fig.c

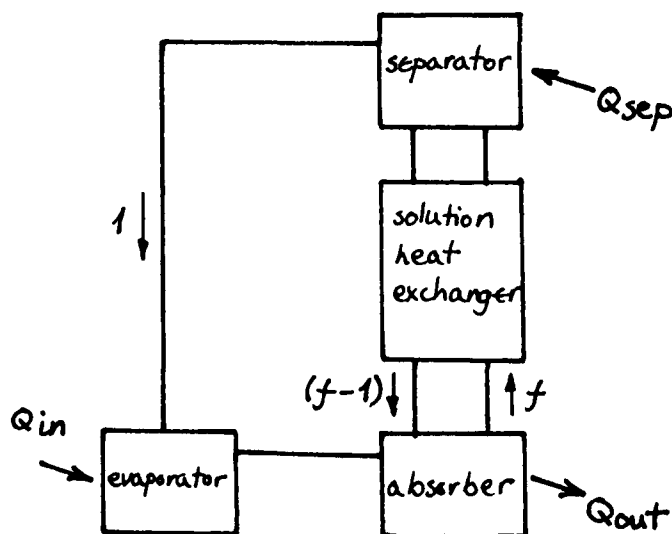


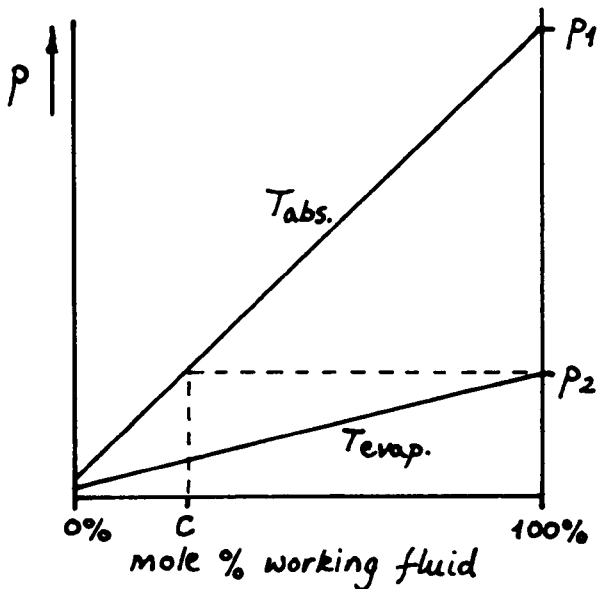
Fig.d

A solution heat exchanger would still be necessary and the heat input would amount to the net heat imbalance of this component with any additional losses. The above diagram is only one example of a potential system; other possibilities may exist with multicomponent mixtures or mixtures subject to additional pressure changes for separation: azeotropic formation is also likely with such mixtures since such a property reflects similar molecular behaviour as that which exists for partial miscibility.

Chemical thermodynamics can only serve to a limited extent as a tool for prediction and selection of potential mixtures, needing extensive information on the solutions to evaluate activity coefficients, excess free energies, excess enthalpies, (Ref.41). On the other hand there is little experimental information apart from a systematic coverage of mixtures with consolute temperatures by A.W. Francis, (Ref.42). Even this is of limited value since most of the mixtures listed are incapable of satisfying the primary requirement of a satisfactory temperature lift between evaporator and absorber. (Ref.43) refers to a patent based on similar methods of separation specifically for heat pumping applications, and a variety of mixtures are listed including several high molecular weight poly-ethers and poly-glycols as absorbents for water. However, the temperature lifts considered appear far too low ($<45^{\circ}\text{C}$) and the system does not appear to have been analysed in any detail.

In selecting potential fluids for such a system, the requirement for a working fluid with a high latent heat of vaporisation may become less stringent if one can select a separation process at a temperature close to the operating temperature of the absorber. The lower capacity of the 'solution heat exchanger' will result in the overall performance being less sensitive to losses in such a component, and so allow for higher absorbent solution flows caused by the use of a lower latent heat working fluid. The first tentative steps for selecting suitable fluids may be as follows; let us assume the mixture behaves in an ideal manner; this is unlikely to be the case at absorber temperatures since the non-ideality of the mixture is being exploited at the separation temperature. A sudden change in intermolecular forces between solvent and solute would be necessary between the absorber and separator if ideality was to exist in the former component. However, the assumption allows one to obtain an idea of the necessary strengths of absorbent solution since we can apply Raoult's law to the mixture, (i.e. that there is a linear relationship between the vapour pressure of the mixture and its strength, in mole fraction). If a working fluid is selected with known vapour pressures at evaporator and absorber temperatures the necessary strength of a mixture may be estimated assuming that the vapour pressure of the pure absorbent is

negligible. This is shown in Fig.e with the mass fraction of working fluid derived.



$$r_p = \frac{p_1}{p_2}$$

$$C = 1/r_p$$

% weight of working fluid;

$$x = \frac{1}{1 + (r_p - 1)\alpha}$$

where $\alpha = \frac{M}{m}$

M : mol.wt. of absorbent

m : mol.wt. of working fluid

Fig. e.

selecting R12 as a working fluid

$$p_2 = 3.1 \text{ bar} \quad r_p = 6.1 \quad C = 16\%$$

$$M = 121; \quad \text{if } \alpha = 2 \quad x = 19\%$$

$$\alpha = 0.2 \quad x = 50\%$$

Although no absorbent has been specified the effect of its molecular weight relative to that of the working fluid can be seen. A high concentration of working fluid is desirable on two accounts, to permit lower solution flow rates, f , and also to increase the likelihood of finding a suitable partially immiscible absorbent. For a small value of x (<10%) an even more dilute solution will exit the absorber and it is unlikely that this solution will separate at any temperature close to that of the absorber. It is therefore desirable to select a combination with a low value of x and this also applies to non-ideal solutions.

In addition, a low value of r_p is desirable: this makes water unattractive as a working fluid since it has a value of $r_p = 50$ for evaporator/absorber equilibrium temperatures of $0^\circ\text{C}/70^\circ\text{C}$ respectively. In addition its low molecular weight will lead to high values of x and therefore make suitable absorbents very unlikely. These reasons could also be applied to a conventional absorption system were it not for the fact that absorbents exhibiting large negative deviations from Raoult's law are employed, so permitting water to be used with its attractive high

latent heat of vaporisation.

The search for a suitable combination of fluids relies on the ability to predict intermolecular forces between liquids, involving a thorough understanding of hydrogen bonding, molecular dipole moments, charge distribution effects of radicals on organic molecules, etc.. This is the area for the physical chemist and chemical engineer: undoubtedly the chemical industry have the largest contribution to make in such areas of technology, being capable of synthesising molecules with specifically designed intermolecular behaviour.

Another alternative to the existing absorption cycle is a system which avoids the use of a solution heat exchanger by transferring the working fluid only between the generator and absorber, employing an osmotic membrane through which only the solvent passes, (Ref.44). Operating the generator and absorber with solutions of slightly different concentrations (ca 1%), and separating these two components with a suitable membrane, results in a pressure difference to drive the working fluid from one to the other. Both the heat exchanger and solution pump are thus eliminated simplifying the whole system considerably. A schematic diagram of the system is shown in Fig.f, with the cycle on the p-T-x diagram in Fig.g. A bleed valve is shown between generator and absorber to restrengthen the solution in the latter component should the membrane be imperfect, with a transport of solute to the generator over a period of time.

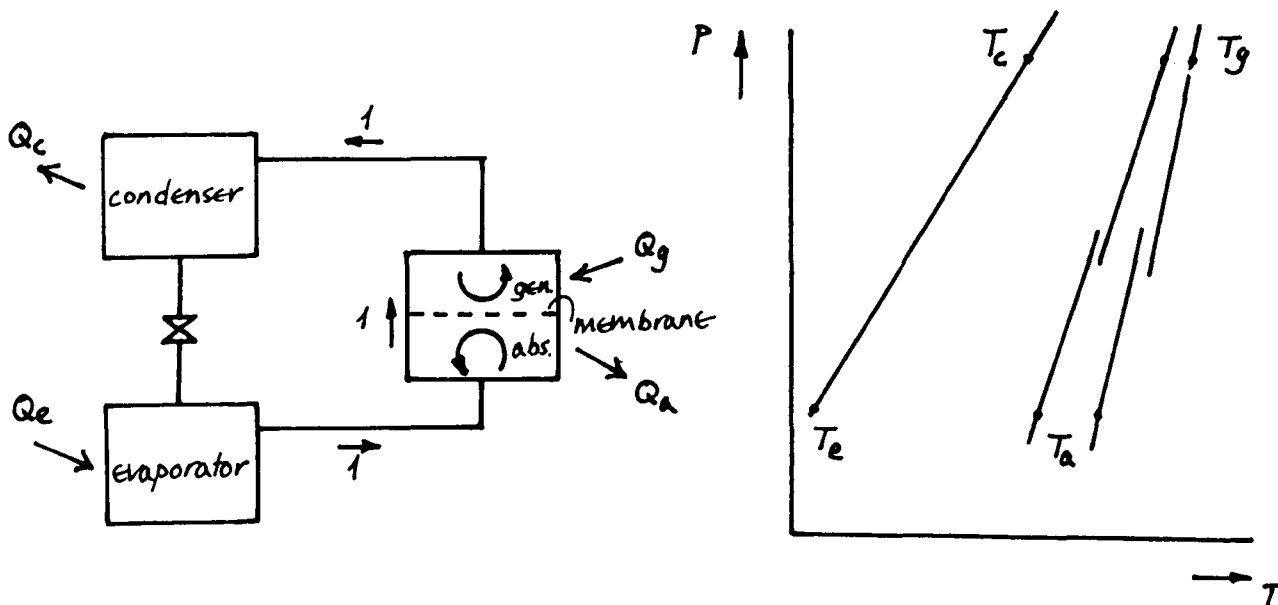


Fig. f.

Fig. g.

The cycle suffers from the fundamental problem of providing a suitable surface area of membrane for fluid transport yet minimising a direct flow of heat from generator to absorber. Of course such a system is entirely dependant on a suitable membrane being constructed needing to withstand both temperature, pressure, and possibly highly aggressive media. However, the range of suitable fluid combinations is considerably enlarged from those which can be considered for the more conventional cycle; since solution flows are not present between absorber and generator the use of a low latent heat working fluid will not necessarily impair performance. Also absorbent/working fluid combinations with positive heats of solution may be considered since despite a larger concentration of absorbent than otherwise, the working fluid flow may not be increased between absorber and generator: as a consequence the performance is automatically improved as illustrated in the introduction.

REFERENCES

1. Haseler, L.E.
Robertson, J.M. Absorption cycle heat pumps for
domestic heating. AERE-G 1049.
AERE Harwell. Sept. 1978
2. Haseler, L.E. Heat Transformers
AERE-R 10111, AERE Harwell.
Apr. 1982
3. Ellington, R.T.
et al. The absorption cooling process
Inst. of Gas Technology
research bulletin 14, Aug. 1957
4. Grossman, G Solar cooling and air
conditioning Prog. Energy
Comb. Sci. Vol.7, 1981,
pp 185-228
5. Thevenot, R. The history of refrigeration
throughout the world
translated J. Fidler.
Int. Inst. of Refrigeration
Paris 1979.
6. British Gas
Corporation Private communications 1981
7. Leach, G. A low energy strategy for the
United Kingdom Science
Reviews, London, 1979
8. Dr.M.B. Green Private communications,
1983 British Gas,
Watson House,
London
9. Wood, R. Ph.D. Thesis, Cranfield Inst.
of Tech., 1984
10. Dr. M.B. Green Private communications, 1982
British Gas, Watson House,
London
11. Alefield, G.
Radermacher, R. Wkg. fluids for abs. heat pumps.
Int. seminar on 'Thermochemical
energy storage'. Edited by
G. Wettermark, Stockholm,
Jan. 1980 ISBN 91-540-3301-2

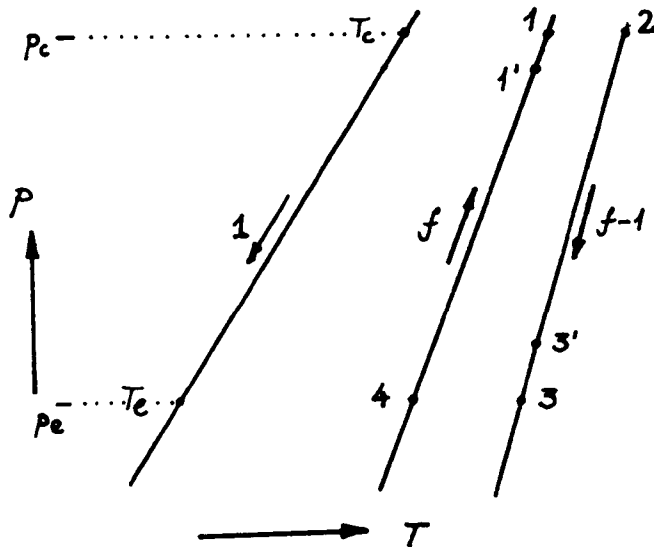
12. Blomberg, P. Proceedings of a workshop
 'New wkg. pairs for absorption
 processes' edited by W. Raldow
 Berlin, Apr. 1982 ISBN
 91-540-3829-4
13. Fitt, P. Proceedings of the grant
 holders meeting on heat pumps.
 Edited J. Foster, Rutherford
 Laboratory, Oxon.
 RL-81-059, Jun.1981
14. Steimle et al. Investigation of wkg. fluids
 for gas-fired absorption
 plants 16th Int. Congress of
 Ref., Paris, 1983
15. El-Shamarka, S. Ph.D. Thesis, Cranfield Inst.
 of Tech., 1981
16. Koebal and Aegerter Ki-Klima-kaelte Ingenieur,
 Apr., 1981
17. Smith, I.E.
 et al. Design and development of
 absorption heat pumps
 Progress report no.1,
 Cranfield Inst. of Tech., 1981
18. Buxton, B.J. Private communications, 1981
 ICI Ltd., Mond Div., Runcorn,
 Chesire
19. Gallagher-Daggitt,
 et al. A Thermo-chemical heat
 pump/energy storage scheme
 based on the sulphuric
 acid-water system
 Rutherford Laboratory, Oxon.
 RL-79-041, Apr. 1979
20. McBride, J. Ph.D. Thesis, Open University,
 1982
21. Clark, E. Industrial heat recovery using
 a modified absorption cycle.
 Int. Symp. on 'The industrial
 application of heat pumps'.
 Coventry, U.K., Mar. 1982
22. Dipl.Ing.H.Bokelmann Private communications, 1983
 University of Essen, F.R.G.

23. Raben, I.A.
et al. A study of nucleate pool boiling of water at low pressure. 6th Nat. Heat Transfer Conference AICLE-ASME Aug.1963
24. Collier, J.T. Convective boiling and condensation McGraw Hill, London, 1972
25. Sukhatme, S.
Rohsenow, W. Heat transfer during film condensation of a liquid metal vapour. J. of Heat Transfer, Trans. ASME, Feb.1966
26. Jameison, D. The condensation coefficient of water National Engineering Laboratory, Report No.186, May.1965
27. Materials in Design Engineering Vol.6, Nov.1961, p.141
28. Gawrilov, G. Chemical nickel plating Portcullis Press
29. Poeton Ltd., Glos. Private communications, 1983
30. J.V. Dawson Private communications, 1983 British Cast Iron Research Association, Birmingham
31. Smith, I.E.
et al. Design and development of absorption heat pumps Progress report no.3, Cranfield Inst. of Tech.,1983
32. Grossman, G. Simultaneous heat and mass transfer in absorption of gases in laminar liquid films. Oak Ridge National laboratory ORNL/TM-8366 Sept.1982
33. Ramm, V.M. Absorption of Gases Israel program for scientific translations, Jerusalem 1968

34. Salazar, A. Ph.D. thesis 1979
Toulouse Polytechnic
France
35. Alloush, A. Ph.D. thesis 1983
Kings College, London
36. Haselden, G.G.
Malaty, S.A. Heat and Mass transfer
accompanying the absorption
of ammonia in water
Trans. Instn. Chem. Engrs.
Vol.37,1959 p.137-146
37. Norman, W.S. Absorption, Distillation
and Cooling Towers
Longmans, Aberdeen, 1962
38. Danckwerts, P.V. Gas-liquid reactions
McGraw Hill, 1970
39. Atkins, P.W. Physical Chemistry
Oxford University Press,
1977
40. Smith, B.E. Basic chemical thermodynamics
Clarendon Press, 1977
41. Rowlinson, J.S. Liquids and liquid mixtures
Butterworths, London
2nd edition
42. Francis, A.W. Critical solution temperatures
Advances in Chemistry Series,
No.31, 1961
43. British Pat. No. 1,582,247
44. German Pat. DE 3009820 A1
45. Wong, H.Y. Heat Transfer for Engineers
Longman, London, 1977
46. Perry, J.H. ed. Chemical Engineers handbook
4th edition McGraw Hill,
NewYork, 1963
47. Leybold-Heraeus GMBH Vacuum technology its
foundations
formulae and tables
48. Howatson, A.M. et al. Engineering Tables and Data
Chapman and Hall 1972

Appendix A

Performance of H₂SO₄/H₂O and NaOH/H₂O Systems



$$\xi = \frac{\Delta T_{23'}}{\Delta T_{24}} = \frac{f C_p \Delta T_{1'4}}{(f-1) C_p \Delta T_{24}}$$

ξ is the effectiveness of the solution heat exchanger*
 f is the circulation flow defined in Fig.1

$$\Delta h_s = \frac{R_o \ln r_p}{M \Delta(1/T)}$$

from Clausius Clapeyron where
 $r_p = p_c/p_e$, Δh_s is the heat of vaporisation of the solution, M is the mol.wt. of water

$$\begin{aligned} \text{COP} &= 1 + \text{COP}_{\text{ref}} \\ &= 1 + \frac{(1-x)\Delta h_o}{\Delta h_s + \alpha + \beta} \end{aligned}$$

Δh_o is the heat of vaporisation of water at evaporator temperature
 x is the mass fraction of condensate flashed

$$\alpha = f C_p \Delta T_{1'1}$$

sensible heat input to generator

$$\beta = (f - \frac{1}{2}) C_p \Delta T_{12}$$

sensible heat input over generator temperature range

$$(1-x) C_p \Delta T_{ce} = x \Delta h_o$$

heat balance for condensate flashed

$$R_o = 8.31 \times 10^3 \text{ J/kmolK}$$

$$\text{for water } M = 18 \text{ kg/kmol}$$

$$\text{for } r_p = 100, \quad \Delta h_s = \frac{2.126}{\Delta(1/T)} \text{ kJ/kg}$$

* The specific heat C_p refers to the fluid that is being transferred across the given temperature range ΔT .

$$\text{for } T_e = 0^\circ\text{C} \quad T_c = T_4 = 70^\circ\text{C} \quad T_3 = 80^\circ\text{C}$$

$$(1-x)\Delta h_o = 2.24 \text{ MJ/kg}$$

H₂SO₄

$$T_1 \approx 155^\circ\text{C} \quad T_2 \approx 170^\circ\text{C} \quad (\text{see fig A.1})$$

$$\Delta_c \approx 3\% , \quad 77 - 80\%$$

$$f \approx 27$$

$$\Delta h_s \approx 3.18 \text{ MJ/kg}$$

$$\text{for } \epsilon = 90\% \quad T_{3'} = 80^\circ\text{C}$$

$$\text{so } T_{1'} = 156^\circ\text{C}$$

$$\alpha \approx -0.06 \text{ MJ/kg}$$

$$\beta \approx 0.83 \text{ MJ/kg}$$

$$\text{hence } \quad \underline{\text{COP} \approx 1.57}$$

NaOH

$$T_1 \approx 140^\circ\text{C} \quad T_2 \approx 147^\circ\text{C} \quad (\text{see fig 3})$$

$$\Delta_c \approx 3\% , \quad 60 - 63\%$$

$$f \approx 27$$

$$\Delta h_s \approx 3.75 \text{ MJ/kg}$$

$$\text{for } \epsilon = 90\% \quad T_{3'} \approx 78^\circ\text{C}$$

$$\text{so } T_{1'} = 135^\circ\text{C}$$

$$\alpha \approx -0.12$$

$$\beta \approx 0.42$$

$$\text{hence } \quad \underline{\text{COP} \approx 1.50}$$

Appendix BPower available from flashing condensate

The maximum quantity of vapour produced, on flashing, is with isenthalpic expansion but this can do no work.

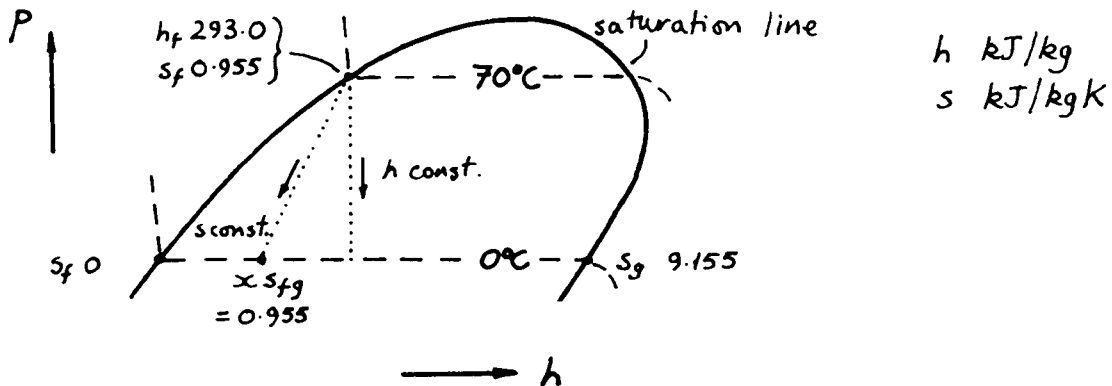
From the steady state energy equation,

$$Q - W = \Delta h$$

Since $Q = 0$ and $\Delta h = 0$ then $W = 0$

For maximum available work, one must expand isentropically giving a smaller fraction of vapour x , than if isenthalpic expansion. The remaining liquid is not completely cooled to the evaporator temperature, however, requiring further external cooling.

From steam tables;



$$x = \frac{0.955}{9.155} = 0.1043$$

$$h_x = x h_{fg} = 260.87 \text{ kJ/kg}$$

$$\text{hence } \Delta h = 293.0 - 260.87 = 32.13 \text{ kJ/kg}$$

for a 1g/s flow of water, power available W is;

$$\begin{aligned} W &= \dot{m} \cdot \Delta h \\ &= 32.1 \text{ W} \end{aligned}$$

This power however must be multiplied by an efficiency of the pump before the true available work has been evaluated.

Loss in performance from heat pump cycling with dilution required.

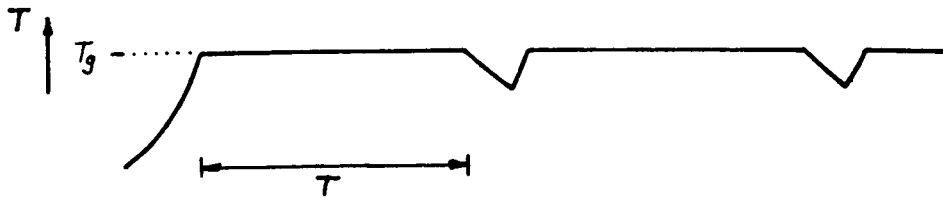


Fig.i

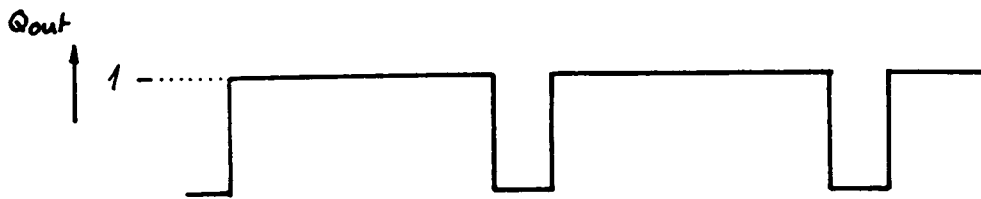


Fig.ii

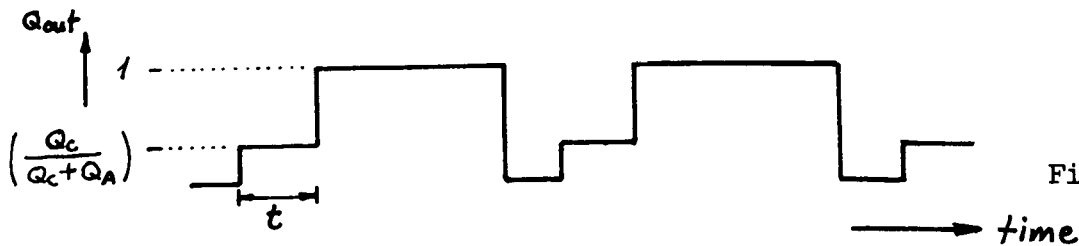


Fig.iii

Fig.i shows the variation in generator temperature with time; starting from an initial ambient temperature the solution is heated until it reaches an approximately constant operating temperature T_g . At this point, for a heat pump without dilution requirements, the full heat output from both condenser and absorber will be delivered and this is shown in Fig.ii. However for a heat pump with dilution requirements, only the condenser will initially be delivering useful heat; when the solution becomes sufficiently concentrated then the absorber will also deliver heat as shown in Fig.iii. The loss in performance may be estimated as follows;

solution inventory, M kg say 7 kg
dilution requirement, d kg H₂O/kg strong soln.

$$\text{hence } t = \frac{d \times M \times h_s}{Q_g}$$

ratio of heat delivered with and without dilution per cycle is,

$$\frac{Q_2}{Q_1} = \frac{t(Q_c / (Q_c + Q_a)) + (T-t)}{T}$$

$$\text{for } Q_A/Q_C = 1.5; \quad Q_2/Q_1 = 1 - 0.4t/T$$

$$\text{for } d = 0.17 \text{ kg/kg, } h_s = 4 \text{ MJ/kg, } Q_g = 10 \text{ kW, then } t = 8 \text{ min.}$$

$$\text{for } T = 1 \text{ hour; } \quad Q_2/Q_1 = 95\%$$

Appendix C

HEAT EXCHANGER AND GENERAL COMPONENT DESIGN

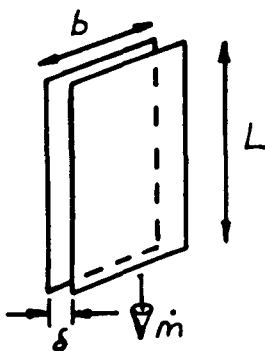
1. Solution Heat Exchanger

The sizing of the solution heat exchanger is largely dependant on the concentration change obtained in the absorber and generator as shown by Fig.5. This could not be predicted due to lack of information on the characteristics of the absorption process. A solution heat exchanger of equal capacity to the systems heat output was arbitrarily chosen. This corresponds to concentration changes of the order of 3% requiring solution flows of about 15g/s for a 3kw heat output.

for $\mu = 0.01 \text{ kg/ms}$, $D = 1 \text{ cm}$:

$$Re = 200$$

It may be seen that turbulent flow is almost impossible to achieve with these flows, for reducing the pipe diameter further would result in prohibitive pressure drops, (see App.C). Low heat transfer coefficients are likely therefore on both sides and a heat exchanger with large surface area and yet low pressure drop (<0.1 bar) is required. The 'plate' heat exchanger is probably the most promising arrangement being compact and yet achieving a low pressure drop by separating the flow into many parallel paths. Thus a design on this basis will be made:



$$Re = \frac{\dot{m}D}{A\mu} \quad D = 2\delta$$

$$A = b\delta$$

$$\text{So } Re = \frac{2\dot{m}}{b\mu}$$

$$\dot{m} = 15 \text{ g/s} \quad \mu = 10^{-2} \text{ kg/ms}$$

$$\text{for } b = 100 \text{ mm} : Re = 30$$

$$C_p = 3.0 \text{ kJ/kgK} \quad k = 0.7 \text{ W/mK}$$

$$Pr = 43$$

$$\text{for } \delta = 1 \text{ mm} \quad L = 500 \text{ mm} : \frac{2\delta}{L} = 4 \times 10^{-3}$$

$$\text{now } (RePr \frac{2\delta}{L}) = 5.2$$

since $(\text{RePr} \frac{2\delta}{L}) < 70$, $\text{Nu} = 7.54$ (Ref.45).

hence $h = 2.6 \text{ kW/m}^2\text{K}$

Since the solution flow on each side of the plate is very similar we have neglecting resistance of plate ($>20h$), an overall heat transfer coefficient U :

$$U = h/2$$

$$U = 1.3 \text{ kW/m}^2\text{K}$$

for a capacity of 3kW and a $\Delta T_{lm} = 5^\circ\text{C}$:

$$a = 0.46 \text{ m}^2$$

area of one plate: $a_p = 0.05 \text{ m}^2$

no. of plates: $n = 10$

Several plates will reduce Re below the previous value but Nu will remain unchanged. Despite the arbitrary dimensions chosen it may be shown that it is difficult to increase the Nu above 7.54 by increasing the factor $(\text{RePr} \frac{2\delta}{L}) > 70$:

For the same solution properties etc., but excluding plate dimensions:

$$\text{Re} = \frac{6}{nb} \quad (\text{for } n \text{ plates flow reduced to } 2\dot{m}/n)$$

$$\text{now } n = a/a_p$$

$$\text{but } a = 0.46 \times \delta \text{ m}^2 \quad (\delta \text{ in mm})$$

$$\text{and } a_p = bL$$

$$\text{hence } \text{RePr} \frac{2\delta}{L} = 6/nb \times 43 \times 2\delta/L$$

$$= 1.12$$

So the condition for $\text{Nu} > 7.54$ can never be attained with these conditions.

It is also necessary to evaluate the pressure drop across the heat exchanger:

pressure drop from dynamic head: $\Delta p_\delta = \frac{1}{2} \rho u_m^2$

pressure drop from skin friction: $\Delta p_\sigma = 4C_f (\frac{1}{2} \rho u_m^2) \frac{L}{D}$

total pressure drop through heat exchanger:

($u_m = \dot{m}/\rho A$);

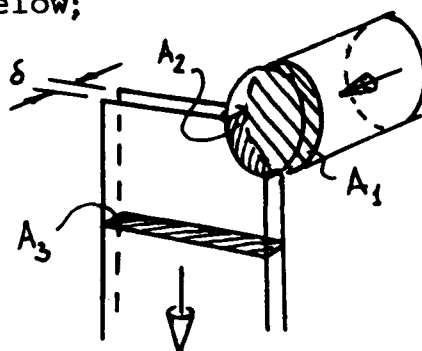
$$\Delta p_T = \frac{1}{2} \frac{\dot{m}^2}{\rho A_1^2} + \frac{8}{n^2} \left(\frac{1}{2} \frac{\dot{m}^2}{A_2^2} \right) + \frac{4}{n^2} \left(4C_f \frac{1}{2} \frac{\dot{m}^2}{A_3^2} \frac{L}{D} \right)$$

$$\left[\Delta p_\delta \text{ inlet to s.h.x.} \right] + \left[2x \Delta p_\delta \text{ inlet and exit to plate} \right] + \left[(\Delta p_\sigma \text{ through plate}) \right]$$

typically; $A_1 = 100 \text{ mm}^2$, $A_2 = \delta^2$, $A_3 = b\delta$ *

With these approximate relations and given the previous solution conditions a variety of configurations may be tried to realise the effect of the various heat exchanger dimensions. Some results are shown below;

δ /mm	L/mm	b/mm	p/mbar
1	500	100	80
1	500	50	26
1.5	500	50	7
1.5	1000	50	29



Bearing in mind that the total area is proportioned to the plate spacing δ , it is preferable to select a narrow spacing without increasing the pressure drop over, say, 100 mbar. Higher pressure drops would require condenser temperatures of at least 50°C to achieve these solution flow rates and this is not taking into account possible pressure losses in any absorber distribution device.

An initial design of heat exchanger proved to be ineffective on account of bad flow distribution across the plates and inadequate sealing of plates with PTFE gaskets.

In the event, a commercial plate was employed on the grounds of expediency, having pressed corrugations for good distribution of liquid and being constructed with a built in rubber gasket for effective vacuum sealing.

* The middle term provides the greatest contribution by nearly an order of magnitude for $A_2 = \delta^2$ since $b \gg \delta$. However for the commercial plate that was eventually used A_2 is at least five times larger and the skin friction term then dominates.

APV Junior paraflow plates : stainless steel type
316 with butyl rubber
gaskets.

area of plate a_p : 0.0258 m² (L=420mm b=50 mm)

no. of plates n : 23

total area a : 0.594 m²

mean spacing δ : 1.9 mm

It may be noted that the corrugations increase the plane face plate area by 23% although the pressure drop is also increased. Normally such corrugations serve the purpose of strengthening the plates for high differential pressures and also for providing turbulence across the plate by periodic "pinching" of the flow. However, neither of these benefits could be realised in this situation.

One final point has to be considered when employing a heat exchanger with a high temperature gradient across its length, and that is the effect of heat being conducted along the length of the plates reducing effective counterflow conditions.

Heat loss $Q = k/L A \Delta T$

L 500mm

k 16 W/mk (stn.st.)

A : cross sectional area of metal

$$A = \underset{\text{plate}}{nb \delta} + \underset{\text{endplate}}{2b \delta}$$

$$= 1750 \text{ mm}^2$$

$$\Delta T = 100^\circ\text{C}$$

hence $Q = 5.6 \text{ W}$

2. Absorber Heat Exchanger

The absorber heat exchanger was sized to half the capacity of the solution heat exchanger. Twelve similar APV plates were used, but because larger temperature differences were being employed in the former component, with inlet cooling water temperatures of around 15°C, the numbers of plates could have been further reduced.

3. Condenser

A water cooled tube condenser was proposed, comprising of a horizontal coil made from closely wound 5mm bore stainless steel tubing. This can be analysed as a horizontal pipe with condensation occurring on both sides. The external heat transfer coefficient can be derived from the Nusselt relation for condensation on the outside of a horizontal pipe;

$$h_o = 0.95 k_L \left[\frac{(\rho_l - \rho_g) \rho_l g}{\mu_l \Gamma} \right]^{1/3}$$

for 1.5 kW : $\dot{m} = 0.6 \text{ g/s}$

for a coil 0.2m long : $\Gamma = 3 \times 10^{-3} \text{ kg/sm}$

for less favourable conditions at condenser temperatures of 50 - 60°C,

$k = 0.65 \text{ W/mK}$, $\mu_l = 0.5 \times 10^{-3} \text{ kg/ms}$, $\rho_l = 10^3 \text{ kg/m}^3$, $\rho_g \ll \rho_l$

then $h_o = 11.5 \text{ kW/m}^2\text{K}$

For condensation on the inside of the spiral coil a factor of 0.8 may be applied to the above value which may be combined to give an average external heat transfer coefficient of

$$\bar{h}_o = 10.4 \text{ kW/m}^2\text{K}$$

Internal heat transfer coefficient:

For 1.5kW heat output but with a large water temperature change between inlet and outlet of 40°C to give a lower estimate of ;

$$\dot{m} = 9.0 \text{ g/s}$$

and for $D = 5 \text{ mm}$: $Re = 2900$

The modified Dittus-Boelter relation may be used for turbulent flow, where $0.6 < Pr < 100$ (Ref.45).;

$$Nu = 0.027 Re^{0.8} Pr^{0.33} \left(\frac{\mu}{\mu_w} \right)$$

$Pr = 5.4$ and $\frac{\mu}{\mu_w} = 1$

hence $Nu = 27$

$$h_i = 3.4 \text{ kW/m}^2\text{K}$$

If fully developed laminar flow exists at lower powers one may use the equation;

$$Nu = \frac{0.07 (RePrD/L)}{1 + 0.04 (RePrD/L)^{2/3}} + 3.65 \quad (\text{Ref.48})$$

Neglecting the conduction resistance of the pipe, the overall heat transfer coefficient U is found from

$$\frac{1}{U} = \frac{1}{h_o} + \frac{1}{h_i}$$

hence $U = 2.6 \text{ kW/m}^2 \text{ K}$

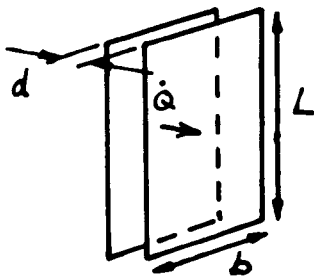
for 1.5kW and a log mean ΔT of 5°C ,

$$A = 0.12 \text{ m}^2$$

Taking a coil with a diameter of 0.1m and length of 0.2m., this gives a 'pipe' surface area of about 0.12m^2 despite the actual area being greater by a factor of about 50%.

4. Heat Loss From Generator To Condenser

Since the generator and condenser are only separated by a stainless steel metal plate, it is necessary to evaluate the heat loss by radiation and convection from the end plate to condenser coil. Considering this as two plates at generator and condenser temperature respectively;



$$L = 150\text{mm}$$

$$d = 50\text{mm}$$

$$b = 100\text{mm}$$

$$\text{Radiation heat loss; } h = \epsilon \sigma \bar{T}^4$$

$$\Delta T = 100^\circ\text{C}$$

$$\epsilon = 1 \quad \bar{T} = 400\text{K} \quad h = 3.6 \text{ W/m}^2 \text{ K}$$

$$\text{for } A = 1.5 \times 10^{-2} \text{ m}^2 \quad \Delta T = 100^\circ\text{C};$$

$$Q_r = 5.4 \text{ W.}$$

Since the vapour velocities are very low, additional losses may be estimated assuming natural convection;

$$\text{Gr} = \frac{g \rho^2 \Delta T d^3}{T_\mu^2}$$

$$\rho = 0.2 \text{ kg/m}^3, \quad \Delta T = 100^\circ\text{C}, \quad T = 350\text{K}, \quad \mu = 10^{-5} \text{ kg/ms}$$

$$\text{hence} \quad \text{Gr} = 1.4 \times 10^5$$

for these conditions

$$\text{Nu} = 0.18 \text{ Gr}^{\frac{1}{4}} \frac{L}{d}^{-\frac{1}{9}} \quad (\text{Ref. 45})$$

$$\text{Nu} = 3.1$$

$$k = 2.2 \times 10^{-2} \text{ W/mK} : h = 1.4 \text{ W/m}^2\text{K}$$

$$\text{and } Q_c = 2.1 \text{ W.}$$

These results show that direct heat loss from generator to condenser is less than 1% for condenser outputs of 0.7kW and can consequently be neglected.

5. Packed Column Design

On account of the low absolute pressures in the evaporator <6 mbar, it is essential that the vapour pressure drop through the packing is kept to a minimum. Probably the most suitable compilation of data from which to estimate pressure drops is that given in the Chemical Engineers handbook (Ref.46); the most recent correlation presented is from the work of Eckert where it is necessary to evaluate two groups,

$$A = \frac{G^2 F \psi \mu^{0.2}}{\rho_g \rho_l g} \quad \text{and} \quad B = \frac{L}{G} \sqrt{\frac{\rho_g}{\rho_l}}$$

ρ_g vapour density $5 \times 10^{-3} \text{ kg/m}^3$ for $t_e 0^\circ\text{C}$

ρ_l absorbent solution density 1500 kg/m^3

μ solution viscosity 0.02 kg/ms

F a factor depending on the characteristics of the packing. For ceramic 1/2" Intalox saddles = 200

G vapour mass flow per unit cross sectional area
For a 15cm column and 1.5kW evaporator load
= $5.1 \times 10^{-3} \text{ kg/sm}^2$

L solution mass flow per unit c.s.a.

Hence $L/G = f = 30$ maximum. This assumes that the liquid is uniformly distributed over the c.s.a

ψ ratio of density of water to density of solution = 0.67

The two groups may now be evaluated, although it is necessary to convert the former to Imperial units for reference to the data in (Ref.46).

The results are:

$$A = 1.16 \times 10^{-2} \quad \text{and} \quad B = 5.5 \times 10^{-2}$$

The data of Eckert shows that for these conditions the pressure drop is considerably less than,

0.42 mbar per metre height of column.

In addition the column is operating well below its 'flooding' point where the liquid flow is sufficiently great to result in a phase inversion with the vapour bubbling through the liquid.

The maximum available height of packing was 0.3m. giving a predicted pressure drop of <0.13 mbar, and for lower evaporator powers this would be even smaller. For 1/2" Intalox saddles with a quoted area of $480 \text{m}^2/\text{m}^3$ the maximum dry surface area of packing is 2.5m^2 .

Distribution

Good liquid distribution across the cross section of the column is essential. The liquid can either be insufficiently dispersed or alternatively it can migrate to the side walls of the column; both of these conditions result in the packing becoming ineffective. To avoid liquid migration, column diameter/packing diameter ratios greater than ten are recommended (Ref.46), this is satisfied with 1/2" Intalox saddles in a 6" (150mm) diameter column. For effective distribution there are additional recommendations of at least one liquid stream for every 30cm^2 which requires at least six liquid streams for the aforementioned column.

6. Pressure Drops For Vapour And Solution Flows

Dynamic head pressure drop;

$$\Delta p_{\delta} = \frac{1}{2} \rho u_m^2 = \frac{1}{2} \frac{\dot{m}^2}{\rho A^2}$$

Skin friction pressure drop

$$\Delta p_{\sigma} = 4 C_f \left(\frac{1}{2} \rho u_m^2 \right) \frac{L}{D} = 4 C_f \Delta p_{\delta} \frac{L}{D}$$

i) Evaporator-absorber pipe vapour pipe

$$t_e = 0^\circ \text{C} \quad \Delta h_o = 2500 \text{ kJ/kg} \quad v_g = 206 \text{ m}^3/\text{kg} \quad \mu_g = 8.5 \times 10^{-6} \text{ kg/ms}$$

$$\text{for } 1.5 \text{ kW} : \quad \dot{m} = 0.6 \text{ g/s}$$

$$\text{for } D = 5 \text{ cm} : \quad \underline{\Delta p_{\delta} = 9 \text{ N/m}^2}$$

$$\text{Re} = 1800, \text{ say laminar} : \quad C_f = 0.0089$$

$$\text{for } L = 50 \text{ cm} : \quad \underline{\Delta p_{\sigma} = 5 \text{ N/m}^2}$$

These pressure drops are very small (1mbar = 100N/m²) so 5cm pipe x 20cm length is acceptable. It is also necessary to check for possible compressible flow of the water vapour at these low pressures.

For similar conditions as above,

$$q = 0.12 \text{ m}^3/\text{s}$$

$$u_m = 60 \text{ m/s}$$

$$\text{speed of sound : } a = \sqrt{\gamma RT} \quad (R=R_0/M^1, \gamma = \frac{C_p}{C_p - R})$$

$$C_p = 1.85 \text{ kJ/kgK} : \quad \gamma = 1.33$$

$$T = 273 \text{ K} : \quad a = 409 \text{ m/s}$$

$$\begin{aligned} \text{hence} \quad M &= \frac{u_m}{a} \\ &= 0.15 \end{aligned}$$

We can neglect compressible effects since they are negligible for $M < 0.3$.

ii) Generator-condenser Vapour Pipe

$$\text{for 2kW in generator : } \dot{m} = 0.6 \text{ g/s}$$

$$\text{for } A = 1 \text{ cm}^2 : \quad \Delta p_\delta = \frac{18}{\rho} \text{ N/m}^2$$

$$\text{for a mean density at } 70 \text{ C} : \quad v_g = 5.0 \text{ m}^3/\text{kg}$$

$$\Delta p_\delta = 90 \text{ N/m}^2$$

Δp_σ is negligible since an orifice is employed between generator and condenser.

$$\text{Take } D = 2\text{cm}, A = 3\text{cm}^2 : \Delta p_\delta = 10 \text{ N/m}^2$$

Despite the pressure loss of several dynamic heads due to tortuous path through separator cap, preventing solution carryover, the pressure drop is still <1mbar.

iii) Absorbent Solution Pipes

From earlier COP calculations, $\Delta T_a = 5^\circ\text{C}$ gives $f = 60$ for $\Delta T_{ae} = 70^\circ\text{C}$ hence solution flow 36 g/s.

for $D = 1\text{cm}$: $\Delta p_\delta = 69 \text{ N/m}^2$

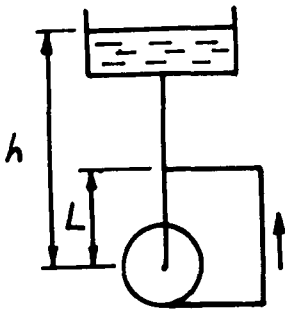
$\mu = 0.02 \text{ kg/ms}$: $\text{Re} = 230$

since laminar flow : $C_f = 16/\text{Re}$

for $L = 1\text{m}$: $\Delta p_\sigma = 1.9 \times 10^3 \text{ N/m}^2$

Even at these very high solution flow rates the pressure drops are acceptable with this diameter pipe.

iv) Possible Cavitation At Pump Inlet



Cavitation is most likely when full flow is passing through by-pass

Since solution is at saturation pressure in absorber to avoid cavitation;

$$\Delta p_h > L \Delta p_\delta + \Delta p_\sigma$$

$\Delta p_h = \rho g h$; $L \Delta p_\delta$ is pressure loss at pump inlet

Δp_σ is skin friction loss over length L

Worst conditions;

$Q = 0.19 \text{ l/s}$ $\rho = 1.52$ $h = 0.3\text{m}$ $L = 0.25\text{m}$

$\Delta p_h = 4.5 \times 10^3 \text{ N/m}^2$

for $D = 1\text{cm}$: $\Delta p_\delta = 4.4 \times 10^3 \text{ N/m}^2$

for cold solution $\mu = 0.08 \text{ kg/ms}$: $\text{Re} = 460$

Since laminar flow : $C_f = 16/\text{Re}$

$L/D = 25$: $\Delta p_\sigma = 15.3 \times 10^3 \text{ N/m}^2$

These results show that cavitation is likely.

Increasing D to 1.5 cm :

$$\Delta p_{\delta} = 0.9 \times 10^3 \text{ N/m}^2$$

Re still laminar so

$$\Delta p_{\delta} = 3.0 \times 10^3 \text{ N/m}^2$$

Since $4.5 > 3.0 + 0.9$, cavitation is very unlikely even with using cold highly viscous solutions.

Appendix DVacuum Considerations

See (Ref.47)

1. Pump Down Times

Vacuum pump : Sliding Vane
Leybold Heraeus type D2A

Pumping speed $S = 0.69$ l/s, constant $p > 10$ mbar

Water vapour tolerance : 40 mbar

Approx volume of system : $V = 35$ l

Pumping from 1 bar to : 10 1 10 mbar

Pumping factor σ from (Ref.47) : 4.2 6.7 9.0

Pump downtime $\frac{\sigma V}{S}$: 3.5 5.7 7.6 min.

2. Vapour Loss For Continuous Pumping

For a maximum partial pressure due to ingressing air we must open throttle to achieve a certain pumping rate. The maximum water vapour loss \dot{m} may be estimated for a given temperature, assuming 100% vapour passes through throttle.

Maximum permitted leak : $\lambda = 10^{-2}$ mbarl/s

This corresponds to a pressure rise of 1 mbar/h

for p : < 0.1 mbar < 1 mbar

S : > 0.1 l/s > 0.01 l/s

at 15°C : $v_g = 78$ l/g

\dot{m} : > 4.6 g/h > 0.5 g/h

at 70°C : $v_g = 3.7$ l/g

\dot{m} : > 97 g/h > 9.7 g/h

The water loss of 97 g/h would be nearly 5% of water flow

round the heat pump circuit when operating at full output and even more when running at lower outputs. However a low partial air pressure of 0.1 mbar would not be necessary at these condenser pressures of over 300 mbar (at 70 °C) and 1 mbar would be an acceptable limit, reducing the water loss considerably.

3. Sizing Of Throttle For Balancing Leaks

Specifying a permissible leak and partial air pressure one can find the necessary pumping speed; knowing the pumping speed of the vacuum pump S_p , then gives the conductance C of the throttle (inverse of resistance to flow) which may be used to give an idea of size (Ref.47).

$$\lambda = 10^{-2} \text{ mbar l/s} \quad p_a = 0.1 \text{ mbar} : S = 0.11/\text{s}$$

$$\text{D2A type pump: } S_p = 0.69 \text{ l/s down to 0.1 mbar}$$

$$\frac{1}{S} = \frac{1}{S_p} + \frac{1}{C}$$

$$\text{so } C = 0.12 \text{ l/s}$$

To find expression for conductance we must determine nature of flow i.e. molecular, Knudsen, or laminar. Laminar flow exists for $D\bar{p} > 0.6 \text{ mbar cm}$ where \bar{p} is average pressure across throttle. This is likely to be the case even for low evaporator temperatures providing the throttle diameter D is not smaller than about one millimetre.

$$\text{For laminar flow : } C = 135 \frac{D^4}{L} \bar{p} \quad (\text{mbar, cm})$$

$$\text{For } \bar{p} = 1 \text{ mbar : } \frac{D^4}{L} = 0.87 \times 10^{-3} \text{ cm}^3$$

$$\text{For } \frac{L}{D} = 10 : \quad D = 0.3 \text{ cm} \quad L = 3.0 \text{ cm}$$

$$\text{For } \bar{p} = 5 \text{ mbar} \quad D = 0.06 \text{ cm} \quad L = 0.6 \text{ cm}$$

These approximate dimensions show that it is not necessary to use a highly accurate needle valve with fine adjustment: a simpler and cheaper 1/4" BSP should be adequate.

APPENDIX EABSORPTION PROCESS WITH LAMINAR LIQUID FILMS

With reference to the report by Grossman (Ref.32);

For a constant temperature surface the Nusselt number, given by

$$Nu = \frac{h \delta}{k}$$

h heat transfer coeff from vap/liq. interface to solid wall W/m^2K
 δ film thickness
k conductivity of solution W/mK

attains a constant value of 4.25 at a normalised distance of $\zeta_c \sim 1$ where

$$\zeta = \frac{x}{\delta} \frac{1}{Pe} \quad x \text{ distance along film}$$

Pe Peclet number

Now $Pe = \frac{\Gamma}{\nu \alpha} \quad \alpha \text{ thermal diffusivity} = \frac{k}{C_p \rho}$

δ may be related to Γ by using the Nusselt equation for a laminar film flowing down a vertical wall;

$$\delta = \frac{3\mu\Gamma}{\rho^2 g}^{1/3}$$

At typical absorber conditions,

$$\mu = 20 \times 10^{-3} \text{ kg/ms}, \rho = 1600 \text{ kg/m}^3, k = 0.7 \text{ W/mk}$$

$$C_p = 2.7 \text{ kJ/kgK}$$

For a low value of $\Gamma = 10^{-3} \text{ kg/sm}$, if this can actually be achieved,

$$Pe = 3.9$$

$$\delta = 0.13 \text{ mm}$$

$$\text{and } x = 0.52 \text{ mm}$$

After this distance $Nu = 4.25$ from which the heat transfer coefficient is

$$h = 22 \text{ kW/m}^2\text{K}$$

For a high value of $\Gamma = 10^{-1} \text{ kg/sm}$,

$$Pe = 390$$

$\delta = 0.60\text{mm}$
 and $x = 230\text{mm}$
 where $h = 4.7 \text{ kW/m}^2\text{K}$

For distances less than ζ_c there is a slight improvement in Nu with higher wetting rates and the heat transfer coefficient may be expressed as

$$h \propto \Gamma^{0.02}$$

If the wall is adiabatic as is the case in a packed column absorber, the value of $\zeta_c = 0.1$ after which $\text{Nu} = 4.23$.

However, the Sherwood number, given by

$$\text{Sh} = \frac{h_M \delta}{D} \quad \frac{h_M}{D} \quad \begin{array}{l} \text{mass transfer coefficient m/s} \\ \text{diffusion coefficient m}^2/\text{s} \end{array}$$

attains a constant value after a considerably longer distance than Nu. To find this distance it is necessary to first evaluate the Lewis number which is the ratio of material diffusivity to thermal diffusivity, given by

$$\text{Le} = \frac{D}{\alpha}$$

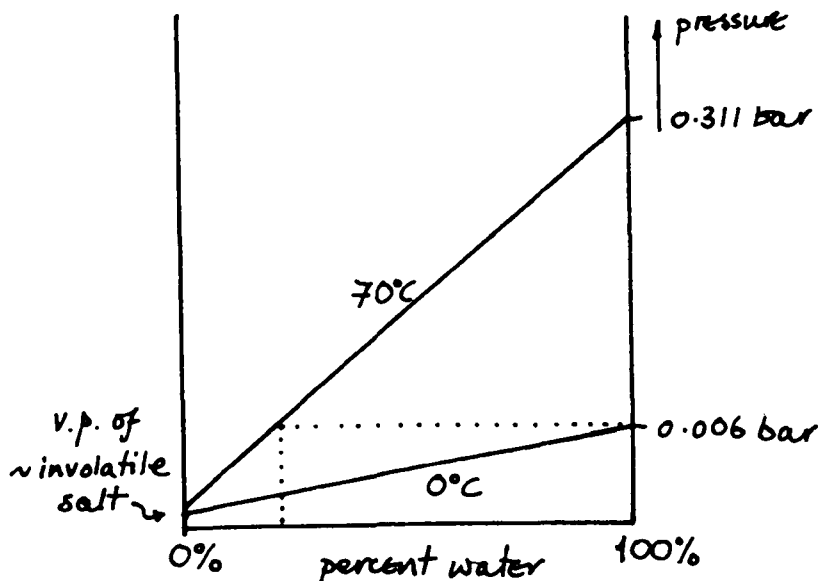
As no experiments were undertaken to evaluate the diffusion coefficient, it must be evaluated by other means. Shamarka (Ref.15), and Alloush (Ref.35), applied the Wilkes and Chang formula to predict the diffusion coefficient with some success for their methanol/mixed bromide solutions, however, this formula is strictly for dilute salt solutions. It is preferred in this instance to take a value of $10^{-10} \text{ m}^2/\text{s}$ and bear in mind that this is to within an order of magnitude. Hence $\text{Le} = 10^{-4}$ which gives a normalised distance $\zeta_c = 10^3$ after which $\text{Sh}_1 = 3.5$. For the previous wetting rates of 10^{-3} kg/sm and 10^{-1} kg/sm , the distance x to achieve this constant value of Sh is 0.52m and 230m respectively. At distances below these values $\text{Sh} \propto \Gamma^{0.6}$ from which the mass transfer coefficient $h_M \propto \Gamma^{0.27}$. The corresponding values of h_M are

$$30 \times 10^{-7} \text{ m/s and } 8 \times 10^{-7} \text{ m/s}$$

Because it is not possible to determine with accuracy the concentration difference across the film, the evaluation of h_M is of little use in determining the power density expressed in kW/m^2 . It is the Lewis no. which conveys more useful information; being a low value this directly shows that the mass transfer is the limiting factor on the power output from the absorber, rather than the heat transfer. Consequently an absorber must be designed to produce hydrodynamic conditions in the solution which maximises the former.

Appendix F

Minimum energy change on mixing



$$x_w = \frac{0.006}{0.311} = 0.019$$

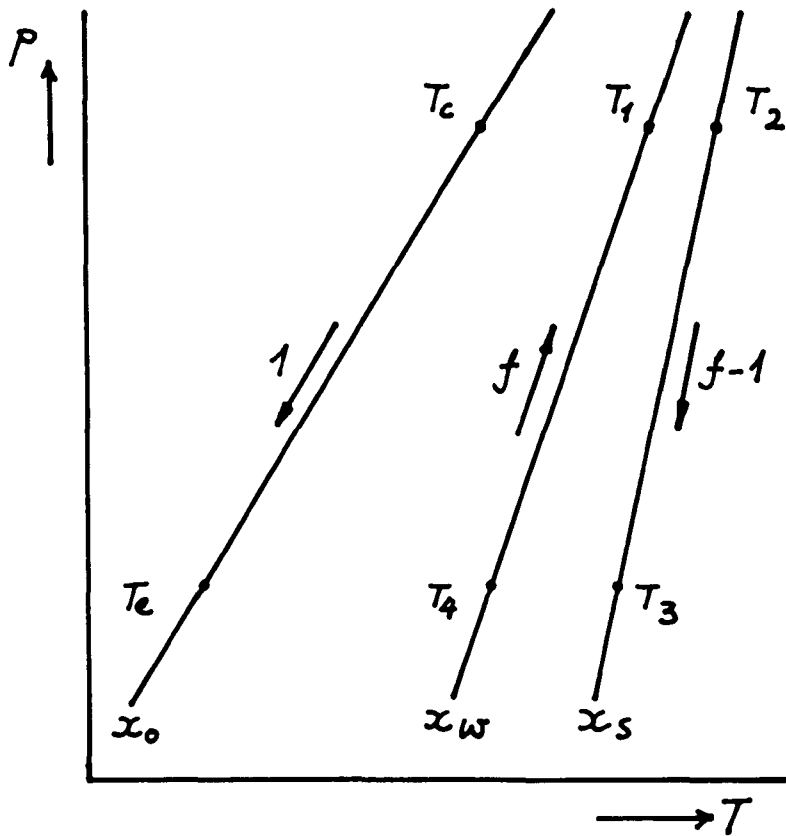
To establish the free energy change on mixing (or separating) for an ideal solution of water and an involatile salt, it will be assumed that there is an infinite quantity of solution at a concentration x_s , and this is unchanged on mixing 1 mol. or 1 kg. of water.

Before mixing;

$$\mu_1 = (\mu_s^{\circ} + RT \ln x_s) + \mu_w^{\circ} \quad \begin{array}{l} s \text{ solution} \\ w \text{ water} \end{array}$$

After mixing;

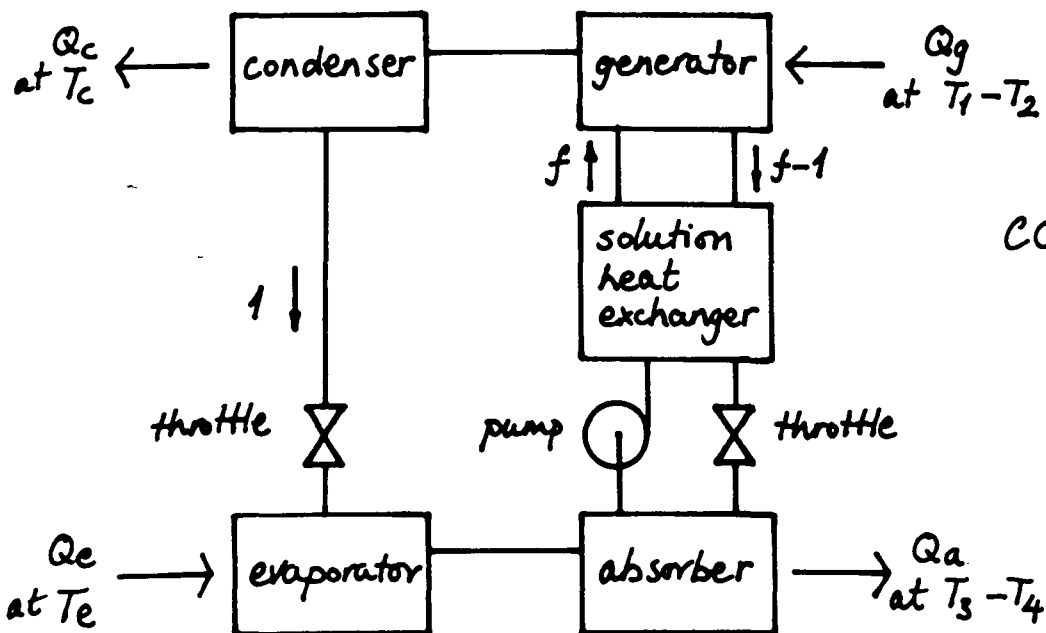
$$\begin{aligned} \mu_2 &= (\mu_s^{\circ} + RT \ln x_s) + (\mu_w^{\circ} + RT \ln x_w) \\ \Delta\mu &= RT \ln x_w \quad (T \text{ temp. of mixing}) \\ &= 8.31 \times 10^3 \times 343 \times \ln (0.019) \\ &= 11.3 \text{ MJ/kg mol.} \\ &\underline{\underline{\text{or } 0.628 \text{ MJ/kg}}} \end{aligned}$$



$$f = \frac{x_s}{x_s - x_w}$$

- x_0 working fluid
- x_w weak absorbent solution
- x_s strong sororbent solution

Fig. 1 p-T-x diagram for absorption cycle



$$COP = \frac{Q_a + Q_c}{Q_g}$$

Fig. 2 A schematic diagram of an absorption cycle

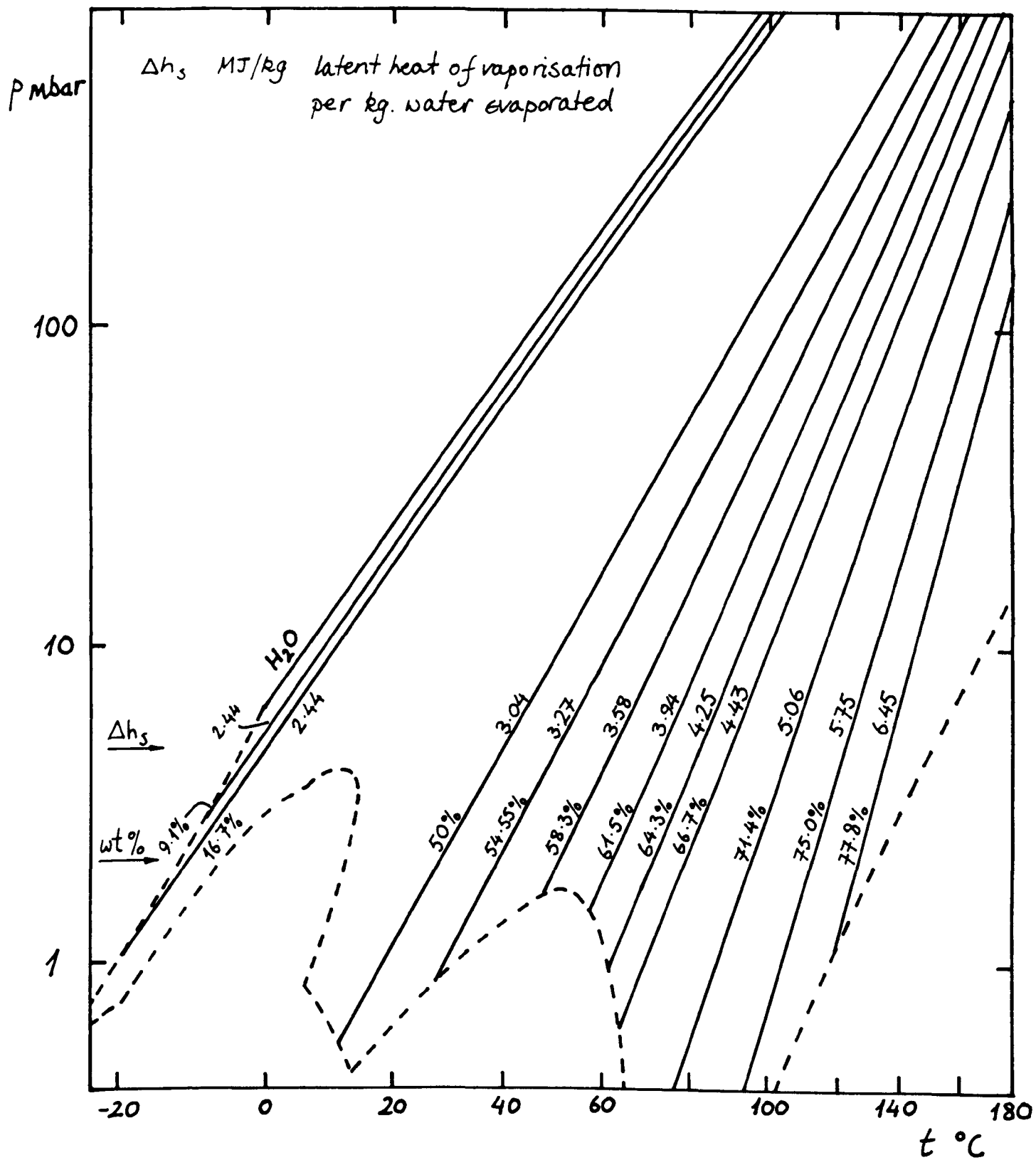


Fig. 3 p-T-x diagram for the NaOH/H₂O system

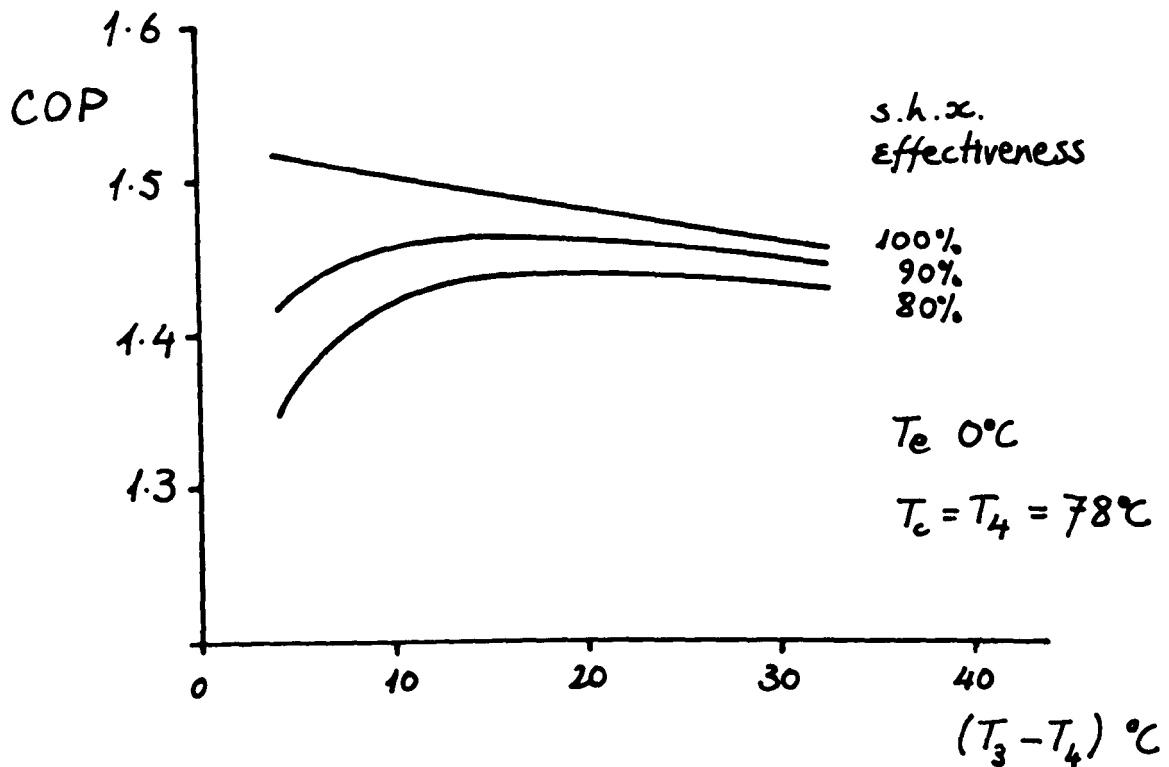
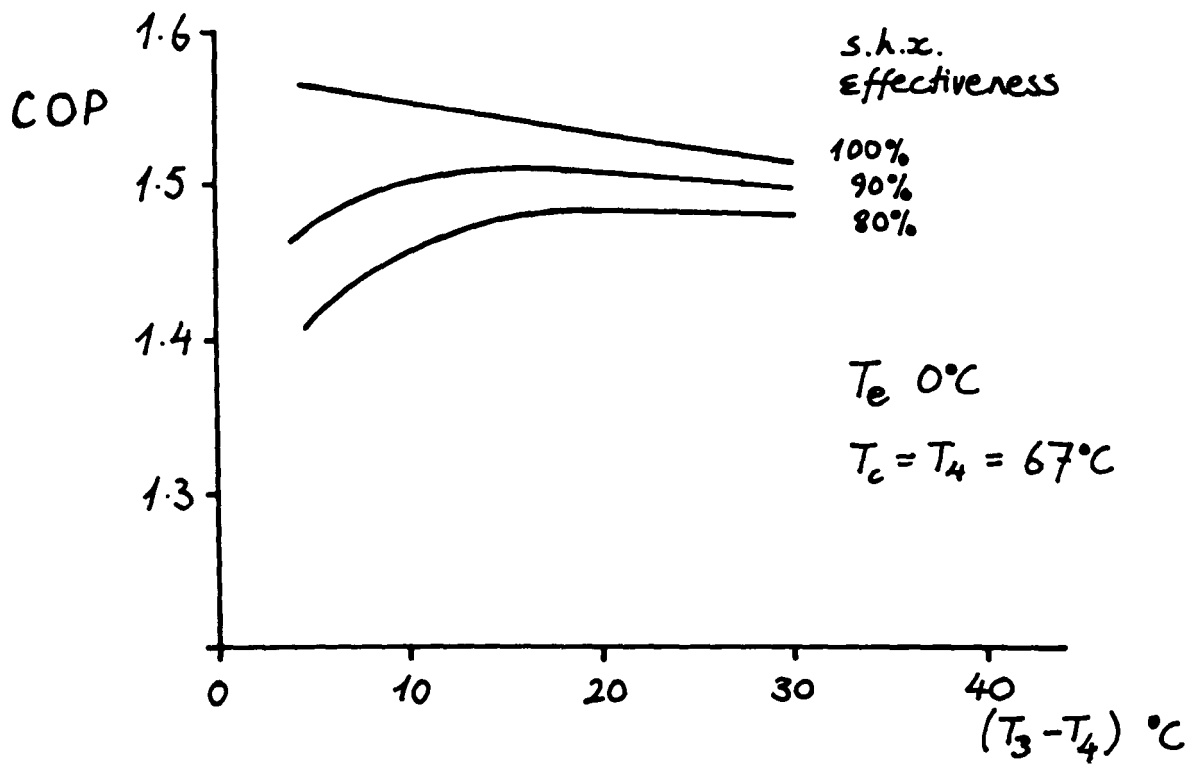


Fig. 4 Theoretical performance for the NaOH/H₂O system

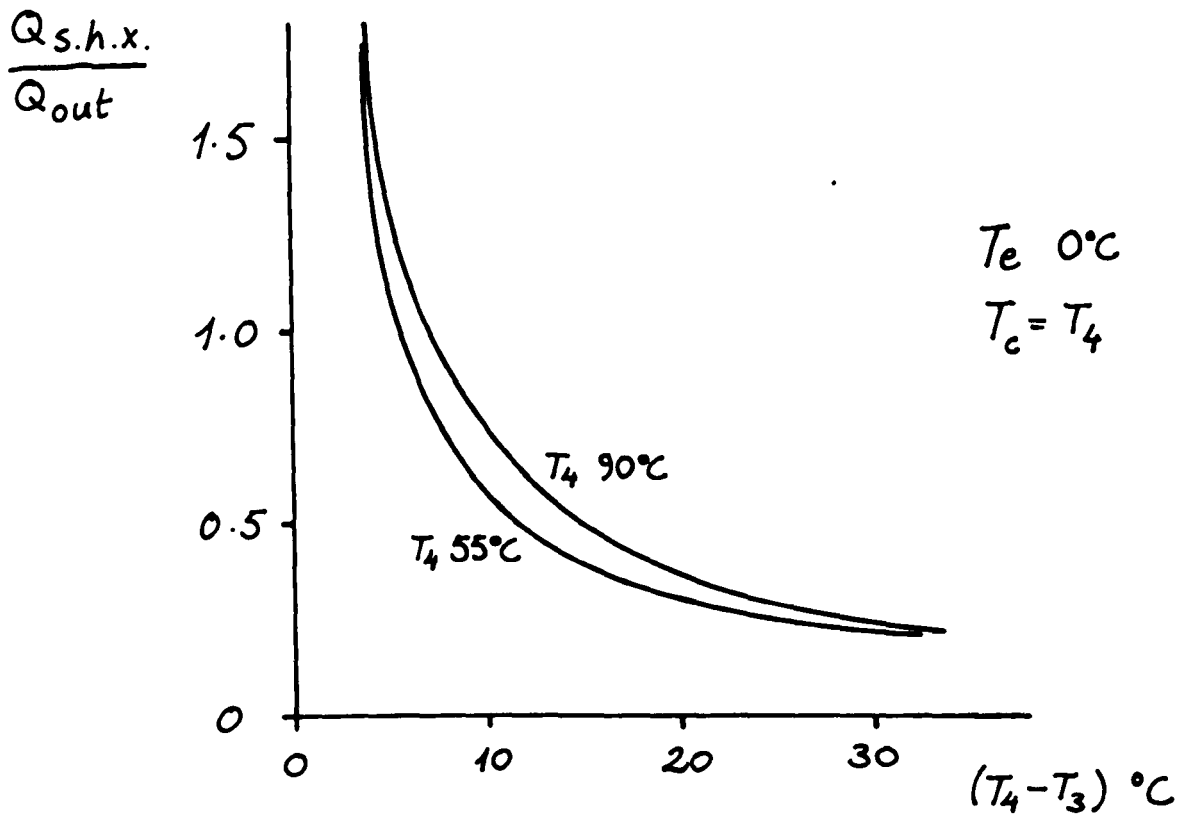


Fig. 5 Solution heat exchanger capacity vs. absorber temperature range

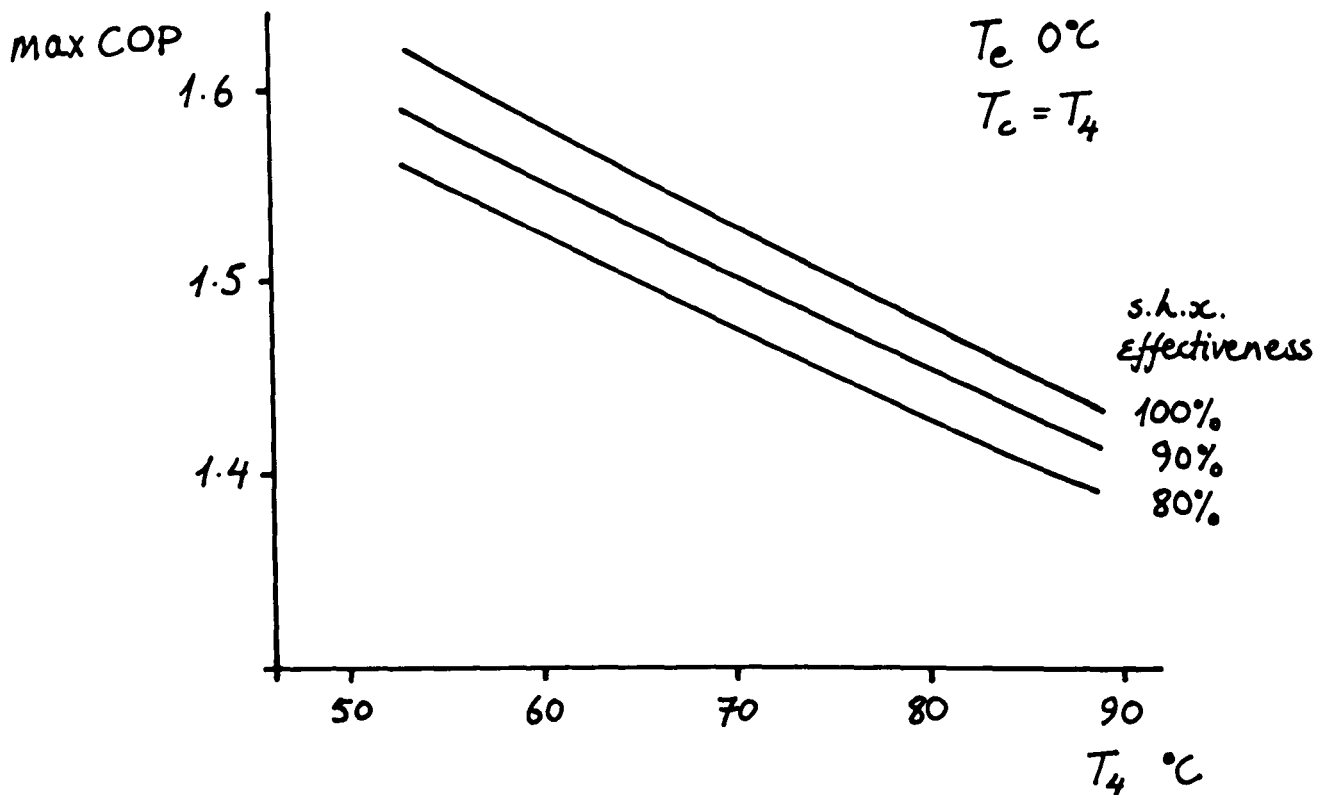


Fig. 6 Dependence of maximum COP on temperature lift

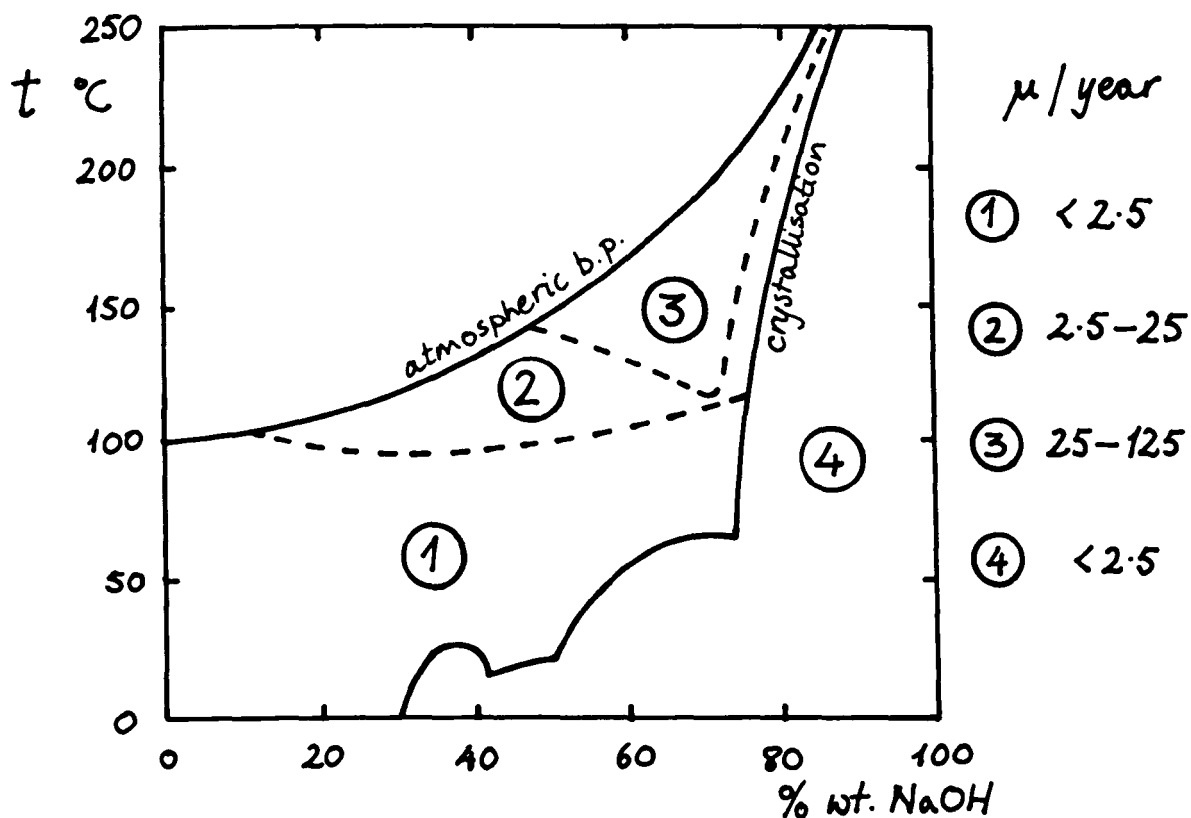


Fig. 7 Corrosion chart for nickel with NaOH solutions - courtesy ICI Ltd

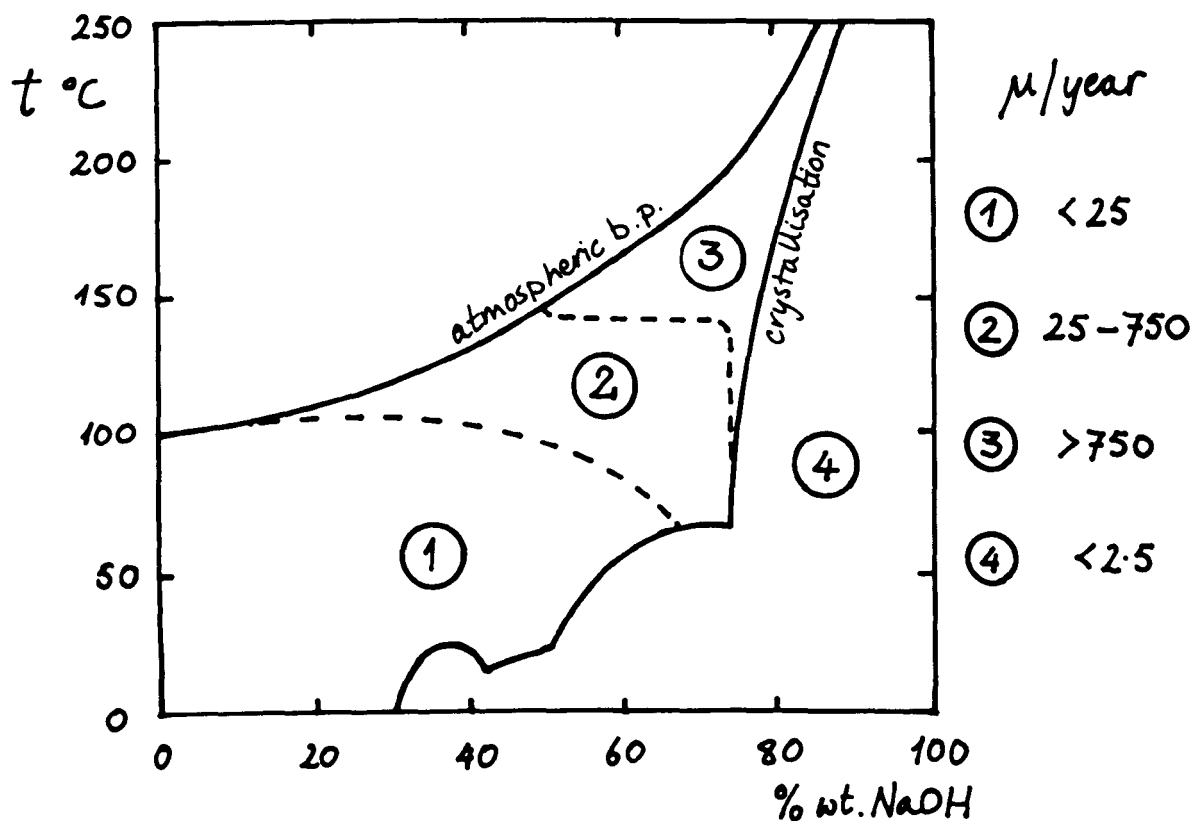


Fig. 8 Corrosion chart for austenitic stainless steel with NaOH solutions - courtesy ICI Ltd

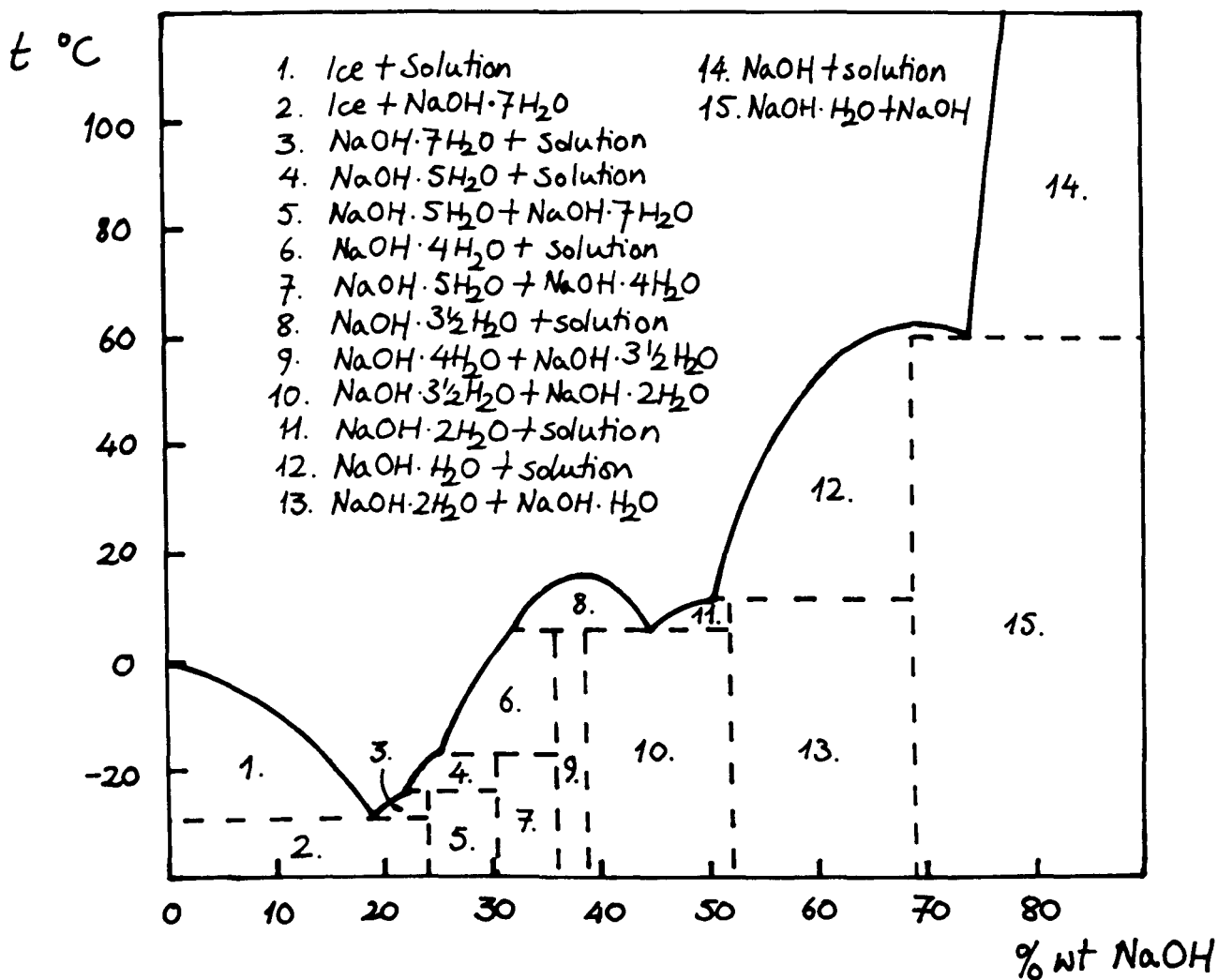


Fig. 9 Crystallisation temperature - concentration chart for NaOH solutions

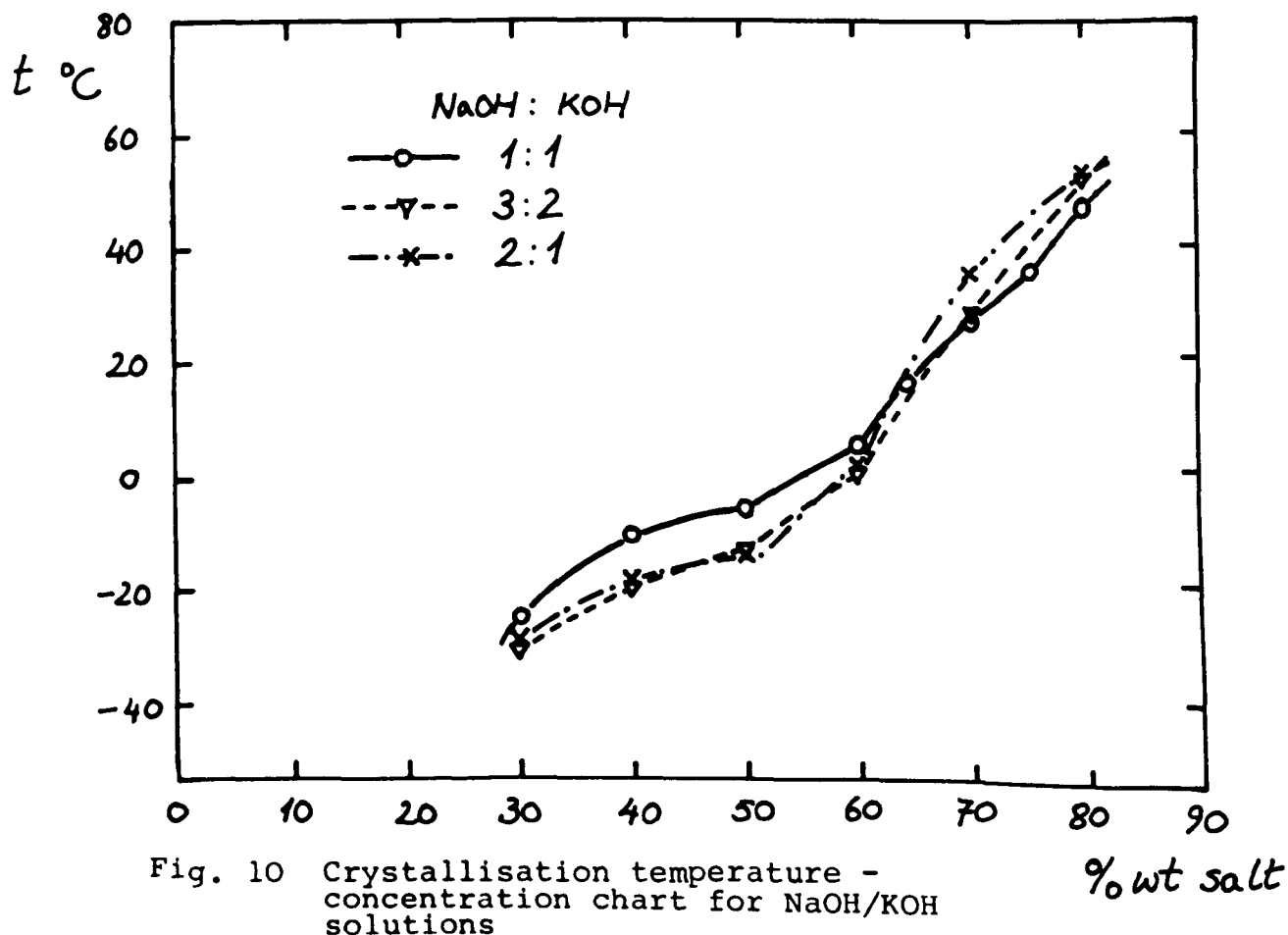


Fig. 10 Crystallisation temperature - concentration chart for NaOH/KOH solutions

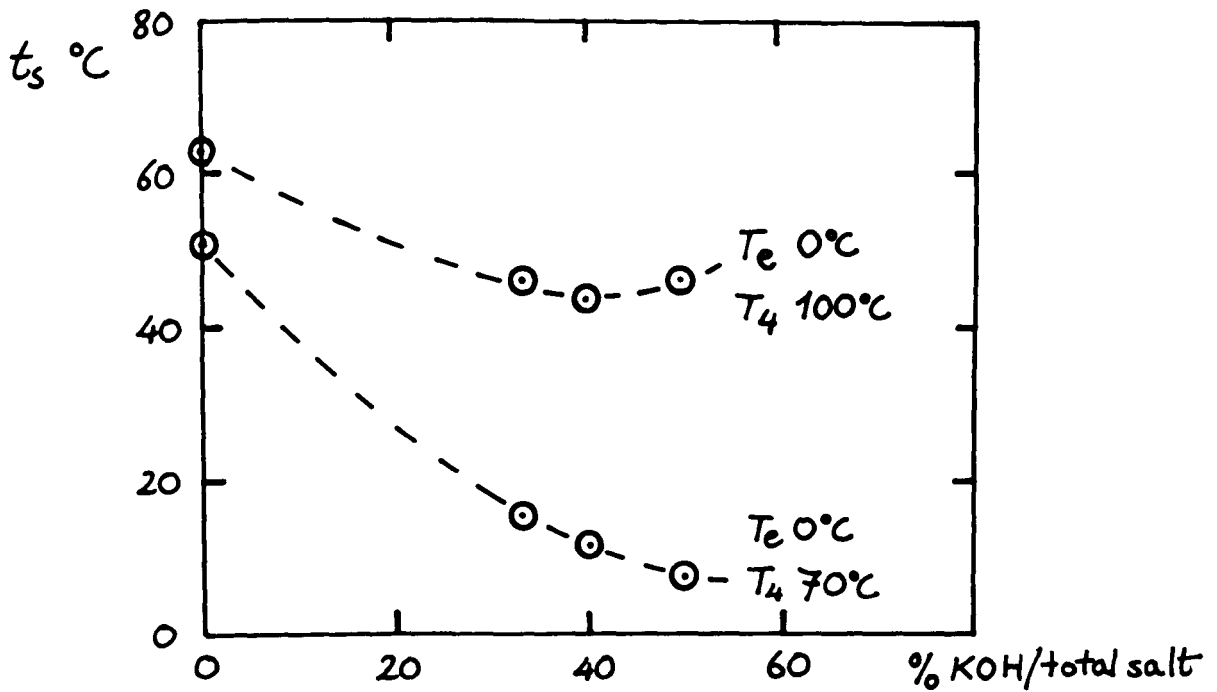


Fig. 11 Effect of % KOH on crystallisation temperature

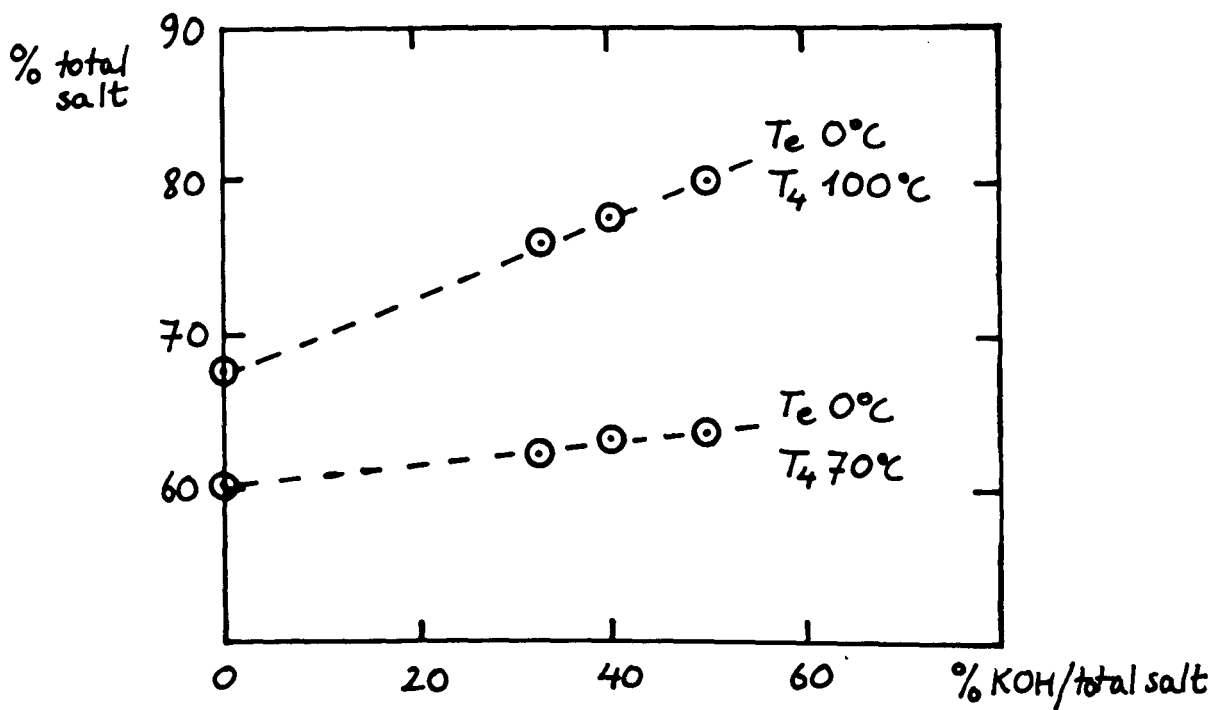


Fig. 12 Effect of % KOH on total % salt necessary for a given temperature lift

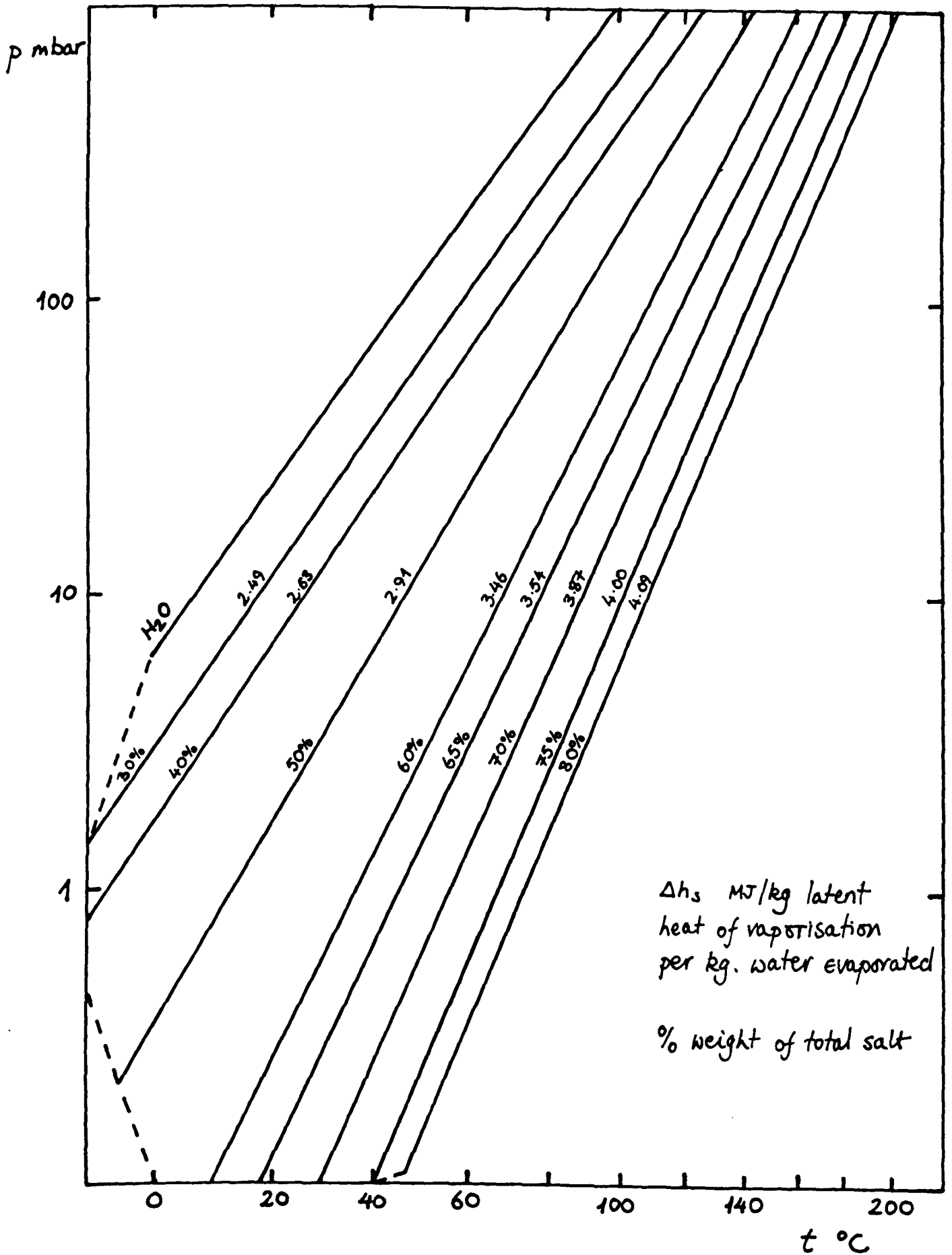


Fig. 13 p-T-x diagram for the NaOH/KOH/H₂O system with equal weight proportions of salt. (Ref.31)

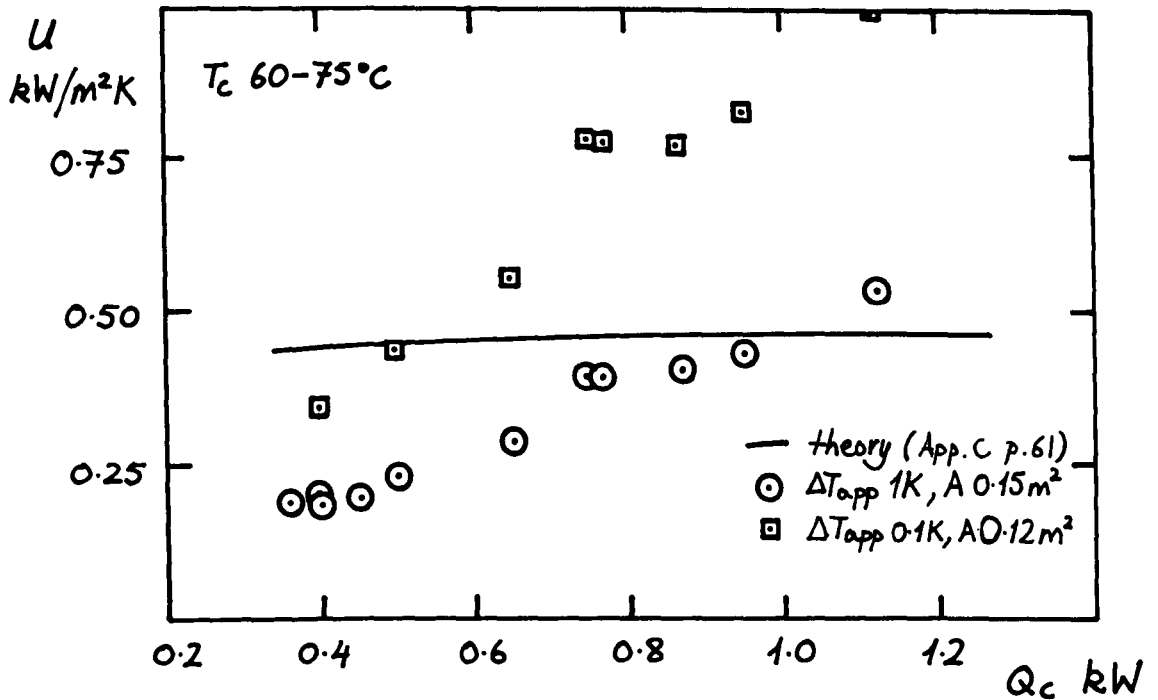


Fig. 14 Overall heat transfer coefficient for the condenser coil

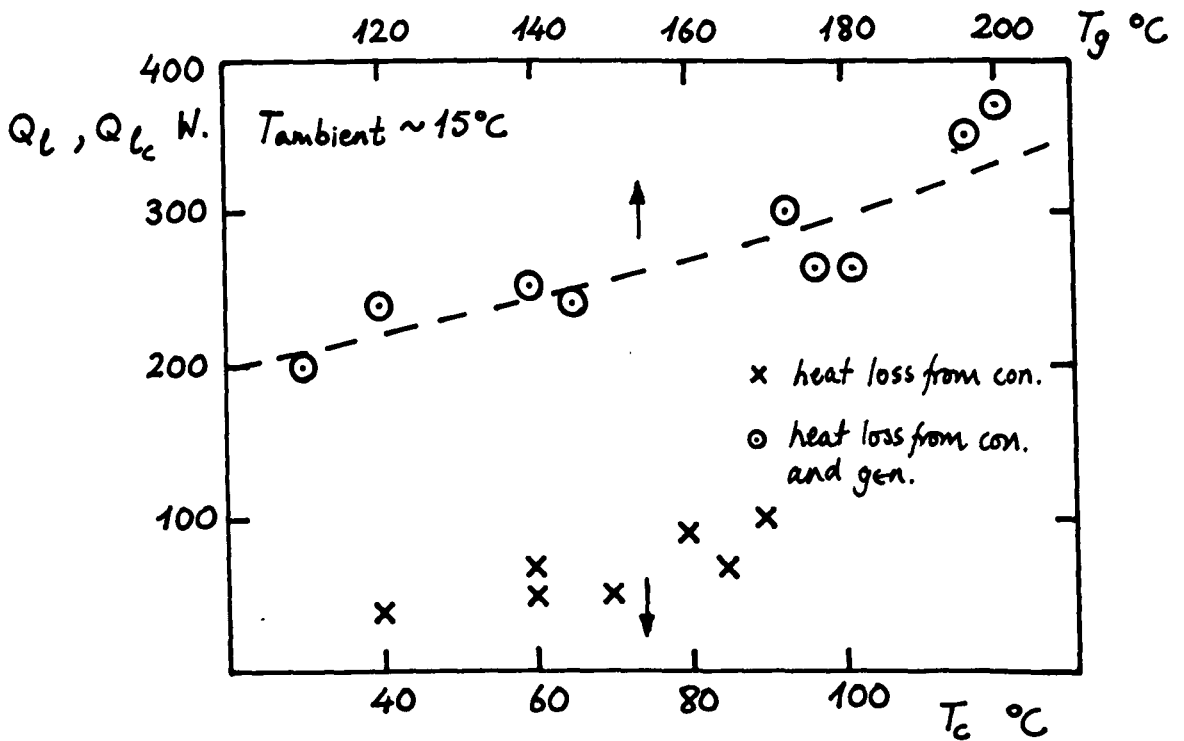


Fig. 15 Heat loss from generator and condenser

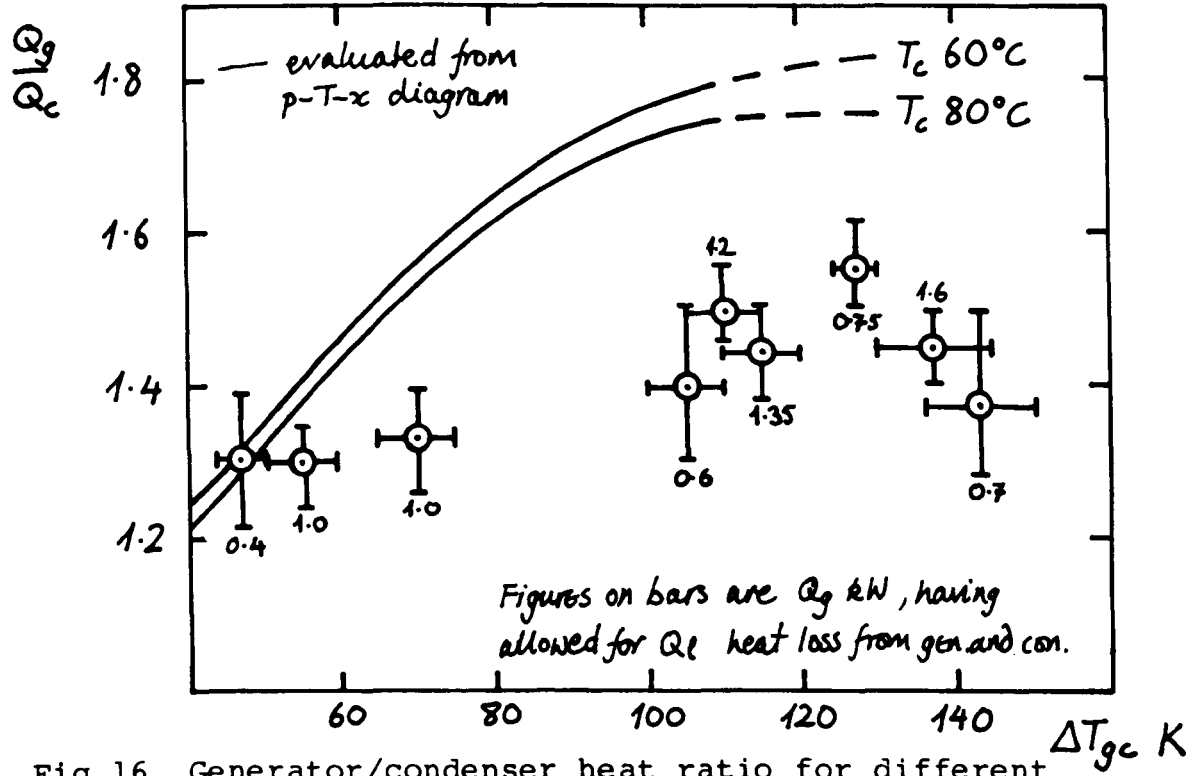


Fig. 16 Generator/condenser heat ratio for different strengths of solution

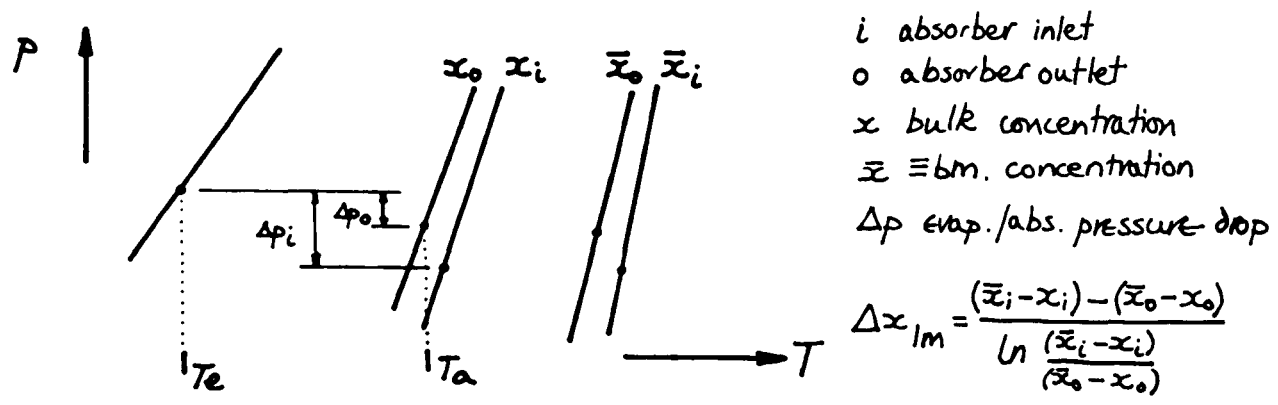


Fig. 17 Evaluation of concentration driving potential from p-T-x diagram

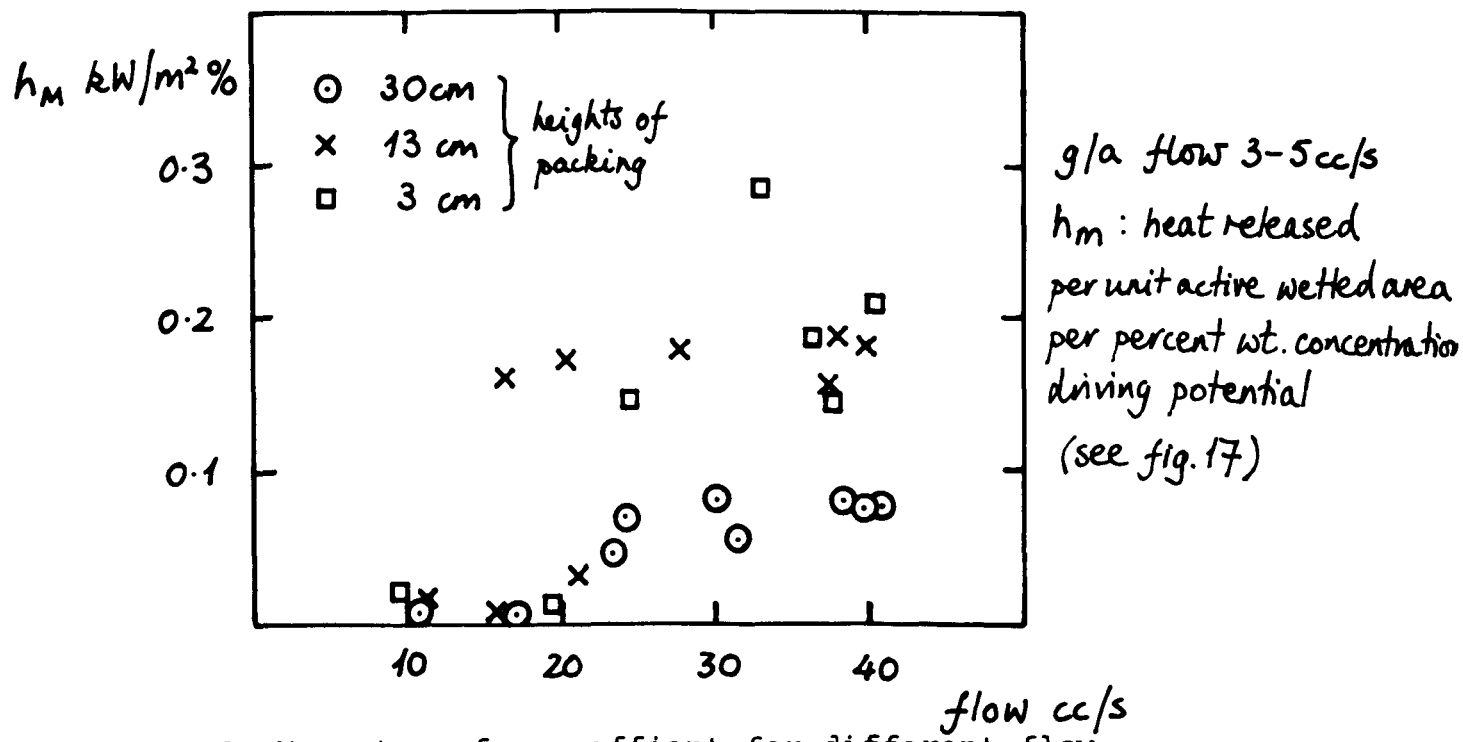


Fig. 18 Mass transfer coefficient for different flow rates over the packed column

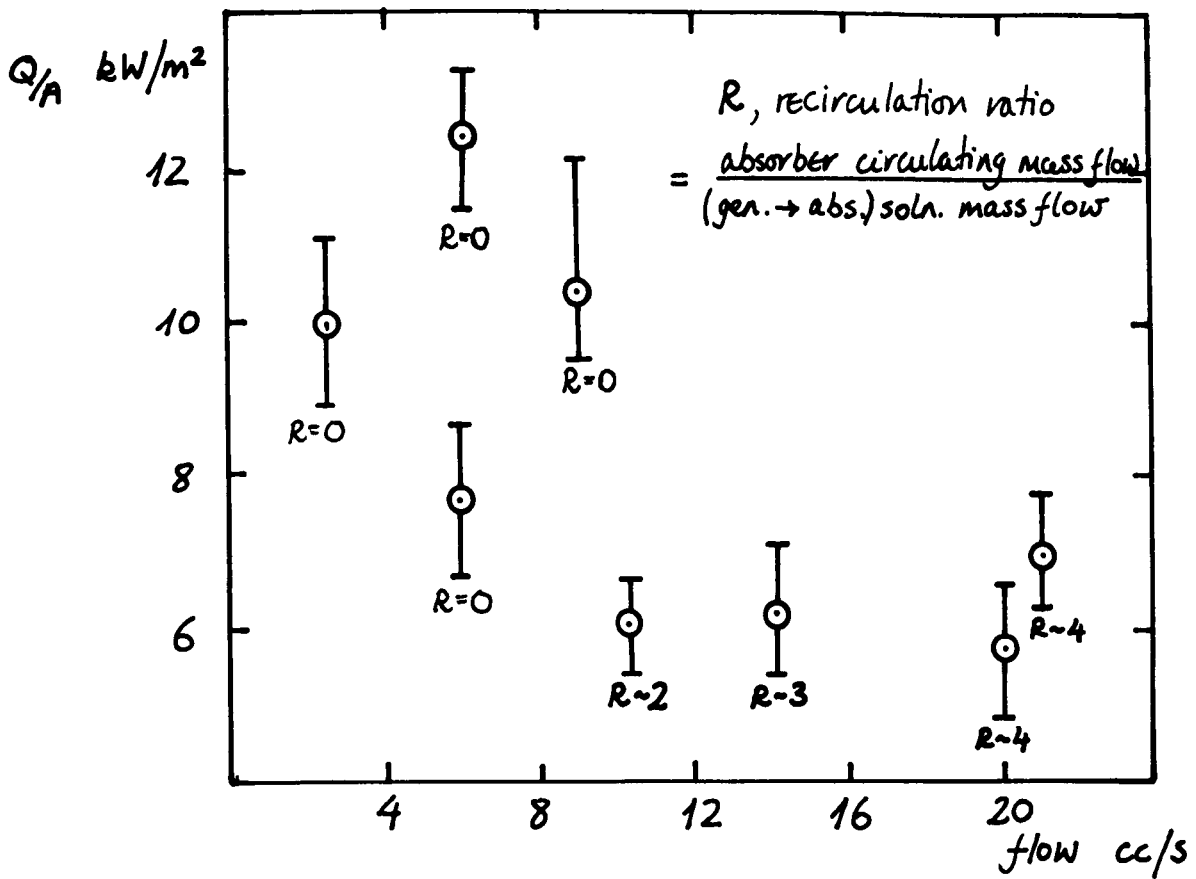


Fig. 19 Power density against solution flow for the isothermal absorber

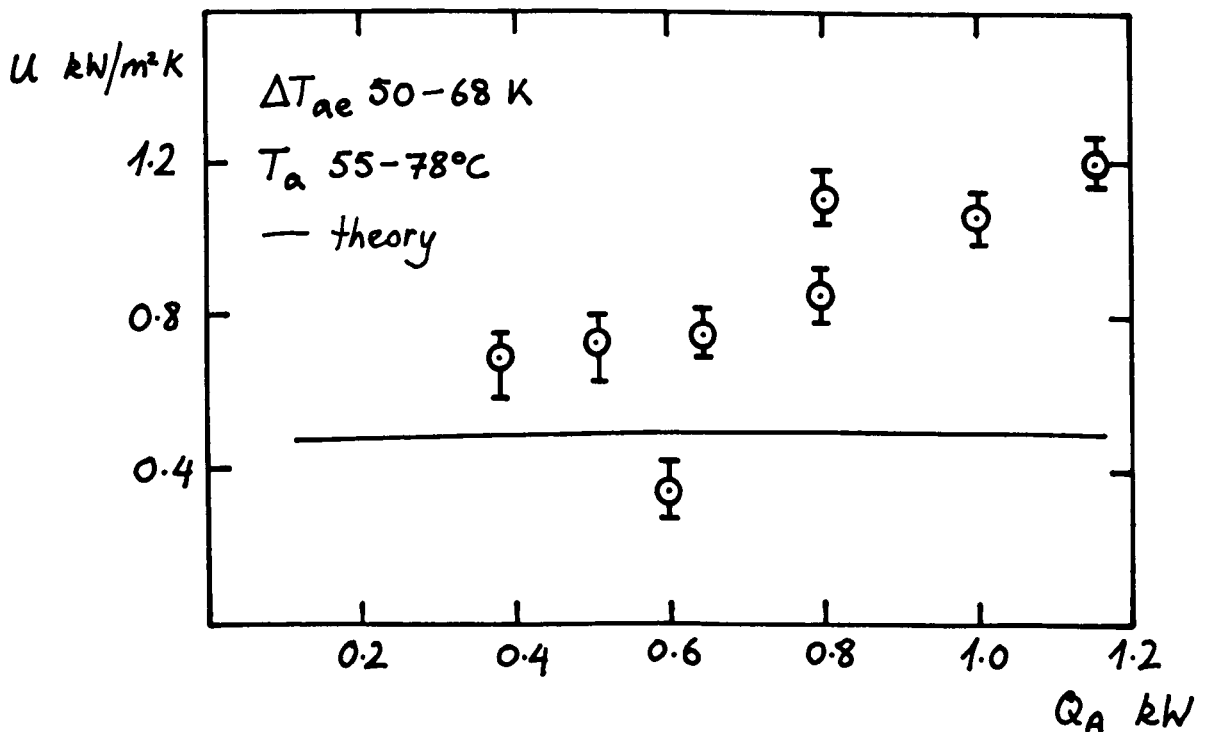


Fig. 20 Overall heat transfer coefficient for the isothermal absorber

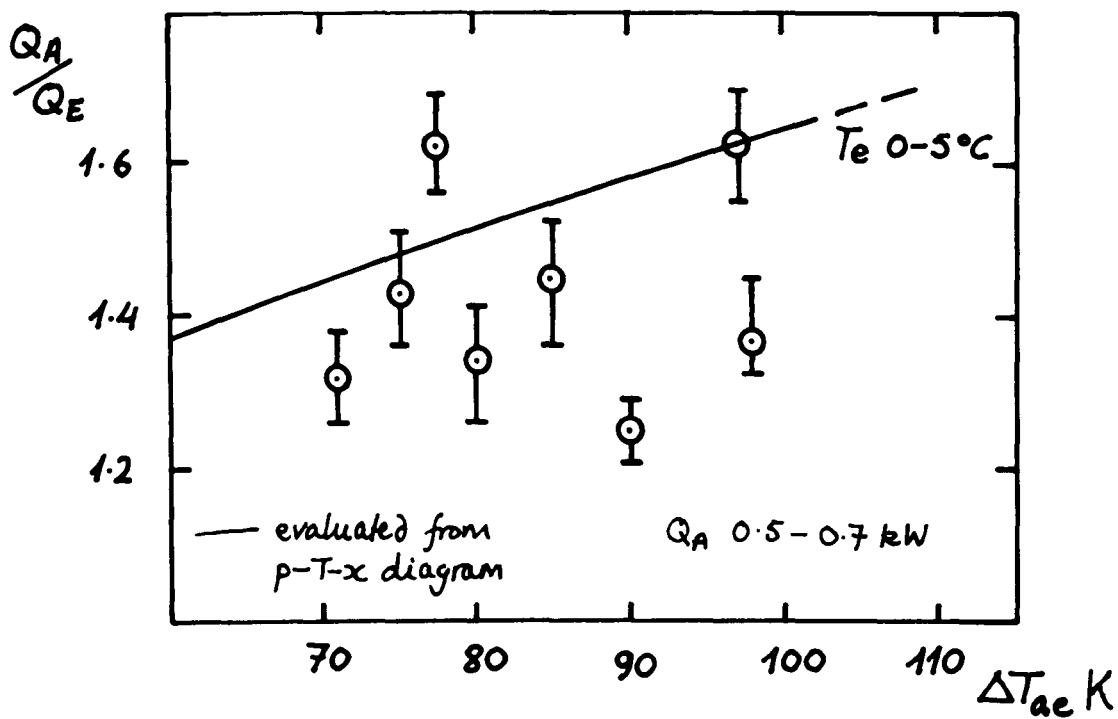


Fig. 21 Absorber/evaporator heat ratio for different strengths of solution

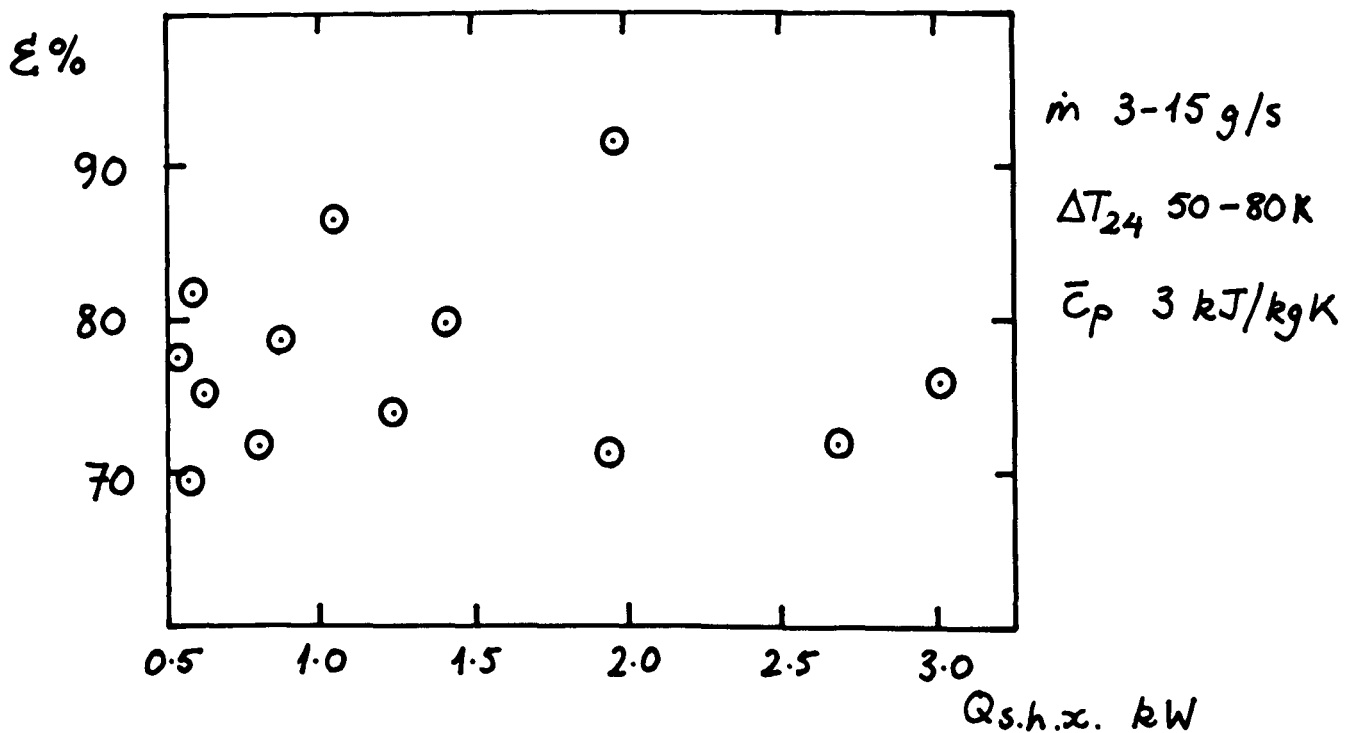
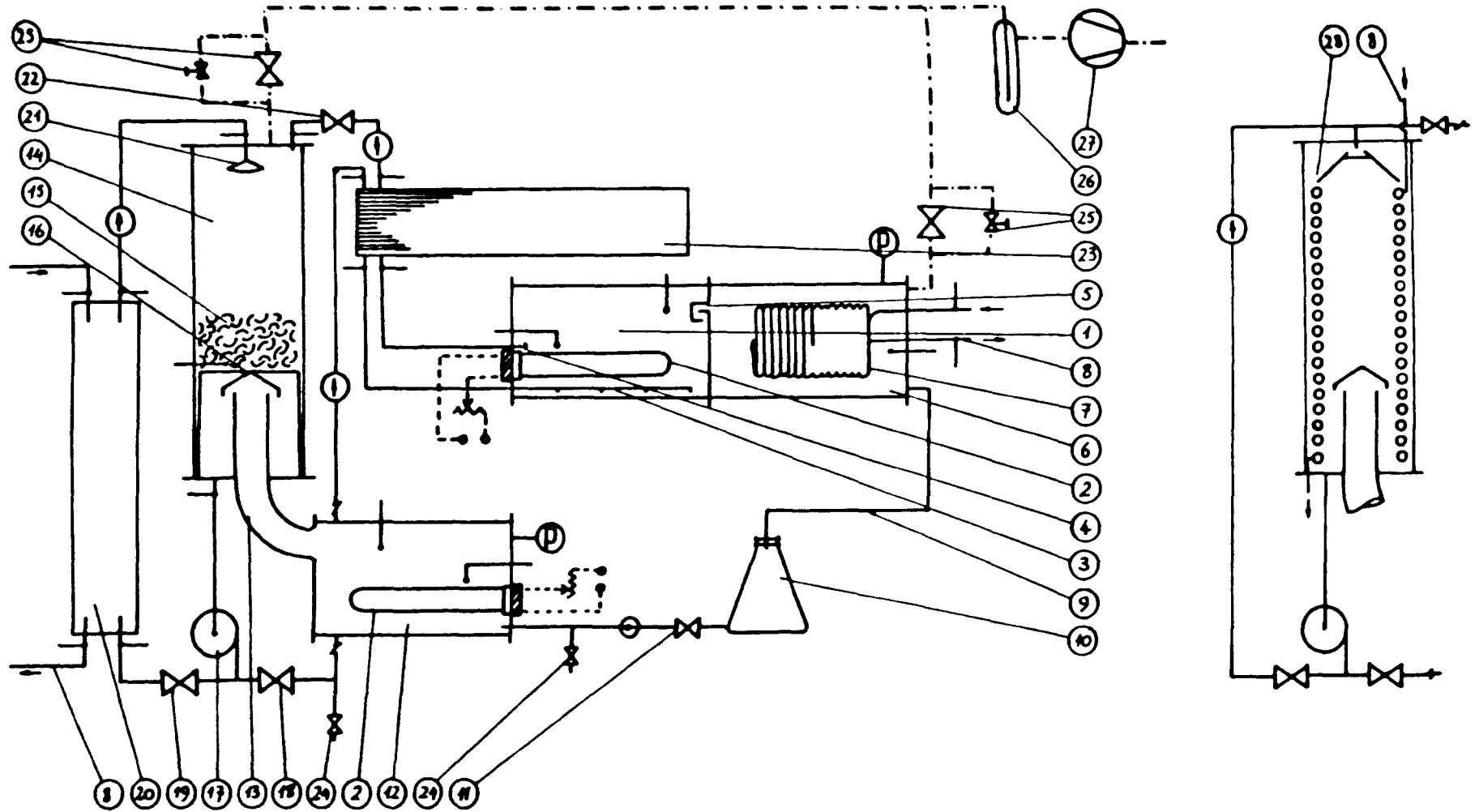


Fig. 22 Solution heat exchanger effectiveness

Drawing 1 Schematic diagram of experimental rig



- | | | | |
|-----------------------------|------------------------------|-------------------------------|-----------------------------|
| Ⓧ Capsule pressure gauge | ⑤ Vapour baffle cap | ⑬ Vapour pipe | ⑳ Distributor rose |
| — Thermocouple | ⑥ Condenser | ⑭ Absorber | ㉑ Gen./abs. expansion valve |
| - - - Vacuum line | ⑦ Condenser coil | ⑮ Ceramic packing | ㉒ Solution heat exchanger |
| - - - Power line to heaters | ⑧ Cooling water | ⑯ Vapour baffle cap | ㉓ Drain valves |
| Ⓛ Flowmeter | ⑨ Condensate outlet | ⑰ Solution pump | ㉔ Vacuum valves |
| ① Generator | ⑩ Condensate receiver | ⑱ Valve for flow to generator | ㉕ LN ₂ trap |
| ② 1kW heater | ⑪ Con./evap. expansion valve | ㉖ Valve for abs. recirc. flow | ㉖ Vacuum pump |
| ③ Solution inlet | ⑫ Evaporator | ㉗ Abs. plate heat exchanger | ㉗ Isothermal abs. coil |
| ④ Solution outlet | | | |

Fig. 23 Details of experimental rig

Main vessels :

- ① 150mm ϕ borosilicate glass pipe, min. wall thickness
 - ⑥ 6 mm, 300 mm long (⑭ x 500 mm). Stainless steel
 - ⑫ end plates, type 321 6 mm thick, sealed with butyl
 - ⑭ rubber gaskets (PTFE for ①).
-

Areas :

- ② A = 0.01 m², nickel plated.
 - ⑦ A = 0.15 - 0.12 m², stn. st. 321; 6 mm ϕ turns, 6 mm pitch.
 - ⑮ A = 8.48 m²/m pckng. height, $\frac{1}{2}$ " Intalox saddles.
 - ⑳ A = 0.31 m² see App. C for details.
 - ㉓ A = 0.59 m² see App. C for details.
 - ㉔ A = 0.23 m², stn. st. 321; 6 mm ϕ , 29 turns, 12/15 mm pitch.
-

Thermal capacities :

- ① 18-25 kJ/K including solution inventory.
 - ⑥ 5 kJ/K including cooling water.
 - ⑫ 17 kJ/K including water inventory.
 - ⑭/⑮ 7-10 kJ/K 3-30 cm of packing.
 - ⑳ 4 kJ/K including cooling water, excluding solution.
 - ㉓ 4 kJ/K excluding solution, 12 kJ/K including solution.
 - ⑭/㉔ 8 kJ/K including cooling water.
-

General :

Pipes : Stn. st. 6-10 mm ϕ .
 Valves : 'QVF' glass with PTFE gland.
 Pump : 'Micropump' PTFE/stn. st. gear pump, maximum delivery 45 cc/S.
 Gaskets, connections, etc : natural and butyl rubber.

Instrumentation :

- Stn. st. sheathed chromel/alumel, calibrated $\pm \frac{1}{2}^{\circ}\text{C}$.
 - Ⓟ 'Diavac K' capsule gauge.
 - Ⓢ Taper glass rotameters.
 - ⚡ 3 kW variac, calibrated ± 10 W.
-

Insulation :

40 mm - 60 mm thick glass fibre wool with aluminium foil backing.

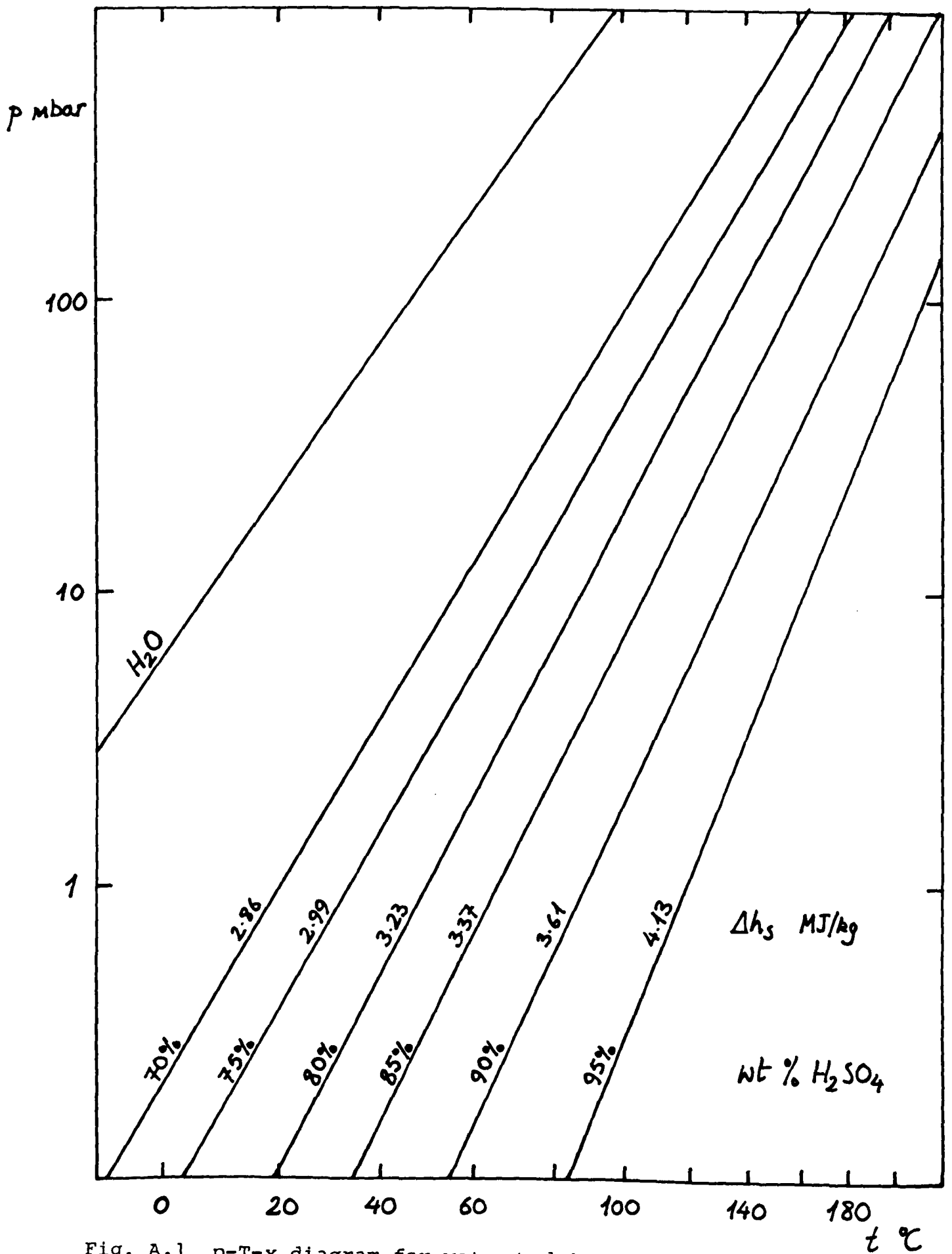


Fig. A.1 p-T-x diagram for water/sulphuric acid solutions

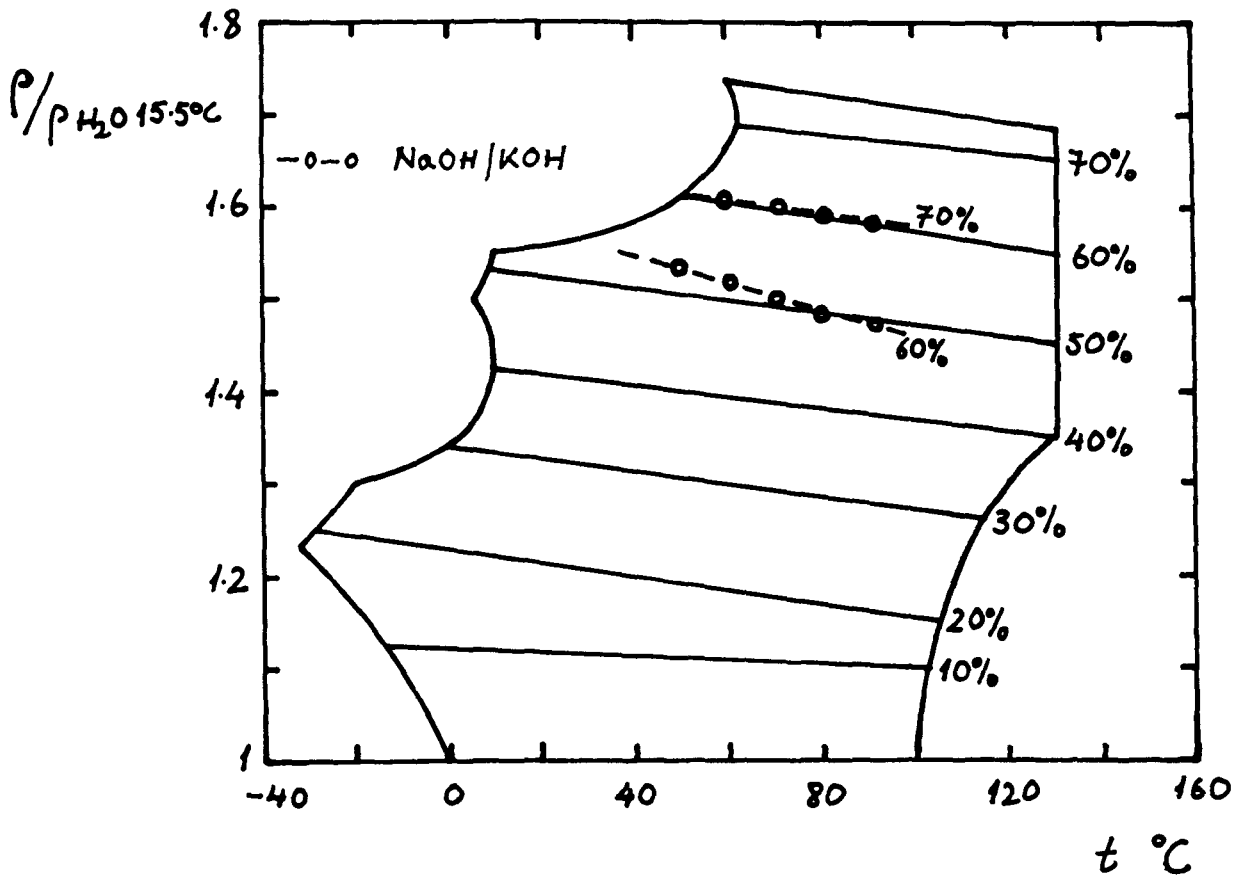


Fig. C.1 Densities of NaOH and NaOH/KOH (1:1) solutions - courtesy ICI Ltd

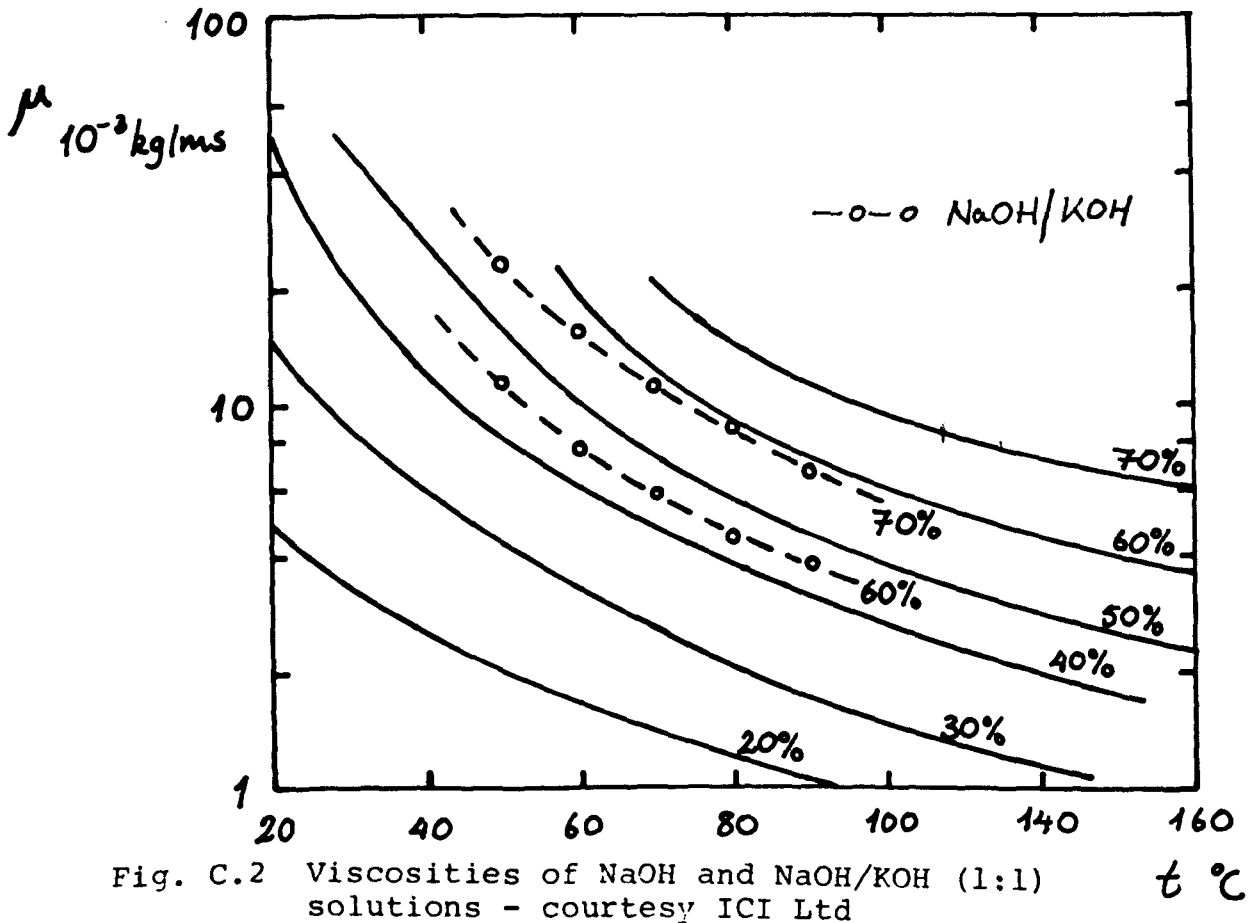


Fig. C.2 Viscosities of NaOH and NaOH/KOH (1:1) solutions - courtesy ICI Ltd

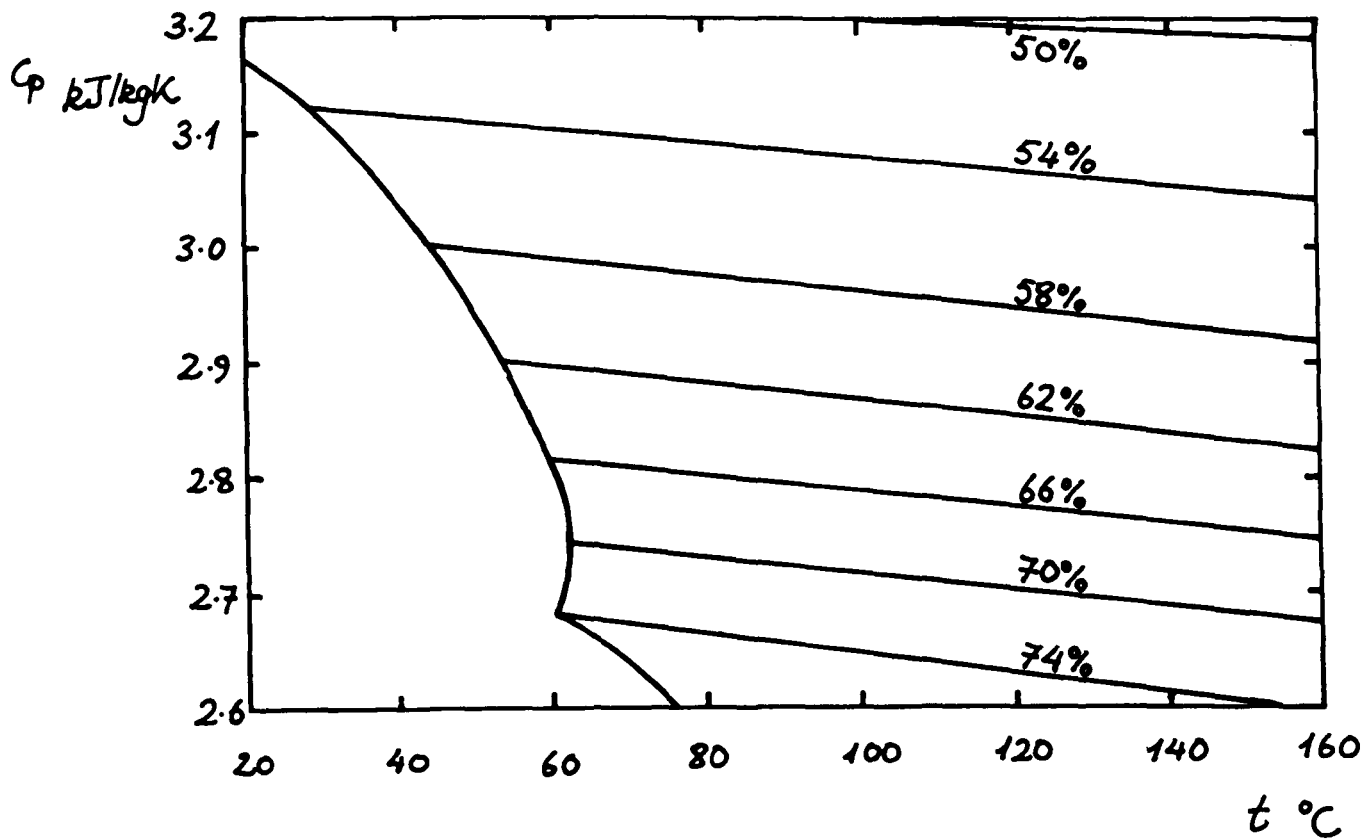


Fig. C.3 Specific heats of NaOH solutions - courtesy ICI Ltd

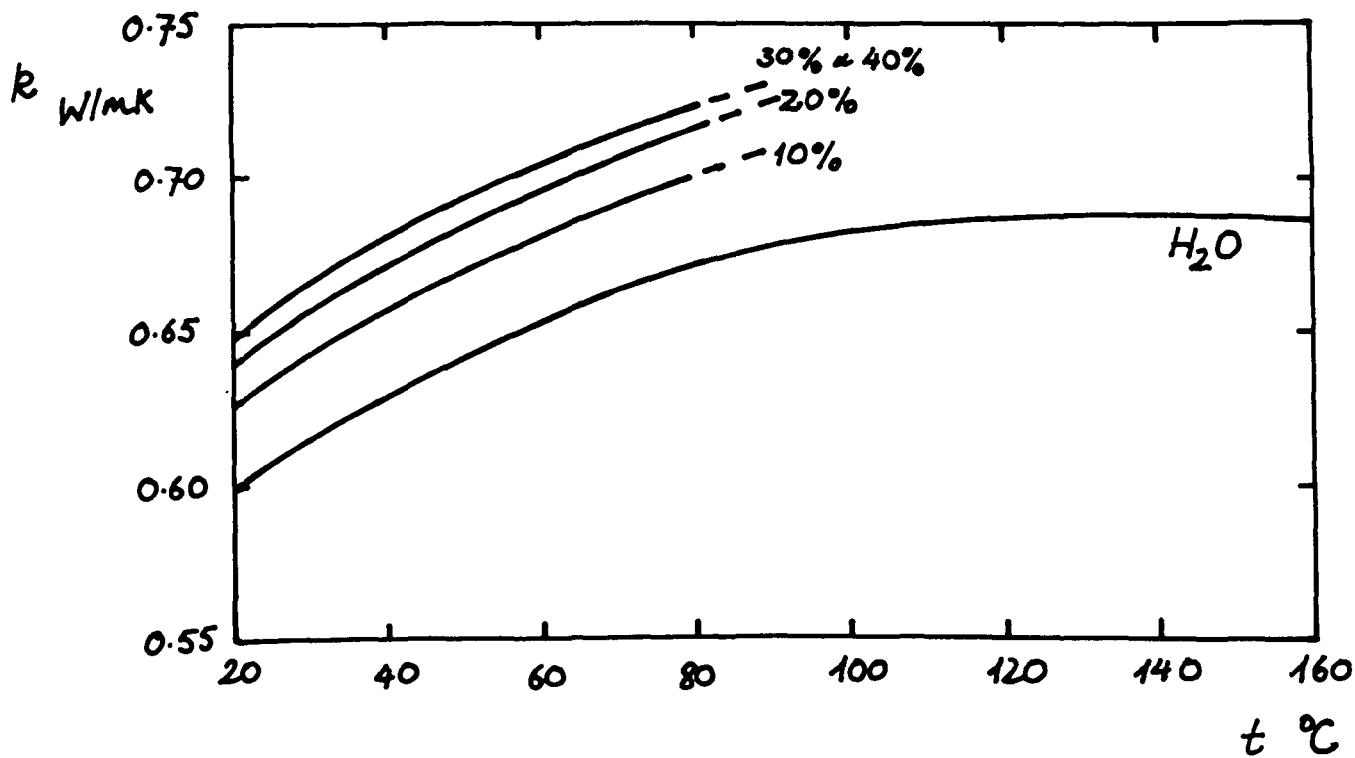


Fig. C.4 Conductivity of NaOH solutions - courtesy ICI Ltd

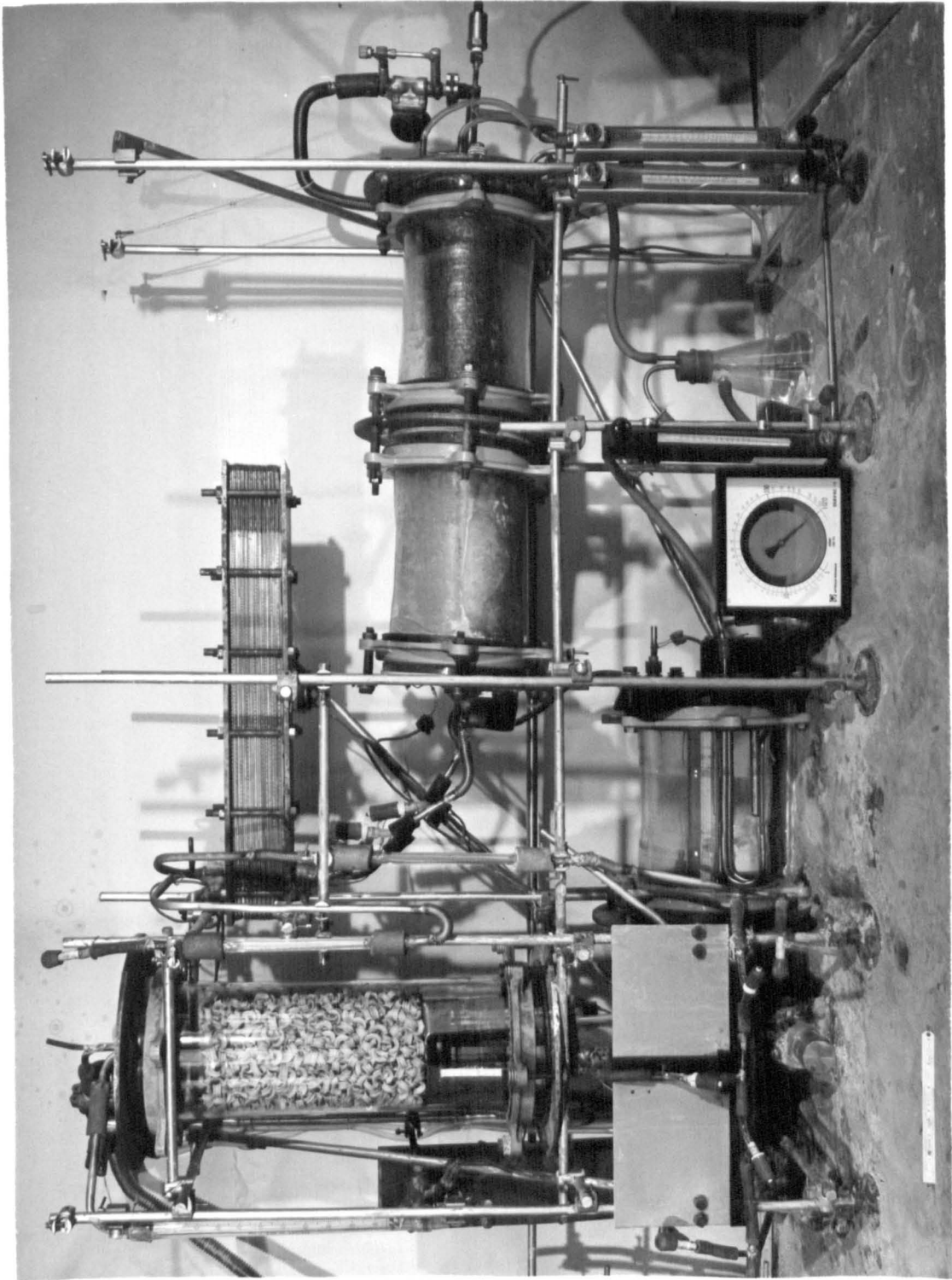


photo.1 EXPERIMENTAL RIG

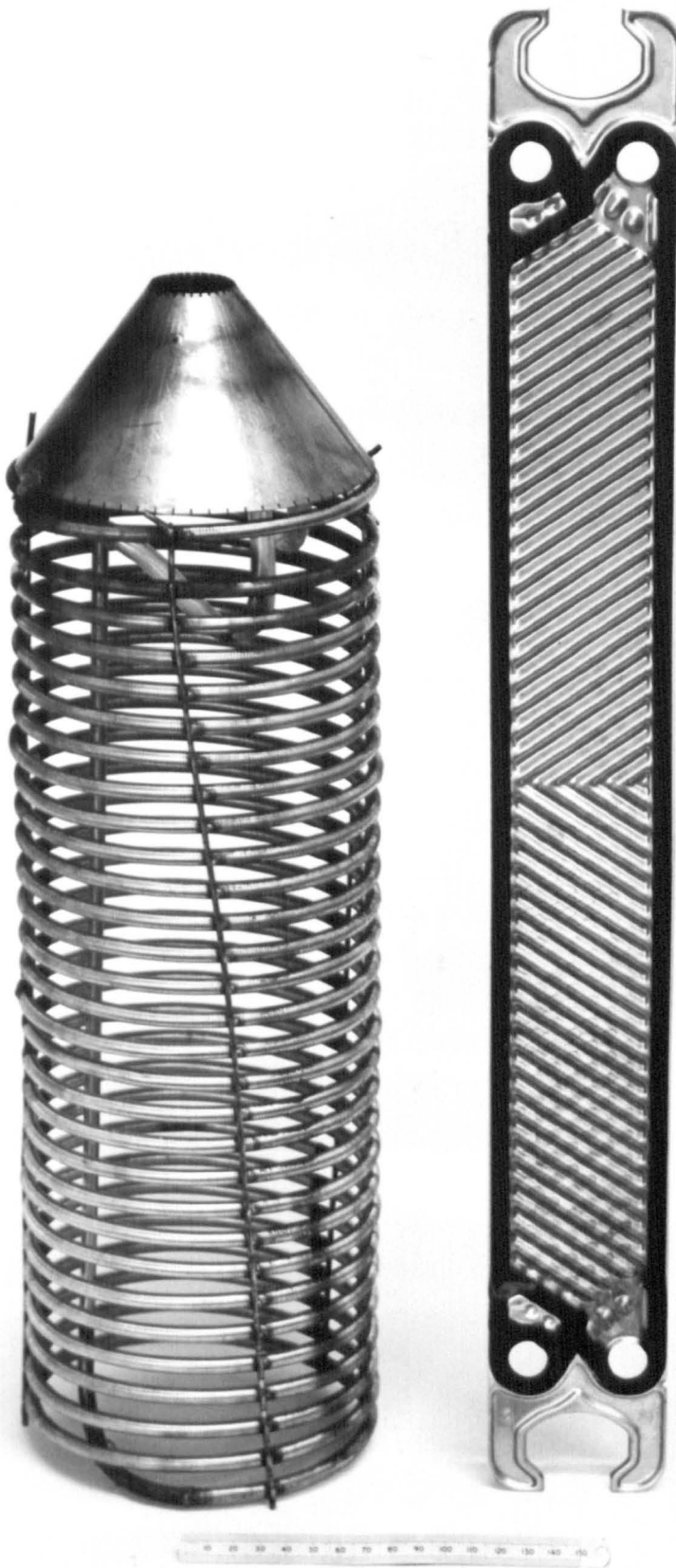


photo.2 ABSORBER COIL AND SINGLE HEAT EXCHANGER PLATE

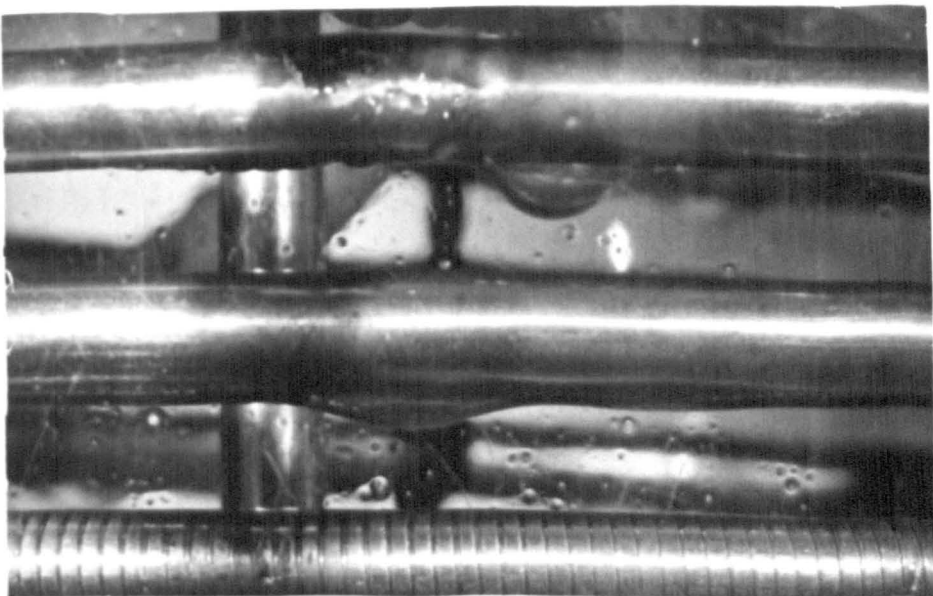
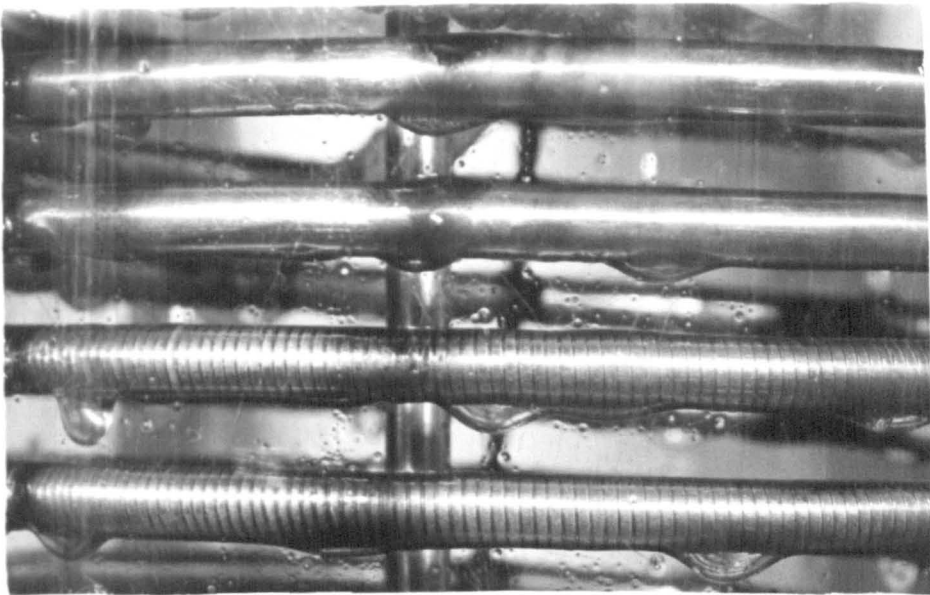
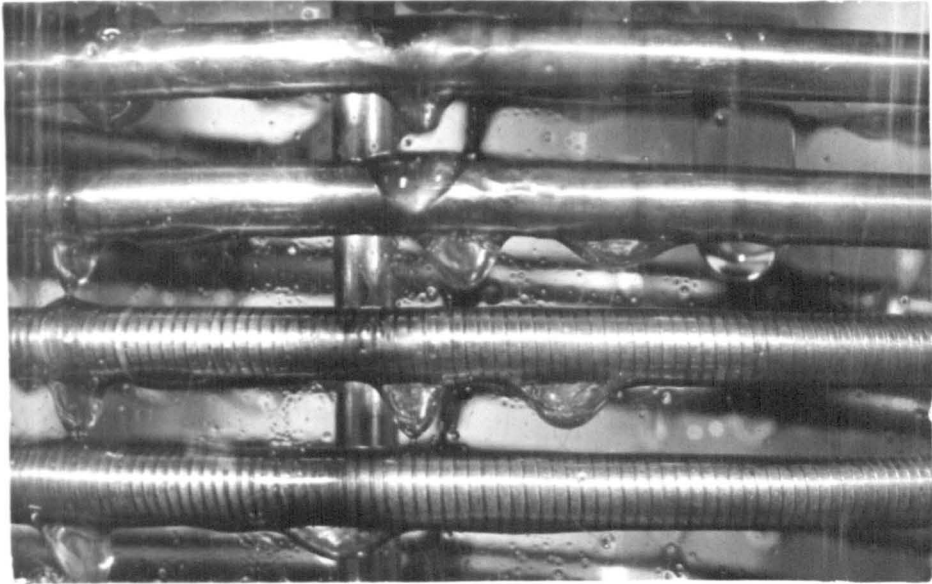


photo.3 "SHIMMERING" ON ABSORBER COIL